Investment Planning Models and Optimal Incentive Design for System Planners and Investors to Integrate Renewables

by

Indrajit Das

A thesis
presented to the University of Waterloo
in fulfillment of the
thesis requirement for the degree of
Doctor of Philosophy
in
Electrical and Computer Engineering

Waterloo, Ontario, Canada, 2014

I hereby declare that I am the sole author of this thesis. This is a true copy of the thesis, including any required final revisions, as accepted by my examiners.

I understand that my thesis may be made electronically available to the public.

Abstract

Emissions from fossil fuel based energy sources is a global concern with respect to environmental degradation. Thus, a diversification of energy sources in the supply mix of power systems to include renewable sources of energy has become necessary in order to reduce emissions. In addition to renewable integration, the incorporation of energy conservation also helps in emissions reduction, thereby, becoming an increasingly important aspect of generation expansion planning (GEP). However, the relatively high cost of renewable energy sources (RES) is a hindrance in achieving a cleaner and more diverse energy supply mix. Therefore, it is imperative to develop and analyze a system planning model for determining optimal incentives that will encourage both renewable integration and conservation, while allowing investors to make optimal investment decisions on RES projects.

In recent years, solar energy, particularly solar photovoltaic (PV), based generation has become one of the fastest growing energy sources in the electricity sector. Hence, the first part of this thesis presents a novel sensitivity analysis framework, based on duality theory (DT), to examine the sensitivity of an investor's profit to changes in parameters of a solar PV investment planning model previously proposed. The computed sensitivity indices are utilized for assessing the risk of a specific solar PV investment project for a realistic model of the Ontario grid. The results demonstrate that sensitivity indices obtained using DT-based method are very close to the true sensitivities obtained using a finite difference (FD) approach and also those obtained using Monte Carlo simulations, but at lower computational costs. Furthermore, a novel interpretation of the sensitivity indices is developed, by proposing mathematical formulas that help to evaluate the risk indices of a solar PV investment project.

In the second part of this thesis, a novel holistic GEP model, from a system planner's perspective, has been proposed to enable a central planning authority (CPA) or a regulator to determine optimal incentives for renewable energy integration and energy conservation, while considering investors' constraints. The proposed GEP model is also designed to determine the siting, sizing, timing, and technology of the new capacities required to adequately supply the demand over the planning horizon. Various case studies relevant to Ontario and based on realistic data, comprising presence/absence and variations in RES penetration and/or energy conservation targets,

variations in maximum payback-period limits of RES, and other input parameter changes are presented and discussed. Furthermore, Monte Carlo simulations are performed to understand the effects that uncertainties on non-dispatchable wind and solar generation availabilities have on the GEP outcome, particularly on the optimal RES incentives.

Acknowledgements

First and foremost, I convey my gratitude and appreciations to my supervisors, Professor Kankar Bhattacharya and Professor Claudio Cañizares, for their invaluable support and guidance at every stage of my PhD studies. Their professionalism and dedication have always been inspiring to me, and working with them has been a truly enriching experience. I consider the opportunity to complete my studies under their supervision as the highest degree of privilege.

I would like to convey my deepest gratitude to the following members of my PhD committee for their valuable comments and inputs: Professor Bala Venkatesh from the Department of Electrical and Computer Engineering at Ryerson University; Professor Olaf Weber from the School of Environment, Enterprise and Development at the University of Waterloo; and Professor Daniel Miller and Professor Magdy M. A. Salama from the Department of Electrical and Computer Engineering at the University of Waterloo.

I gratefully acknowledge the funding and support provided by the Ontario Centres of Excellence (OCE), National Science and Engineering Research Council (NSERC) Canada, Hydro One Inc., ABB USA Corporate Research, IBM Canada, First Solar Inc., and London Hydro Research Grant.

I extend my heartfelt gratitude to my beloved uncle, father, and mother for their unconditional love, support, and encouragement.

I warmly thank all my current and past colleagues in the Electricity Market Simulation and Optimization Laboratory (EMSOL) for providing a pleasant and friendly working environment in the years of my studies.

A very special word of thanks goes to Saptarsi and Ronita for their exceptional encouragement and friendship that I am privileged to have.

Finally, I owe my loving thanks to my wife Chandrani for being there with me during all the ups and downs, and for the many sacrifices that she has made to support me in undertaking my doctoral studies. Thank you my dear for building my inner strength with your endless love and encouragement.

I dedicate this thesis to my wife *Chandrani*.

Table of Contents

List of Tables

List of Figures

Glossary

AHP	Analytical Hierarchy Process
BAU	Business-As-Usual
BIO	Bio-based power generation
COAL	Coal-based power generation
c.d.f.	Cumulative Distribution Function
CL	Confidence Level
CPA	Central Planning Authority
DISCO	Distribution Company
DSM	Demand Side Management
DT	Duality Theory
FD	Finite Difference
FIT	Feed-in-Tariff
GAS	Gas-based power generation
GENCO	Generation Company
GEP	Generation Expansion Plan
GPV	Ground-mounted PV based power generation
GRM	Generation Reserve Margin
HNR	Market-price-based hydro power generation
HOEP	Hourly Ontario Energy Price
HR	Regulated-price-based hydro power generation
IEA	International Energy Agency
IESO	Independent Electricity System Operator

IPSP	Integrated Power System Plan
IRP	Integrated Resource Planning
IRR	Internal Rate of Return
KKT	Karush-Kuhn-Tucker
LDC	Local Distribution Company
LMP	Locational Marginal Price
LP	Linear programming
MILP	Mixed Integer Linear Programming
MINLP	Mixed Integer Non-Linear Programming
MVP	Mean-Variance Portfolio
NCP	Contract-price-based nuclear power generation
NLP	Non-Linear Programming
NPV	Net Present Value
NR	Regulated-price-based nuclear power generation
O&M	Operation and Maintenance
OAT	One-factor-at-A-Time
OEB	Ontario Energy Board
OIL	Oil-based power generation
OPA	Ontario Power Authority
OPF	Optimal Power Flow
PBP	Pay-Back Period
p.d.f.	probability density function
PV	Photo-Voltaic
PVPS	PV Power Systems
RES	Renewable Energy Sources
RPV	Roof-top PV based power generation
VaR	Value at Risk
WON	Onshore wind based power generation
WOF	Offshore wind based power generation

Nomenclature

Subscripts and superscripts

$base$	Base case optimization output
$Conv$	Value related to conventional generation
Dem	Demand
DT	Duality Theory
Ex	Quantities related to existing capacities
Exp	Export
FD	Finite Difference
Gen	Generation
GPV	Value related to ground-mounted PV generation
ICV	Incentive-based quantities
Imp	Import
in	Input data
irr	Internal rate of return
Max	Maximum value
MC	Monte Carlo
Min	Minimum value
MP	Market price
New	Quantities related to new capacities
$newFD$	Re-optimization output after parameter perturbation in FD method
o	Profit at a given Confidence Level

out	Output data
Pft	Quantities related to solar PV investment model
RP	Regulated price
Sys	Quantities related to central planning model
$\%$	Quantity in percentage
\$	Quantity in dollars

Sets and Indices

b	Index for base, intermediate and peak load blocks
i, j	Index for transmission zones
J	Set of indexes of active inequality constraints
k	Index of years of study horizon
l	Index of equality constraints
m	Index of all inequality constraints
p	Set of parameters of the solar PV investment plan model
q	Index for binary variables
r	Index of solar PV plan model parameters
s	Set of all generation technologies
$s1$	Set of technologies receiving market price based payments from Central Planning Authority (CP
$s2$	Set of technologies receiving payments from CPA based on regulated price
$s3$	Set of technologies receiving payments from CPA based on incentives
$s4$	Set of technologies connected at distribution level
$s5$	Set of technologies connected at transmission level
$s6$	Set of dispatchable generation technologies
$s7$	Set of non-dispatchable generation technologies
$s8$	Set of renewable energy sources based technologies
t	Time
w	Index of parameters p

Functions

$CP(\cdot)$	Cumulative Distribution Function
$f(\cdot)$	Objective function
$g(\cdot)$	Inequality constraints
$h(\cdot)$	Equality constraints
$z(\cdot)$	Primal optimization problem objective function
$z_D(\cdot)$	Dual optimization problem objective function
$\mathcal{L}(\cdot)$	Lagrangian function
$\Omega_{Pft}(\cdot)$	NPV of profit objective function [$]
$\Omega_{Sys}(\cdot)$	NPV of total system costs and payments objective function [$]

Parameters

a_0	Incentive rate for energy conservation [$/MWh]
a_b	Incentive rate for demand reduction [$/MW]
b_0	Generation reserve margin (GRM) [%]
a, b, c	Vector of parameters or known coefficients
ABG	Annual budget of solar PV investor [$]
AF	Annualization factor
B	Zonal transmission matrix [p.u.]
c_0	Confidence level
Cap^{Ex}	Existing generation capacity [MW]
CC	Capital cost [$/kW]
CF	Capacity factor [%]
CF^{Min}	Minimum capacity factor for existing sources [%]
CN	Annual energy conservation target [GWh/year]
DB	Initial number of years of zero investment [years]
DF	Discount Factor
ED	Energy demand [MWh]

Em	Emission per unit energy generation [kg of $eq\text{CO}_2$/MWh]
g	Gestation period [years]
ir	Inflation rate [%]
L	Number of equality constraints
LF	Transmission loss factor [%]
LT	Life-time of solar PV units [years]
LbC	Labour cost [$/kW]
LdC	Land cost [$/kW]
M	Number of inequality constraints
m_J	Number of non-zero active inequality constraints
N	Years of study horizon [years]
N_1	Period of new installations [years]
n	Number of variables
OM	Operation and maintenance (O&M) cost [$/kWh]
OMF	Fixed O&M cost [$/kW]
OMV	Variable O&M cost [$/MWh]
PD	Peak power demand [MW]
PDE	Effective peak power demand [MW]
PT^{Max}	maximum power transfer between zones [MW]
Q	Number of binary variables for technologies
TBG	Total budget of solar PV investor [$]
TC	Transportation cost [$/kW]
UC	Equipment cost [$/kW]
Z	Number of transmission zones
α	Discount rate [%]
α_{irr}	Internal rate of return [%]
β	Fuel prices [$/MWh]
Δt_b	Time duration of load blocks [hours]
μ	Mean value of a data set
ν^{MP}	Market price of electrical energy [$/MWh]

ν^{RP}	Regulated price of electrical energy [$/MWh]
ϕ	Payback period [years]
ρ^{Ex}	Incentive rates for existing capacities [$/MWh]
ψ	Minimum power generation at all time [%]
σ	Standard deviation of a data set
θ	Capital recovery factor
ζ	Emission penalty [$ / ton of $eq\mathrm{CO}_2$]
ϑ_s	Unit size of new capacity additions [MW]
ϖ	Target penetration level of *s8* technologies [%]
Γ	Zonal capacity addition potentials [MW]
Υ	Annual energy generation potentials [MWh]

Variables

C	Sum of O&M, fuel and installation costs [$]
Cap^{New}	New capacities installed over the plan horizon [MW]
Cap	Total capacities, both existing and new [MW]
CFL	Fuel costs [$]
CI	Installation costs of new capacity additions [$]
COM	O&M costs [$]
CST	Total project cost [$]
DR	Demand reduction [MW]
E	Energy generation [MWh]
EC	Emission cost [$]
ECP	Incentive payments for energy conservation [$]
ET	Energy transfer between zones [MWh]
NC	New capacity additions (integer) [MW]
O	Output of finite difference approach
PC	Project cost [$]
P	Power generated [MW]

PT	Power transfer across zones [MW]
R	Payment from CPA to gencos using ν or ρ [$]
REV	Project revenue [$]
VaR	Value at Risk [$]
W	Binary variables
x	Vector of variables
x_1, x_2, y	Individual variables
γ	Lagrange multiplier for inequality constraints
δ	Bus angle [rad]
λ	Lagrange multiplier for equality constraints
ξ	Sensitivity index
ρ^{New}	Incentives for new RES based electrical energy generation [$/MWh]
Ω	NPV of cash flow [$]

Chapter 1

Introduction

1.1 Motivation

Traditional fossil fuel based power generation facilities contribute significantly to climatic concerns by emitting substantial amount of greenhouse gases, particularly CO_2. The resulting environmental degradation is prompting the electric power industry to search for sustainable solutions. Hence, considering the ever increasing demand for electricity, entities responsible for generation, transmission and distribution of electrical energy, are facing a difficult task in selecting new generation technologies to supply the growing energy demand, while reducing the carbon emission levels.

The power industry realized in the last decade that the introduction of relatively low carbon emitting energy sources in the generation portfolio, coupled with a reduction in energy consumption, is the best solution to meet the climate challenge while addressing the perennial energy challenge. Thus, the impact of energy demand and generation sources on emissions can be evaluated based on the following empirical relation quantifying total CO_2 emission for a given population PP of any jurisdiction [1]:

$$CO_2 = PP \times (E/PP) \times (CO_2/E) \tag{1.1}$$

where *E/PP* is the per capita energy consumption, and CO_2/E is the emission per unit energy generation.

Electricity generated from renewable energy sources (RES), particularly sun and wind, are attractive since they are non-polluting and freely available. However, because of their high capital cost, these are not the preferred options for private investors who seek to maximize their profit, as these projects do not accrue acceptable levels of rate of return. Hence, in order to encourage investments in capital intensive RES-based projects, there is a need to compensate the investors so as to render these projects financially feasible. This is achieved through various financial instruments, such as the following [2]:

- *Enhanced Feed-in-Tariff (FIT)*: This is an explicit monetary reward for producing electricity using RES, paid at a rate per kWh somewhat higher than the retail electricity rate.
- *Capital Subsidies*: These are direct financial subsidies aimed at tackling the up-front cost barrier, either for specific equipment or total installed RES system cost.
- *Green Electricity Certificates*: These allow customers to purchase electricity based on RES from the electricity authority, usually at a premium price.
- *Renewable Portfolio Standards (RPS)*: These are mandated requirements that the electricity utility (often the electricity retailer) includes a portion of renewable energy in its electricity supply.

Of the RES technologies, solar photovoltaic (PV) based generation capacity has achieved a global average yearly growth rate in excess of 50% in the last decade [3], making it one of the fastest growing at present. The global capacity additions grew from 7.2 GW in 2009 to more than 25 GW in both 2011 and 2012 [4], for a total installed capacity of nearly 96.6 GW, with a capability of producing around 150 TWh of electrical energy every year. The cumulative global installed solar PV capacity, as presented in the International Energy Agency's (IEA) PV Power Systems (PVPS) program survey report [4], is shown in Figure 1.1. The cumulative installed solar PV capacity in Canada, as of December 2012, in off-grid domestic/non-domestic and grid-connected centralized/distributed sectors is shown in Figure 1.2 [5].

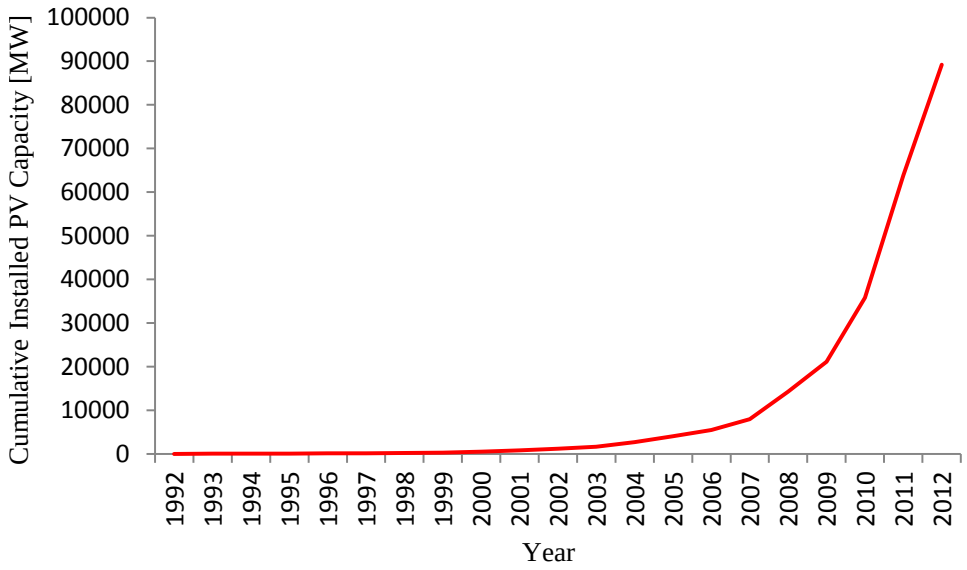

Figure 1.1: Global cumulative installed solar PV capacity, as per IEA-PVPS [4].

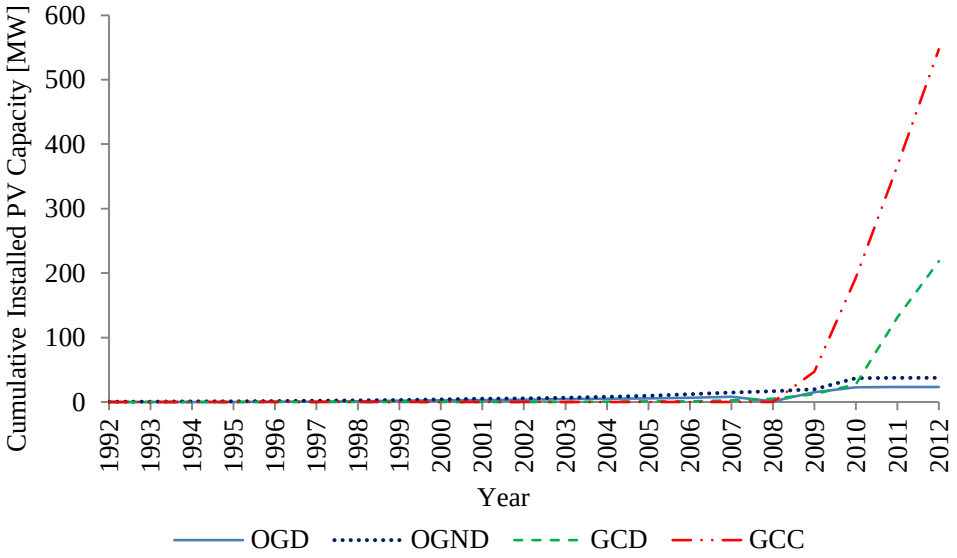

Figure 1.2: Cumulative installed solar PV capacity in Canada (OGD: Off grid domestic; OGND: Off grid non-domestic; GCD: Grid connected distributed; GCC: Grid connected centralized) [5].

The levelized cost of electricity from solar PV has decreased by more than 55% in the most competitive solar PV investment markets (from being over 300 $/MWh in 2010 to less than 150

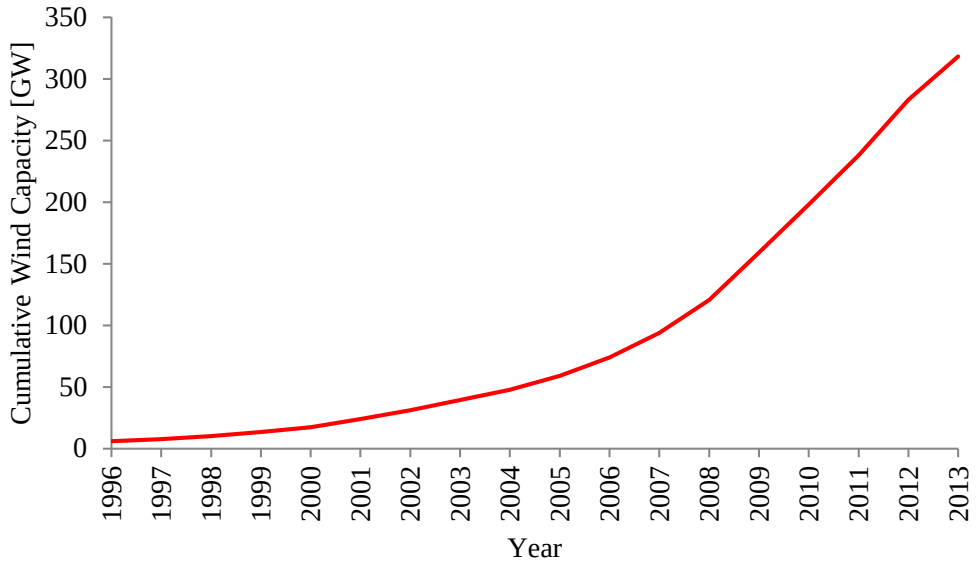

Figure 1.3: Global cumulative installed wind capacity [8].

$/MWh in 2012) [6]. This reduction in cost can be attributed to the declining cost of technology from innovations in design and manufacture of solar cells. The IEA-PVPS survey reports that solar PV module prices have decreased by more than 60% in the last 10 years [4]. This reduction in price renders solar PV technology more acceptable to RES investors, and thus has served as the primary motivating factor for the development and growth of this industry.

In the case of wind energy, as reported by the World Wind Energy Association (WWEA), the global installed capacity reached 318 GW in 2013 for 100 jurisdictions, with the ability to supply almost 3.5% of the world's electricity demand [7]. The cumulative installation of wind capacity, as per WWEA, is shown in Figure 1.3, which depicts a growth of more than 700% in the last decade [8]. In 1993, Canada's first commercial windfarm was installed in Alberta (Cowley Ridge) [9], and the present installed capacity, as of Dec. 2013, is 7.8 GW. This represents 3% of the country's electricity demand, and places it as the ninth largest market for wind energy in the world with a 2.5% share of global installed capacity. In 2013 alone, about 1.6 GW of wind capacity was installed in Canada, which represents a global share of 4.5%, or the fifth largest, of new capacity additions in the world [8]. The province of Ontario leads Canada with almost 2.5 GW of installed wind capacity, which is more than 30% of the country's total wind

installations [10].

Worldwide RES based cumulative capacity has increased by 8.5% to reach 1500 GW in Dec. 2012 [11], where about one-third of it is non-hydro based, e.g., solar, wind, bio, geothermal, ocean. Bio-based power generation achieved a growth of 12% to reach an annual energy production capacity of 350 TWh globally, with a capacity of about 83 GW and an annual consumption of more than 22 million tonnes of wood pellets. Geothermal, on the other hand, has attained an annual energy production level of 223 TWh, of which one-third is electricity generation from 11.7 GW of total plant capacity; the rest is delivered as direct heat. Finally, energy from the oceans, mostly tidal, remained around 530 MW of installed capacity, while hydro power installed capacity increased by 3% to about 1000 GW, generating near 4000 TWh of electricity.

This upsurge in investments in renewable projects, particularly solar and wind, calls for research on analyzing their techno-economic feasibility. Of particular interest is the case of Ontario, Canada, where investments in RES capacities have been accorded high incentives through the FIT and micro-FIT programs [12]. An investment plan on renewable generation projects is required to maximize the investors' profit by providing the optimal sizing, siting, and timing of new installations. Subsequently, it is necessary to analyze and examine the sensitivity of investors' profit to various plan parameters as well as the investment risks associated with the projects.

Most jurisdictions that have initiated or are going to initiate RES support mechanisms are either presently offering or planning to offer FIT for RES projects [11]. The province of Ontario, Canada, has initiated a FIT program [12], which is North America's first comprehensive guaranteed pricing structure for electricity production from RES [13]. The program targets small, medium and large renewable energy projects generating more than 10 kW of electricity. A subset of the FIT program, referred to as the micro-FIT Program, targets very small renewable energy projects generating 10 kW of electricity or less, such as home or small business installations. Prices paid for renewable energy generation under FIT and micro-FIT programs vary by energy source [12]. Under the program, RES projects enter into a 20 year contract to receive a fixed price for the electricity they generate, as detailed in Table 1.1 [12]. The FIT incentives have successfully driven RES investments in Ontario.

Table 1.1: FIT rates for renewables, other than hydro, in Ontario, Canada [12].

Type of Application	Installation Size (in 2009)	Contract Price [¢/kWh]		Revised Size (in 2012)
		Established in 2009	Revised in 2012	
Rooftop mounted solar PV	≤ 10 kW	80.2	54.9	≤ 10 kW
	10 – 250 kW	71.3	54.8	10 – 100 kW
	250 – 500 kW	63.5	53.9	100 – 500 kW
	> 500 kW	53.9	48.7	> 500 kW
Ground mounted solar PV	≤ 10 kW	64.2	44.5	≤ 10 kW
	> 10 kW (Revised in 2010) 10 kW – 10 MW	44.3	38.8	10 – 500 kW
			35.0	500 kW – 5 MW
			34.7	> 5 MW
Onshore wind	Any size	13.5	11.5	Any size
Offshore wind		19.0		
Renewable biomass	≤ 10 MW	13.8		≤ 10 MW
	> 10 MW	13.0		> 10 MW

The FIT scheme has been reported to be the most efficient financial instrument in use today [14], [15], that is effectively promoting RES based electricity generation. It is being utilized in nearly 100 jurisdictions (as of 2012) to promote RES integration [11], with varying degrees of success. It has been observed in recent years that in some jurisdictions, either the initial FIT rates offered were reduced or the scheme was terminated within a few years of its introduction (Tables 1.1 and 1.2). This is mainly because of the extensively high initial FIT rates, which attracted significant RES investment and development, but had a negative impact on electricity prices [19], [20], [21].

Similar to the FIT scheme for investors, local distribution companies (LDC) or DISCOs also need to be encouraged to adapt energy conservation measures through suitable incentive schemes, since the LDCs are, for obvious reasons, more inclined to sell energy than reduce their consumption. Thus, there is a need to design suitable incentives for RES integration and energy conservation, since the design of these incentives is usually driven more by the socio-political factors than techno-economic criteria. Therefore, it is necessary to develop a comprehensive

Table 1.2: Timeline of FIT implementation and reduction/termination in some jurisdictions.

Jurisdiction	FIT Implemented	FIT Reduced	FIT Terminated
Australian Capital Territory [16]	March 2009	July 2013	–
New South Wales, Australia [16]	October 2010	–	December 2011
Queensland, Australia [16]	July 2008	June 2012	July 2014
South Australia [16]	August 2010	September 2011	September 2013
Victoria, Australia [16]	November 2009	January 2013	–
Ontario, Canada [12]	February 2009	2012	–
Spain [17]	February 2007	–	January 2012
United Kingdom [18]	April 2010	August 2011	–

and generic mathematical modeling approach to design the incentives for renewable integration and energy conservation simultaneously, based on techno-economic reasoning used in traditional integrated planning procedures.

1.2 Literature Review

This section presents a critical review of the research reported in the area of generation expansion planning (GEP) considering RES and energy conservation.

1.2.1 Power System Planning

Deterministic approaches, with scenario analysis, have generally been used in power system planning studies in the past [22], [23], [24]. The GEP problem are essentially of linear integer programming type, and traditionally solved using linear, dynamic, and integer programming techniques. Research literature pertaining to modifications and improvements to the traditional GEP model and their solution methodologies have been reviewed in [25], where the application of artificial neural network, analytic hierarchy process (AHP), network flow theory, decomposition techniques, and heuristic optimization techniques, particularly genetic algorithm (GA) and

simulated annealing, to the GEP problem is discussed.

A dynamic programming based approach to long-term planning of power systems is presented in [26] considering uncertainty. The paper suggests a flexible decision-making methodology, where future investment decisions are based on the latest estimates of uncertain parameters. However, the work considers only demand uncertainties, while uncertainties in cost estimates, generation availabilities, etc., are neglected.

In [27], the effect of optimal spot pricing on GEP is examined using an integrated planning framework and socially optimal investment conditions are derived. Optimal spot price forecasts are integrated with direct load control and central dispatch, which produces socially acceptable investment decisions for independent profit maximizing investors. It is suggested that spot pricing can dampen the impact of load and price forecast uncertainties on the GEP.

Reference [28] examines generation investment decisions under time-of-use (TOU) rates, and their relationship to power system planning for an electric utility. Using a non-linear dynamic optimization model, considering social welfare maximization, the optimal capacity additions in base and peaking plants and the optimal TOU pricing structure are determined. However, investor-owned generation is not considered in this work, and thus the effect of a given TOU rate on the investor's profit cannot be analyzed.

Reference [29] assesses the impact of the deviation from least-cost GEP philosophy, resulting from the restructuring of the power industry and the presence of GENCOs, on long-term planning strategy. The work examines the effect this deviation has on electricity prices and suggests trade-off methods for system planners, as it is argued that the investment decisions that are even non-optimal from the planner's point of view may need to be considered.

In [30], a modified GA is presented to solve the least-cost GEP problem. The modified GA incorporates a stochastic crossover technique and an artificial initial population scheme to achieve a faster search mechanism. It is noted that the modified GA achieves a faster execution time than the simple GA and achieves a lower cost solution. However, the main shortcoming of this paper is that the developed model is only applied to test systems, and thus implementation on real power systems needs to be investigated.

Reference [31] presents a planning-cum-production simulation model that determines the

optimal generation mix including distributed resources (DR), transmission upgradation, and investments in demand side management (DSM), while evaluating all central and local investments simultaneously. The model is developed as a coordination of three optimization models: a local area planning model that determinies DR and DSM, an investment model that looks after centralized generation and transmission investments, and a system operation model based on DC load flow with stochastic load and generator availability.

A multi-period, multi-objective, GEP model that minimizes system cost, environmental impact and incorporates risk of fuel price fluctuations is presented in [32]. The model is implemented on the Mexican power system and solved using multi-criteria programming in the first phase to determine a set of non-dominated solutions, and ranked using AHP in the second phase to determine the best solution. However, the best outcome would depend on the decision maker's preference scale of the model objectives, and may result in a non-optimal or socially unacceptable final GEP solution.

A security constrained multi-GENCO GEP model is presented in [33], which includes locational marginal prices (LMP), transmission security, and a capacity payment from the regulator as an incentive to GENCOs for adding new units. The model is based on an iterative framework that combines inter-GENCO competition, simulated by LMP signals derived from an optimal power flow (OPF), and the GENCO-planner coordination, simulated by security signals. The main shortcoming of this paper is that the model is implemented only on test systems and its performance on a real power system needs to be investigated.

An analytical approach, combining conceptual elements of classical capacity planning models and Mean-Variance Portfolio (MVP) theory, is presented in [34], to derive the efficient portfolio structure comprising an arbitrary number of plant technologies, given uncertain fuel prices. A static optimization model is presented to capture the fuel price risks in an MVP framework, where the optimality conditions are derived from a societal point of view. However, no comparison of welfare optimum, investor optimum or market equilibrium is considered in this work. Furthermore, although variance is used as a risk measure, a comparison with other risk indices, such as, lower partial moments or value-at-risk, would be interesting to analyze.

The Ontario Power Authority (OPA) presented an Integrated Power System Plan (IPSP) in

2007 [35]. The IPSP is designed to achieve Ontario's energy goals, such as conservation, phase-out of coal-fired generation, renewable integration, and realization of the smart grid. An integrated planning criterion is applied to prioritize conservation and supply resources, and develop the sequence of installation of resources to determine necessary transmission enhancements. This document is used in this thesis to develop the Ontario system models used in all examples presented throughout this work.

The shortcomings identified in the literature on GEP with RES are, in particular, the lack of real system applications of GEP with proper modeling of RES. Hence, these issues are addressed in the thesis by implementing the proposed GEP model on a realistic model of the power system of the province of Ontario, Canada, with RES technologies modelled appropriately in the context of GEP.

1.2.2 System Planning from Investor's Perspective

In [36], a generation investment planning problem is formulated for a decentralized and profit-maximizing investor, operating in a competitive market. The optimization model analyzes the power plant profitability and optimal timing of new investments under different market designs. However, the model considers a single plant only and assumes that the capacity and location of the plant are given.

In [37], the socio-economic effects, such as social cost, pollution, and investor's return from Ontario's standard offer program (SOP), and an emission cap and tax scheme are examined for renewable energy projects, using an appropriate investment planning model. Various scenarios are considered, such as minimizing social cost, guaranteeing a minimum acceptable rate of return (MARR) to investors, implementing a distributed generation (DG) penetration limit, LDC purchasing of all the energy produced by DGs, and LDC paying for the emission tax. The work observes that the considered SOP prices are quite high, resulting in an internal rate of return (IRR) for investors significantly higher than their MARR. It also reports that the emission taxes are rendered ineffective in reducing pollution when the LDC purchases all the energy produced by the DGs, and the only benefit of implementing these taxes are the influence they may have

in future capital investments. The paper, however, models the wind and solar PV generations as dispatchable sources and does not consider any capacity limits for the feeders and substations.

A coordination framework is proposed in [38], which introduces an approval process for investor-owned DG proposals submitted to the LDC. The framework consists of five modules, one pertaining to investors and the rest to the LDC's DG coordination algorithm. The module for the investors maximizes their individual profits, while deriving the site, size, and time of DG investments. It is demonstrated that the implementation of this framework enables more DG selections, which in turn reduces emission and power losses and improves the voltage profile. However, this work does not consider more than one DG to be installed at a bus, and approves any DG proposal directly whose production is less than the bus demand.

A sensitivity analysis of the IRR of a solar PV investment project with respect to economic factors, such as annual loan interest, normalized initial investment, unit price of electricity from solar PV, etc., are presented in [39]. The project is implemented in three economic scenarios, closely representing the PV markets of Europe, Japan and USA. However, the parameter perturbation approach employed in this work for sensitivity analysis is highly cumbersome and computationally expensive, and there is a need to explore other methods.

Reference [40] proposes an investment planning model to determine the optimal investments in large-scale solar PV projects, from an investor's perspective. The model determines the optimal siting, sizing and timing of investments in solar PV projects, while maximizing the Net Present Value (NPV) of profit for the investor. However, the work considers solar PV generation as a dispatchable source. Moreover, the sensitivity analysis presented in this work to assess the sensitivities of investor's profit to model parameters is cumbersome and computationally expensive.

From the previous discussion, identified shortcomings in the current literature studies on investor planning are the lack of realistic modeling of RES, the lack of consideration of investor's perspective, and the complexity of the risk analysis procedures proposed so far. Thus, this thesis addresses these concerns by modeling the non-dispatchable RES appropriately from both the investor's and central planner's perspective, and the use of a Duality Theory (DT) based parametric sensitivity analysis procedure to simplify the computation of risk indices.

1.2.3 Centralized System Planning considering Renewable Energy Integration

The traditional planning process begins with the forecasting of energy demand and an associated forecast of peak load growth. Renewable generation is included as available during system operation, and the output from committed thermal units is reduced to accommodate this RES energy [41], [42], [43]. The end result is a sub-optimal system planning and operation, because the thermal units are operated below their economic dispatch, resulting in lower efficiency, higher emissions, and higher operating costs.

The emerging practice is to include RES early in the planning process and consider them within the energy growth forecast models, viewing them as negative loads, e.g. [44]. The planning process is thus based on the net load, which is the forecasted peak load less the renewable generation penetration from existing and planned new installations. This renewable generation is obtained from historical renewable resource data. However, a new dimension has been introduced into GEP in [45], with the need for explicitly evaluating generation flexibility, vis-á-vis the variability of net load, on the time-scale of system load following operations. Increased penetration of intermittent renewable generation renders the operational flexibility of the generation portfolio strategically important. This evaluation of flexibility is an important step, as it has a direct impact on the system operating costs.

A flexible capacity planning tool is developed in [46], which determines the most economical mix of capacities from renewable generation units, particularly solar, as well as storage capacities, while meeting reliability requirements against fluctuating demand profiles and weather conditions. The capacity planning tool is based on hybrid (system dynamic model and agent-based model) simulation and a meta-heuristic based optimization algorithm. The main concerns with this work are that only a single-year snapshot plan is obtained, and dynamic capacity addition plans are not discussed. Furthermore, the planning model only considers the cost aspects and ignores the revenues.

In [47], a stochastic chance-constrained planning model to incorporate large-scale grid-connected solar PV power stations is proposed, where solar irradiance is modeled as a stochastic time series. The planning model can directly obtain the peak capacity limits of the solar PV generating

systems. However, the work concentrates on the determination of optimal capacity of solar PV without any consideration to PV cost components.

Reference [48] examines the impact of wind power generation on system operation cost, reliability and utility expansion plans. The capacity factors of wind generation are computed for two configurations: the individual wind farm model and the dispersed wind power system model. However, the transmission system is not considered; thus, the studies on the impact of wind power integration on reliability and utility expansion plans are inconclusive.

In [49], an optimization method is proposed for the optimal expansion planning of fast-response generating capacity (e.g., gas-fired units) in order to accommodate the uncertainty of wind generation. The study utilizes a mixed integer programming based, security constrained unit commitment for analyzing operational and reliability issues. The model is implemented on a six-bus test system only, and consequently its performance on a real test system is not verified.

In [50], the impact of emission mitigation and incentive schemes, such as FITs, RES quota, emission trade, and carbon tax on GEP is studied from a GENCO's perspective. The traditional model for investor's profit maximizing capacity expansion plan is augmented by introducing constraints pertaining to RES quotas, emission limits, FITs, and cash flows resulting from green certificate trading. The uncertainty associated with RES is taken care of by a suitable capacity factor, demonstrating that there is a need for proper incentive mechanisms to render RES economically sustainable. However, the model, implemented for a hypothetical GENCO in the Italian electricity market, does not consider a transmission system and its corresponding power flow bounds.

The issue of uncertainties in GEP with integration of RES (particularly wind) is discussed in [51], where an offline flexibility index is proposed to evaluate the variability of wind generation and examine its effect on GEP and market operation. However, a deterministic approach, similar to unit commitment, is used in this work to consider the uncertainties of wind generation, which is otherwise inherently stochastic.

Reference [52] presents a bi-level optimization approach that designs efficient incentive policies to encourage investments in RES based generation. The optimization model's effectiveness is demonstrated by the incentives' capability to achieve the target RPS. The lower level of the

model is the traditional central planner making decisions on capacity expansion based on cost minimization, while the upper level involves the policy maker designing RES incentives that influences the lower level planner's decision.

The research literature has addressed the GEP problem extensively, as discussed in [53], tackling the inherent uncertainties of integrating non-dispatchable sources (e.g., wind and solar) as well as developing multi-level, multi-criteria models to consider the conflicting objectives of profit maximization of the investor and system cost minimization of the planner. However, little work has been reported addressing the design of optimal incentives to attract investment in RES by GENCOs, which is one of the objectives of this thesis.

1.2.4 Integrated Resource Planning

The traditional power system planning problem considers demand side activities as external factors, i.e., parameters, to the planning model, and renewable generation is incorporated at the operational stage. Hence, to achieve the objectives of incentive design for RES integration and energy conservation, the classical Integrated Resource Planning (IRP) philosophy needs to be re-visited.

IRP takes into account the supply-side and demand-side resources as a whole and uses them in an efficient, economic, and rational way, so as to reduce the investment in new capacity installations and operating expenses while providing adequate energy supply at lowest cost. The resource choices for IRP are conventional and renewable power plants, owned by either large utilities or independent power producers, improvements in the transmission and distribution systems, and DSM [54]. The IRP philosophy was a new approach in the 1990s, evolving alongside electricity industry deregulation, and faced several implementational issues at its developmental stage [55]. The revenue loss of the utilities due to reduced demand, and their failure to consider environmental and social factors were some of the barriers. Thus, it is suggested in [55] that proper financial incentives to LDCs could improve the delivery of DSM services, and environmental and social factors need be incorporated in the IRP.

A multi-objective framework, using compromise programming technique, to simultaneously integrate various DSM options in electric utilities' IRP is presented in [56]. The paper char-

acterizes the DSM options as supply side resources (e.g., efficient lighting as non-dispatchable source, direct load control programmes as thermal generating units) and examines their interaction among themselves along with their simultaneous vis-à-vis sequential integration in the IRP.

Restructuring of the electricity industry and the resulting competitive environment influenced modifications in the classical IRP strategy. From cost minimization and system reliability maximization approach, IRP evolved to a stage where capacity additions are considered as investments toward profitability. Such a modified IRP procedure is proposed in [57], which takes into account the associated uncertainties of production-costing through a segmentation method based, dynamic programming formulation. The work suggests that modified IRP procedures are tailored to match the uniquely specified goals decided by the problem at hand, and a general purpose, universal IRP optimization model does not exist.

A holistic GEP model, based on the classical IRP philosophy, is therefore needed, which is not only able to provide the traditional optimal solution to GEP problems, but is also designed to determine the optimal incentives for both RES integration and energy conservation. Such a model, from the perspective of the central planning authority (CPA) that includes all the economic transactions between itself with GENCOs and LDCs, is developed in this thesis to determine the optimal incentives for the integration of RES, accounting for the investor interests.

1.3 Research Objectives

The main objectives of the research presented in this thesis are as follows:

- Develop an investment planning model for ground-mounted solar PV generation projects in a large inter-connected power system. The planning model, which is from the perspective of a private investor, seeks to determine the optimal size, location, and timing of new solar PV projects while maximizing the investor's profit.
- Apply Duality Theory (DT) based sensitivity techniques to examine the sensitivity of the NPV of investor's profit to changes in parameters of the solar PV investment planning

model. This is used to formulate a novel mathematical relationship to obtain appropriate risk indices for the investment projects.

- Develop a novel holistic GEP model from the perspective of the CPA to determine the optimal incentive rates for RES integration and energy conservation. The proposed GEP model is envisaged to achieve targeted penetration level of RES technologies over a certain time frame, as well as a targeted energy conservation and corresponding demand reduction. In addition, the new model is also designed to perform the traditional task of a GEP framework, i.e., to determine the optimal siting, sizing, timing and technology of new installations. The investor's interests are also represented in this model to be able to obtain adequate incentives.

All the research presented in the thesis considers the Ontario power system as the test case. Hence, a comprehensive modeling of the Ontario grid has been carried out based on real system data.

1.4 Outline of the Thesis

The rest of the thesis is structured as follows: Chapter 2 discusses the background pertaining to the methodologies and techniques used to carry out the presented research. Thus, power system generation planning methodologies from both the CPA's and investor's perspective, along with the determination of sensitivity indices using the DT-based method, FD approach, and Monte Carlo simulations, are presented. This chapter also provides a brief description of optimization problems with appropriate linearization techniques, as well as risk assessment indices.

In Chapter 3, a DT-based method of computing sensitivity indices for a solar PV investment planning model is discussed, and the results of applying this technique to an Ontario planning model are presented and compared with those computed using an FD approach and Monte Carlo simulations. A novel method for computing investor's risk indices for solar PV projects using the DT-based sensitivity indices and its application to the Ontario planning model is also presented.

In Chapter 4, a new holistic GEP model which determines the optimal incentives required to achieve a targeted penetration level of RES and energy conservation over the plan horizon is presented. The model is implemented and demonstrated for Ontario's grid, discussing various scenarios of RES penetration target variations, conservation target variations, fossil-fuel price variations, and others.

Finally, Chapter 5 presents a summary of the research and its major contributions, with brief outline of possible future research directions in this area.

Chapter 2

Background Review

A review of the background topics pertaining to the research presented in this thesis and the tools used for analysis are presented in this chapter. The GEP problem is discussed from both the central planner's and investor's perspective. Sensitivity analysis procedures based on DT, Monte Carlo simulations and FD methods are explained, and a review of risk assessment measures, such as Pay-back-period (PBP), IRR, Value-at-Risk (VaR), are also presented. Finally, Mixed Integer Non-Linear Programing (MINLP) and Mixed Integer Linear Programing (MILP) problems are briefly discussed, describing a linearization technique that is employed here to transform MINLP into MILP problems.

2.1 Traditional GEP

The traditional power system planning problem seeks a least-cost strategy for long-term expansion planning of the generation (GEP), transmission and distribution systems, in order to adequately meet the load forecast under a set of technical and economic constraints [58]. A generic GEP framework is presented in Figure 2.1. The initial step is to choose a planning horizon, with the total budget allocation for executing the plan, with annual budget constraints, and existing related policies framing the plan being usually specified.

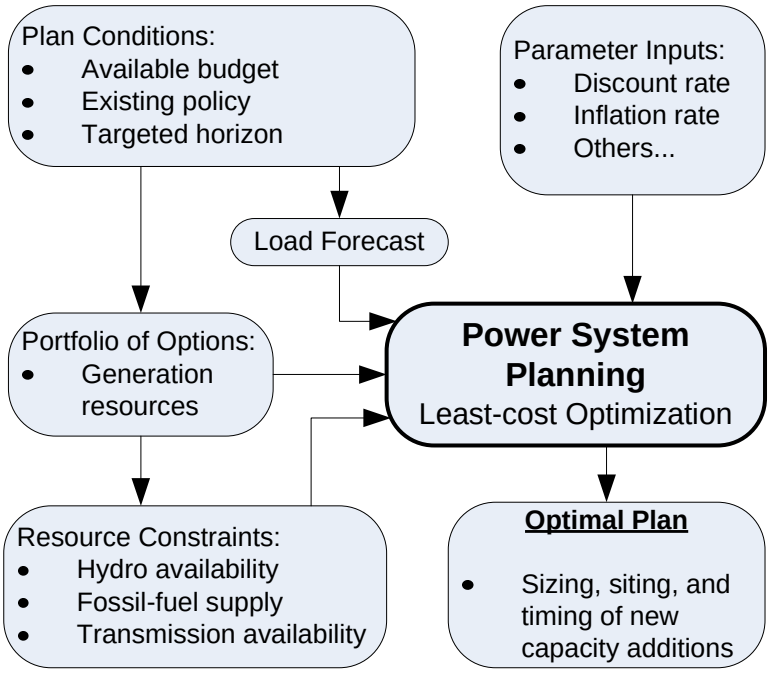

Figure 2.1: Generic framework of traditional GEP.

The next step in the GEP exercise is determining the load forecast over the plan period, which is effectively the main driving parameter. Since inaccurate load forecast may lead to capacity shortages or surplus, which are both undesirable and non-optimal, it is the general practice to create long-term load forecast for three scenarios: base, high and low load growths, where the base case is selected as the basis for the GEP, while the other two define the possible variability of the plan outcome. The load forecast is updated continuously, sometimes on an annual basis, in order to adjust, if possible, the outcome of the initial GEP exercise.

Load forecast is carried out using load duration curves, which are constructed by re-arranging the chronological load curve in descending order of magnitude, as shown in Figure 2.2. A load duration curve determines the number of hours per year when the load is greater or lesser than any particular amount. The load duration curves from previous years provide the past trend of load growth, which, along with the economic growth trends of past years, helps to determine the load forecast. The base, intermediate, and peak load blocks are determined from the approximated load duration curve, as shown in Figure 2.2a, where base load is considered to be present 100%

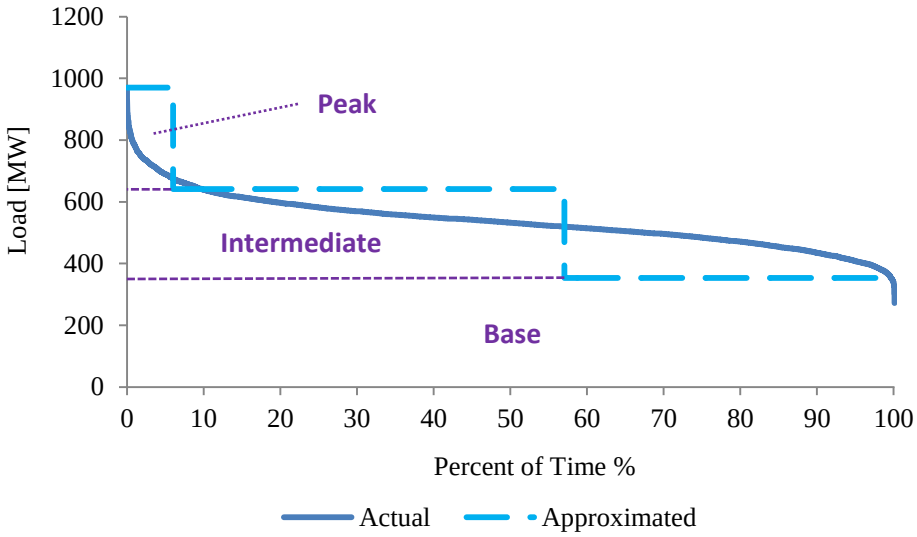

(a) Theoretical concept of base, intermediate, and peak loads.

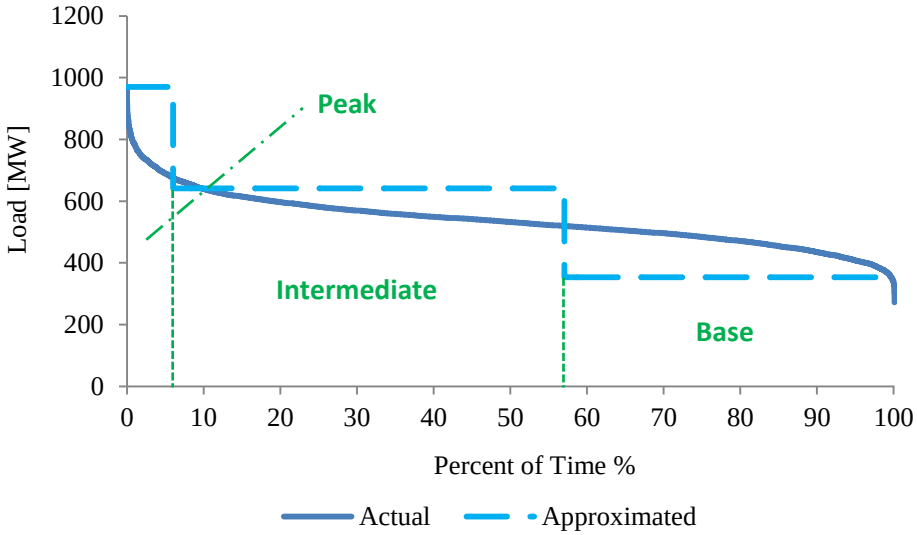

(b) Defining base, intermediate, and peak loads for mathematical modeling.

Figure 2.2: Load duration curve [58].

of time. It is to be noted that, in mathematical models, the load blocks are computed by the time duration of these three load levels, i.e., vertical blocks instead of the horizontal ones [56], as shown in Figure 2.2b. This is done to ensure that the computed power flow, more particularly

energy flow, in a transmission line is unidirectional in each of these base, intermediate, and peak load conditions.

The portfolio of options module in Figure 2.1 include the assessment of supply-side resources, i.e., generation requirements determined primarily from peak demand forecasts [58]. An adequate peak capacity requirement is determined by assuming a minimum generation reserve margin (GRM) beyond the forecasted peak demand [58], [59], so as to ensure high system reliability standards for catering to un-anticipated demand growth, equipment failure, or other unforeseen events. The GRM is defined in [58] as:

$$\text{GRM}(\%) = \frac{\text{Generation capacity} - \text{Peak load}}{\text{Peak load}} \times 100 \tag{2.1}$$

The constraints on resources primarily involve availability of water for existing and potential hydro plants; availability of coal, gas or oil supply linkages for fossil-fuel based power plants; and the transmission availability between new installations and load centers. These constraints, in conjunction with the budgetary and policy conditions, significantly influence plan decisions.

Some other external factors, such as discount rate and inflation rates, are included as parametric inputs to the GEP model. A least-cost optimization is carried out then with inputs from all of the components described earlier, followed by the selected plan's implementation, which is then monitored to make changes in the assumed or forecasted states of the power system.

2.1.1 Central Planner's Perspective

Traditional GEP has been driven by the CPA's perspective. In this context, the GEP takes into account the economic and technical characteristics of existing generation units and resources available for expansion, and also considers the predictable trends of cost variations and technical developments of the available technologies. The economics of GEP primarily include the capital cost, fuel cost, and operation and maintenance (O&M) cost, and the CPA's objective is to minimize the total discounted cost of implementing the plan.

The objective function of the mathematical model for a GEP problem, from the CPA's per-

spective, is the minimization of the total discounted costs, as given by:

$$\text{Min.} \qquad \text{NPV of } CST = \sum_{\text{plan horizon}} CST \;\; DF = \sum_{\text{plan horizon}} (CI + COM + CFL) \;\; DF \tag{2.2}$$

where all variables in this and other equations are defined in the Nomenclature section. The total annual cost CI to install new generation is computed as the product of capital cost, given by CC, and the new capacity of the unit NC, as follows:

$$CI = NC \;\; CC \tag{2.3}$$

The annual O&M cost is generally divided in two components, the annual fixed O&M cost OMF and the annual variable O&M cost OMV, computed using the annual installed capacities Cap and annual energy generation E, respectively, as follows:

$$COM = OMF \;\; Cap + OMV \;\; E \tag{2.4}$$

The CPA, in addition to the above, may have an emissions minimization objective incorporated in the GEP, with emissions being computed as:

$$Total\ Emission = \sum_{\text{plan horizon}} E_m \;\; E \tag{2.5}$$

The primary technical constraints from the CPA's perspective are the traditional, annual energy supply-demand balance, given by:

$$E^{Gen} - E^{Exp} + E^{Imp} = E^{Dem} \tag{2.6}$$

and the annual capacity adequacy constraint, as follows:

$$Cap \geq (1 + b_0)PD \tag{2.7}$$

The total annual energy generated by a power plant can be estimated using an annual average

capacity factor CF of the generator. By definition, the CF of a generator is the ratio of its actual energy output over one year to its potential output if it operated at rated capacity the entire time, as follows:

$$CF = \frac{\text{Annual energy generation in MWh}}{\text{Name plate or rated capacity in MW} \times 8760 \text{ hours}} \tag{2.8}$$

2.1.2 Investor's Perspective

Modern investment evaluation techniques, such as cost-benefit analysis, NPV of profit, IRR, etc., are generally employed to evaluate an investment project [60]. The cost-benefit analysis looks at the project cost components and project revenue generation over the plan horizon. For an investor's profit maximization model, the NPV of profit is computed as:

$$\text{NPV of Profit} = \text{NPV of } REV - \text{NPV of } CST \tag{2.9}$$

where REV is the annual revenue realized from selling energy generated at market-price ν, and RES incentive ρ based capacities, i.e.:

$$REV = \nu\, E^{MP} + \rho\, E^{ICV} \tag{2.10}$$

and CST is defined in (2.2).

The most important project cost component, from an investor's perspective, is the capital cost CC, which is the cost of installing and commissioning new units. It incorporates the cost of equipment UC, the cost of labour LbC to install and commission, the cost of the land LdC required to place the unit, and the cost TC of transporting the unit from its point of purchase to the site where it is installed. All these cost components are computed on the basis of the dollar amount required to install a unit with generation capacity 1 kW, i.e., all these costs have a unit of \$/kW. Mathematically, the CC is represented as follows:

$$CC = UC + LbC + LdC + TC \tag{2.11}$$

The following constraint related to the annual budget ABG can be included, restricting the

amount of money available per year to install new capacities:

$$CI \leq ABG \tag{2.12}$$

and a limit on total available budget TBG is also imposed, as follows:

$$\text{NPV of } CST \leq TBG \tag{2.13}$$

2.2 Sensitivity Analysis

2.2.1 Duality Theory (DT) Method

Sensitivity analysis is of great importance in any mathematical modeling, especially economic modeling. A local sensitivity analysis based on DT is proposed in [61] and [62], which is a perturbation based approach to compute the sensitivities in optimization based models. These sensitivity expressions use the dual variables (Lagrangian multipliers) at the optimal solution and the properties of the Karush-Kuhn-Tucker (KKT) optimality conditions. The DT approach is an alternative to the Monte Carlo simulation [63] and Finite Difference (FD) approaches [64], and it has the ability to determine all the parameter sensitivities simultaneously. A description of the DT based method for obtaining all local sensitivities is discussed next based on [61]. Let consider a primal Non-Linear Programming (NLP) problem as follows:

$$\text{Min.} \quad z = f(x, a) \tag{2.14}$$

$$\text{s.t.} \quad h(x, a) = b \tag{2.15}$$

$$g(x, a) \leq c \tag{2.16}$$

where $h(x,a) = [h_1(x,a), \cdots, h_L(x,a)]^T$ and $g(x,a) = [g_1(x,a), \cdots, g_M(x,a)]^T$. This primal problem has an associated dual problem which can be defined as follows:

$$\begin{aligned} \text{Max.} \quad & z_D = Inf_x \left[\mathcal{L}(x, \lambda, \gamma, a, b, c)\right] \\ \text{s.t.} \quad & \gamma \geq 0 \end{aligned} \tag{2.17}$$

where

$$\mathcal{L}(x, \lambda, \gamma, a, b, c) = f(x,a) + \lambda^T \left[h(x,a) - b\right] + \gamma^T \left[g(x,a) - c\right] \tag{2.18}$$

is the Lagrangian function associated with the primal problem. The primal and dual problems are solved by applying the KKT first order optimality conditions as follows:

$$\nabla_x f(x^*, a) + \lambda^{*T} \nabla_x h(x^*, a) + \gamma^{*T} \nabla_x g(x^*, a) = 0 \tag{2.19}$$

$$h(x^*, a) = b \tag{2.20}$$

$$g(x^*, a) \leq c \tag{2.21}$$

$$\gamma^{*T} \left[g(x^*, a) - c\right] = 0 \tag{2.22}$$

$$\gamma^* \geq 0 \tag{2.23}$$

where x^* and (λ^*, γ^*) are the primal and dual optimal solutions, respectively. Conditions (2.20) and (2.21) are the primal feasibility conditions, while the complementary slackness conditions, referred to as the dual feasibility conditions, are given by (2.22) and (2.23).

In order to simplify the DT method mathematical derivation, the above mentioned parameters a, b, and c are assumed to form a set p, i.e., $p = [a\ b\ c]^T$. The DT method allows determining all the sensitivities at once, i.e., the sensitivities of the optimal solution $(x^*, \lambda^*, \gamma^*, z^*)$ to local changes in the parameters p. This is achieved by introducing a small perturbation Δp in p, which results in a shift of the optimal solution Δx. Mathematically, this can be represented by differentiating the objective function (2.14) and the KKT conditions (2.19) – (2.23) as follows:

$$\nabla_x^T f(x^*, p)\, dx + \nabla_p^T f(x^*, p)\, dp - dz = 0 \tag{2.24}$$

$$\left(\nabla_{xx}\, f\,(x^*,p) + \sum_{l=1}^{L} \lambda_l^*\, \nabla_{xx}\, h_l\,(x^*,p) + \sum_{m=1}^{M} \gamma_m^*\, \nabla_{xx}\, g_m\,(x^*,p)\right) dx$$

$$+\left(\nabla_{xp}\, f\,(x^*,p) + \sum_{l=1}^{L} \lambda_l^*\, \nabla_{xp}\, h_l\,(x^*,p) + \sum_{m=1}^{M} \gamma_m^*\, \nabla_{xp}\, g_m\,(x^*,p)\right) dp$$

$$+\nabla_x\, h\,(x^*,p)\;\, d\lambda + \nabla_x\, g\,(x^*,p)\;\, d\gamma = 0_n \tag{2.25}$$

$$\nabla_x^T\, h\,(x^*,p)\;\, dx + \nabla_p^T\, h\,(x^*,p)\, dp = 0_L \tag{2.26}$$

$$\nabla_x^T\, g_m\,(x^*,p)\;\, dx + \nabla_p^T\, g_m\,(x^*,p)\;\, dp = 0 \qquad \forall\ \gamma_m^* \neq 0\ ;\ m \in J \tag{2.27}$$

$$\nabla_x^T\, g_m\,(x^*,p)\;\, dx + \nabla_p^T\, g_m\,(x^*,p)\;\, dp \leq 0 \qquad \forall\ \gamma_m^* = 0\ ;\ m \in J \tag{2.28}$$

$$-\, d\gamma_m \leq 0 \qquad \forall\ \gamma_m^* = 0\ ;\ m \in J \tag{2.29}$$

$$d\gamma_m \left(\nabla_x^T\, g_m\,(x^*,p)\;\, dx + \nabla_p^T\, g_m\,(x^*,p)\;\, dp\right) = 0 \qquad \forall\ \gamma_m^* = 0\ ;\ m \in J \tag{2.30}$$

where J is the set of all indices m for which $g_m\,(x^*,p) = 0$, i.e., only the active inequality constraints are taken into consideration.

Defining the set of all feasible perturbations as:

$$dq = \begin{bmatrix} dx & dp & d\lambda & d\gamma & dz \end{bmatrix}^T \tag{2.31}$$

Equations (2.24) – (2.30) can be written as:

$$Y_1\; dq = \begin{bmatrix} F_x & F_p & 0 & 0 & -1 \\ F_{xx} & F_{xp} & H_x^T & G_x^T & 0 \\ H_x & H_p & 0 & 0 & 0 \\ G_x^1 & G_p^1 & 0 & 0 & 0 \end{bmatrix} \begin{bmatrix} dx \\ dp \\ d\lambda \\ d\gamma \\ dz \end{bmatrix} = 0 \tag{2.32}$$

$$Y_2\ dq = \begin{bmatrix} G_x^0 & G_p^0 & 0 & 0 & 0 \\ 0 & 0 & 0 & -I_{m_J}^0 & 0 \end{bmatrix} \begin{bmatrix} dx \\ dp \\ d\lambda \\ d\gamma \\ dz \end{bmatrix} \leq 0 \tag{2.33}$$

where the sub-matrices of Y_1 and Y_2 are expressed as follows:

$$F_x = \left[\nabla_x^T f(x^*, p)\right]_{(1\times n)} \tag{2.34}$$

$$F_p = \left[\nabla_p^T f(x^*, p)\right]_{(1\times P)} \tag{2.35}$$

$$H_x = \left[\nabla_x^T h(x^*, p)\right]_{(L\times n)} \tag{2.36}$$

$$H_p = \left[\nabla_p^T h(x^*, p)\right]_{(L\times P)} \tag{2.37}$$

$$G_x = \left[\nabla_x^T g(x^*, p)\right]_{(m_J\times n)} \tag{2.38}$$

$$G_p = \left[\nabla_p^T g(x^*, p)\right]_{(m_J\times P)} \tag{2.39}$$

$$F_{xx} = \left[\nabla_{xx}\ f(x^*, p) + \sum_{l=1}^{L} \lambda_l^*\ \nabla_{xx}\ h_l(x^*, p) + \sum_{m=1}^{m_J} \gamma_m^*\ \nabla_{xx}\ g_m(x^*, p)\right]_{(n\times n)} \tag{2.40}$$

$$F_{xp} = \left[\nabla_{xp}\ f(x^*, p) + \sum_{l=1}^{L} \lambda_l^*\ \nabla_{xp}\ h_l(x^*, p) + \sum_{m=1}^{m_J} \gamma_m^*\ \nabla_{xp}\ g_m(x^*, p)\right]_{(n\times P)} \tag{2.41}$$

and G_x^0 and G_p^0 refer to the sub-matrices of G_x and G_p, respectively, associated with the null γ-multipliers of the active constraints; G_x^1 and G_p^1 refer to the sub-matrices of G_x and G_p, respectively, associated with the non-null γ-multipliers of the active constraints; and $-I_{m_J}^0$ is the negative of a unity matrix after removing all rows $m \in J$ for which $\gamma_m^* \neq 0$.

Re-arranging (2.32) – (2.33) to separate the input perturbation parameters dp and the output perturbation variables from the composite perturbation vector dq, one gets:

$$U\ [dx \quad d\lambda \quad d\gamma \quad dz]^T = S\ dp \tag{2.42}$$

$$V\,[dx \quad d\lambda \quad d\gamma \quad dz]^T \leq T\,dp \tag{2.43}$$

where the matrices U, S, V and T are given by:

$$U = \begin{bmatrix} F_x & 0 & 0 & -1 \\ F_{xx} & H_x^T & G_x^T & 0 \\ H_x & 0 & 0 & 0 \\ G_x^1 & 0 & 0 & 0 \end{bmatrix} \tag{2.44}$$

$$S = -\begin{bmatrix} F_p \\ F_{xp} \\ H_p \\ G_p^1 \end{bmatrix} \tag{2.45}$$

$$V = \begin{bmatrix} G_x^0 & 0 & 0 & 0 \\ 0 & 0 & -I_{m_J}^0 & 0 \end{bmatrix} \tag{2.46}$$

$$T = -\begin{bmatrix} G_p^0 \\ 0 \end{bmatrix} \tag{2.47}$$

The optimization solution generally identifies the active and inactive inequality constraints, i.e., non-zero and zero valued Lagrange multipliers respectively, for a non-degenerate regular case. Matrix U in (2.40) is generally invertible as the solution to the optimization problem $(x^*, \lambda^*, \gamma^*, z^*)$ is typically a regular non-degenerate point. If any degenerate constraint, i.e., a zero-valued Lagrange multiplier of an active constraint, is present, this is removed for computational simplicity, as proposed in [65]. If the degenerate constraints are not removed for constructing U, alternative procedures that are more computationally involved are proposed in [61], [62]. For the computation of sensitivity indices, the non-degenerate inequality constraints are also converted to equality constraints [61], thus reducing the matrices U and S to the following form:

$$U = \begin{bmatrix} F_x & 0 & -1 \\ F_{xx} & H_x^T & 0 \\ H_x & 0 & 0 \end{bmatrix} \tag{2.48}$$

$$S = -\begin{bmatrix} F_p \\ F_{xp} \\ H_p \end{bmatrix} \tag{2.49}$$

It is to be noted here that all the non-basic variables are to be eliminated as well, so as to achieve an invertible matrix H_x. Thus, the matrix U becomes invertible and the solution to (2.42) is unique and is given by:

$$[dx \quad d\lambda \quad d\gamma \quad dz]^T = U^{-1} S \; dp \tag{2.50}$$

while (2.43) is satisfied trivially as V does not exist. Hence, replacing the vector dp in (2.48) by a matrix including several vectors (columns) with the corresponding unit directions, the matrix with all derivatives, i.e., the sensitivity indices, is given by:

$$\begin{bmatrix} \frac{dx}{dp} & \frac{d\lambda}{dp} & \frac{d\gamma}{dp} & \frac{dz}{dp} \end{bmatrix}^T = U^{-1} \; S \tag{2.51}$$

2.2.2 Monte Carlo Simulations

A deterministic problem is shown in Figure 2.3a, in which all the information required (input variables u) for a system f is available, and, therefore, all the output variables y can be computed with certainty. For this deterministic problem, if the input variables are probabilistic in nature, i.e., defined by probability density functions (p.d.f.s) with a mean equal to their respective deterministic values, the output variables will also be p.d.f.s, as shown in Figure 2.3b [66].

Uncertain input variables of f that are represented by their p.d.f.s, can be represented as a set

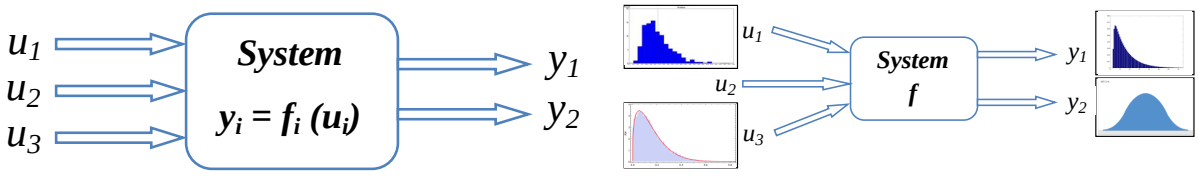

Figure 2.3: (a) Deterministic approach and (b) Monte Carlo simulation [66].

of randomly selected values, generally numbering in thousands, to generate a set of values for each output variable, which in turn define the output p.d.f.s, by applying the deterministic model f to each of these input variable values. This is referred to as the Monte Carlo simulation method, which is useful for simulating a model with uncertainty in the inputs, and thereby can be used to perform sensitivity analysis of the model with respect to its parameters.

For sensitivity analysis, Monte Carlo simulation can be applied to an optimization model on an OAT (One-factor-at-A-Time) basis. Thus, each parameter under consideration as an input (*in*) is assigned a normally distributed p.d.f., since the parameters need to be perturbed symmetrically around their base values in order to obtain unskewed and unbiased sensitivity indices. The latter is due to the fact that in a normally distributed p.d.f. of a parameter, the expected value or mean is the same as the median of the distribution, which allows for a symmetrical variation of the parameter for various standard deviations; additionally, for normally distributed p.d.f., the mode of the variation is also equal to its median, which enables equal perturbation of a parameter around its deterministic value. Therefore, all the parameters in this thesis, are considered to be normally distributed for probabilistic studies with the standard deviation being 1% of its mean value, i.e.,

$$\sigma_{in}^{\%} = 100\left(\frac{\sigma_{in}}{\mu_{in}}\right) \tag{2.52}$$

where μ_{in} is the original value of the parameter. The standard deviation of the resulting output (*out*) can then be computed as a percentage of its mean value, as follows.

$$\sigma_{out}^{\%} = 100\left(\frac{\sigma_{out}}{\mu_{out}}\right) \tag{2.53}$$

Then, the ratio of the standard deviations in percentage of output and input can be considered a sensitivity index computed by the Monte Carlo method, as follows:

$$\xi_{MC}^{\%} = \left(\frac{\sigma_{out}^{\%}}{\sigma_{in}^{\%}}\right) \tag{2.54}$$

Thus, for 1% standard deviation in input parameter, $\xi_{MC}^{\%} = \sigma_{out}^{\%}$.

2.2.3 Finite Difference (FD) Method

The FD approach discussed in [64], is in essence an individual parameter perturbation method. In this approach, each parameter is increased by an $x\%$ (1% in this thesis) of its base value, and the output is computed from the optimization model. The difference between the optimization output with a perturbed parameter (O_{newFD}) and the original output without perturbation (O_{base}) denotes the change in the output for a 1% increase in a given parameter, while other parameter values remain un-altered. This change is the "true" sensitivity index of the system optimization output with respect to the parameter in consideration, i.e.:

$$\xi_{FD} = O_{newFD} - O_{base} \tag{2.55}$$

This sensitivity index can also be represented as a percentage of O_{base} using the following expression:

$$\xi_{FD}^{\%} = 100\left(\frac{O_{newFD} - O_{base}}{O_{base}}\right) \tag{2.56}$$

2.3 Risk Assessment Tools

2.3.1 Investment Assessment [60]

Discounted cash flow techniques, such as the NPV of profit and the IRR, are standard measures for comparative appraisal of long-term investment projects. The NPV of profit from a project is described mathematically as:

$$\Omega = \sum_{t=1}^{N} \frac{REV_t - CST_t}{(1+\alpha)^t} \tag{2.57}$$

A positive NPV indicates that a value is being added to the investment while a negative one signifies loss. A higher value of NPV reflects more return on investment, but this measure fails to compare similar projects with different initial investments. To overcome this downside of NPV analysis, a percentage gain relative to the investment, the IRR, is used as a complement measure to NPV.

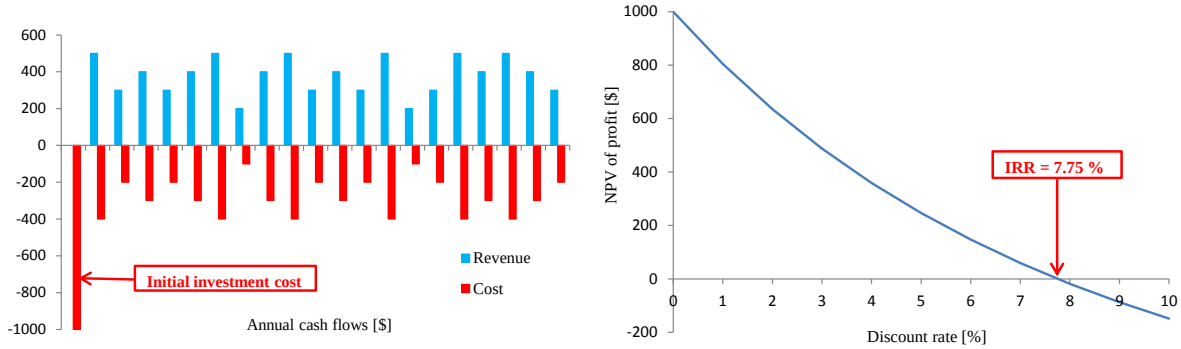

(a) (b)

Figure 2.4: IRR example: (a) annual cash flow and (b) NPV of profit vs. discount rate.

The IRR on an investment is the annualized, compounded rate of return that renders the NPV of the net cash flow from a particular investment to zero. In more specific terms, the IRR of an investment is the discount rate at which the NPV of costs (negative cash flows) equals the NPV of the benefits (positive cash flows), and is given as:

$$\sum_{t=1}^{N} \frac{REV_t}{(1+\alpha_{irr})^t} = \sum_{t=1}^{N} \frac{CST_t}{(1+\alpha_{irr})^t} \tag{2.58}$$

A project having IRR values greater than the discount rate is assessed to be economically feasible, and a higher difference between these rates result in a lower financial risk for the investor; projects with IRR less than the discount rate are either deferred or discarded entirely. The IRR of a project, whose annual cash flows are shown in Figure 2.4a, is explained in Figure 2.4b by plotting the variation of NPV of profit with respect to the discount rate.

The simple PBP method usually refers to the number of years required to recover the initial investment cost. It is computed by adding the annual net cash flows until the sum becomes equal to or greater than the initial investment, which is also known as the break-even point, and the year in which this occurs is the simple PBP. As this procedure does not incorporate the time value of money, a discounted PBP is calculated with the NPV of the annual net cash flows, discounted to the year of initial investment. For the cash flow shown in Fig. 2.4a, the simple PBP is 10 years, and the discounted PBPs are shown in Table 2.1 with variation in the discount rate. For an 8%

Table 2.1: Discounted PBPs with discount rate variations.

α [%]	0	1	2	3	4	5	6	7	8
PBP [Years]	10	11	12	13	14	15	16	18	No PBP

discount rate, which is greater than the IRR of this project, there is no PBP, as the investment is not recovered over the project duration (negative NPV in Fig. 2.4b).

2.3.2 Risk Indices [60]

In risk management, VaR is a widely used risk metric that measures and quantifies the level of financial risk within an investment portfolio over a specific time frame. It is computed using the cumulative distribution function (c.d.f.) of the investment profit or loss portfolio, as shown in Figure 2.5. It gives the measure of the amount of potential profit or loss (depending on whether the c.d.f. is of profit or loss), the probability of occurrence of that amount of profit or loss, and the considered time frame. For example, as shown in Figure 2.5, if the c.d.f. for the NPV of profit Ω_0

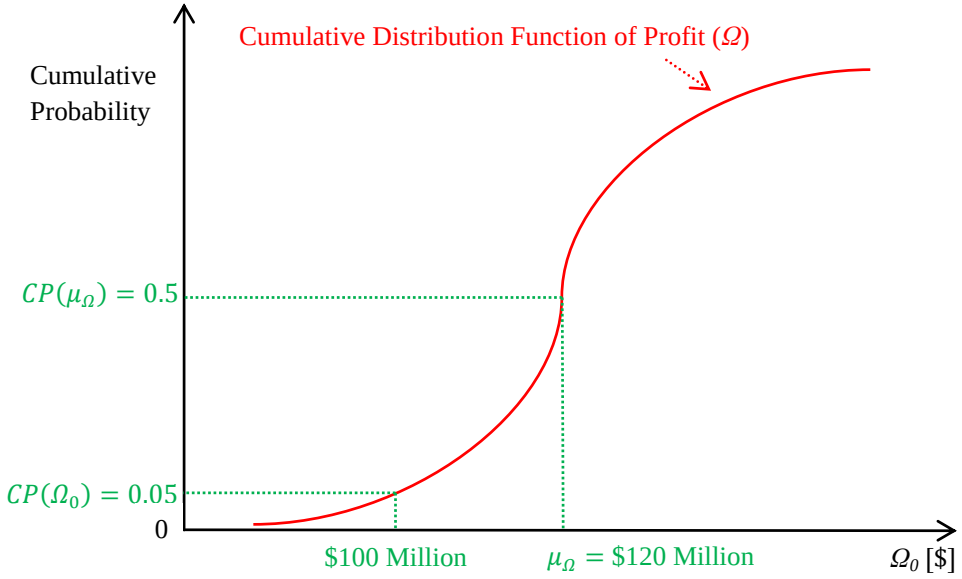

Figure 2.5: Definition of VaR.

in an investment has a value of \$100 million at 5% cumulative probability, i.e., $CP(\Omega_0) = 0.05$, in financial terms it results in a VaR of \$20 million with 5% probability (as μ_Ω = \$120 Million); this signifies that a minimum profit of \$100 million is predicted with a confidence level (CL) of 95%, or, in other words, a 5% probability that the expected profit will reduce by \$20 Million.

2.4 Mathematical Programming [67]

An optimization problem or mathematical programming problem is a mathematical technique that maximizes or minimizes a real function in order to determine the best outcome (such as maximum profit or least cost) of a given mathematical model while satisfying a set of constraints. A typical representation of the optimization problem is expressed in (2.14)–(2.16). An optimization problem with all functions f, h, and g being represented by linear relationships is called a Linear Programming (LP) problem. Its feasible region is a convex polyhedron, which is a set defined by the intersection of several finite half spaces, each of which is defined by a linear inequality. The objective function is a real-valued function defined on this polyhedron. An LP solution algorithm seeks the point on the polyhedron where this objective function has the smallest (or largest) value, if such a point exists. If all the variables in the vector x are integers, then the problem is referred to as an Integer Programming problem and if one or more variables are integers, then the problem becomes a Mixed Integer Linear Programming (MILP) problem.

If there exists at least one non-linear equation in (2.14) to (2.16), then it is termed as a non-linear optimization or Non-Linear Programming (NLP) problem. In addition, if at least one element of the vector x is an integer variable, then the optimization is a Mixed Integer Non-Linear Programming (MINLP) problem. The latter class of optimization problem is the most difficult to solve and is generally tackled in two stages; thus, initially an MINLP is turned into an NLP by relaxing the integer constraints and a solution is derived, and in the next step, the non-integer variables of the NLP solutions are plugged in and the integer constraints are switched on. If the integer constraints are linear, then the second stage becomes an MILP problem, otherwise a linearization technique, like the one described next, may be applied to remove the non-linearity of the integer constraints. If linearization is not possible, then heuristic approaches can be incor-

porated to solve the MINLP problem.

2.4.1 Linearization

If the non-linearity of an MINLP or NLP is quadratic in nature, as is the case of one of the models proposed in this thesis, there are linearization techniques available to render the problem an MILP or LP [68]. Thus, the quadratic term can be a product of any two binary or integer or continuous variables. If the product is given by:

$$y = x_1 \; x_2 \tag{2.59}$$

where both x_1 and x_2 are continuous positive variables, and are bounded by:

$$x_1^{MIN} \leq x_1 \leq x_1^{MAX} \tag{2.60}$$

$$x_2^{MIN} \leq x_2 \leq x_2^{MAX} \tag{2.61}$$

then, with the necessary conditions of $x_1^{MIN} \geq 0$ and $x_2^{MIN} \geq 0$, the product y can be expressed in a linear form by the following two equations:

$$y \leq x_1^{MAX} \; x_2 \tag{2.62}$$

$$y \geq x_1^{MIN} \; x_2 \tag{2.63}$$

The value of x_1 can be deduced from the optimization solution using $x_1 = y/x_2$ for $x_2 \neq 0$, with a further necessary condition that the variable x_1 is not used in any other equation in the model.

2.4.2 Mathematical Programming Tools

The General Algebraic Modeling System (GAMS) [69], designed to solve linear, nonlinear, and mixed integer optimization problems, contains an integrated development environment (IDE) and uses a group of third party optimization solvers. One such solver is CPLEX [70], which is

used in this research work to solve MILP problems. It uses either the simplex method or the branch and cut algorithm; the latter is suitable for MILP problems, which involves running the branch and bound algorithm for the relaxed LP optimization, using cutting planes to tighten the relaxations.

2.5 Summary

This chapter presented a review of the background relevant to the research presented in the next two chapters. The chapter described the basic formulations of the GEP procedure from both an investor's and central planner's perspective. The methods to determine the sensitivities of the objective function to various input parameters of a model were also discussed. The DT based method is the primary procedure applied here to determine sensitivity indices of the solar PV investment model, and is also compared with respect to the indices obtained with the Monte Carlo simulations and the FD approaches. A short discussion on various risk metrics applicable to investment projects was presented next, and the chapter is concluded with a brief background on optimization problems and linearization techniques relevant to the solar PV investment model described in the Chapter 3 and the GEP model of Chapter 4.

Chapter 3

Risk Assessment of Solar PV Investment Projects

3.1 Introduction

In this chapter, the DT-based method discussed in Chapter 2 is applied to a solar PV investment planning model to determine the sensitivity indices of the NPV of profit with respect to the model input parameters. The DT-based method is used to determine how sensitive the NPV is to perturbations of input parameters for a multi-year investment planning model of the Ontario grid. The computed sensitivities are compared with those obtained with Monte Carlo simulation and the FD based approaches. A novel relationship is proposed between the sensitivity indices and investor's profit for a certain confidence level to determine the risk indices for an investor in solar PV projects.

3.2 Solar PV Investment Model

The solar PV investment planning model is based on [71], and is an MILP problem comprising continuous and binary variables, with the objective of maximizing the NPV of the investor's

profit to determine the optimal set of solar PV investment decisions. Thus, the NPV is defined as:

$$\Omega_{Pft} = \sum_{k=1}^{N_{Pft}} \frac{\sum_{i=1}^{Z} (REV_{k,i} - CST_{k,i})}{(1+\alpha)^k} \tag{3.1}$$

where

$$REV_{k,i} = \rho_{PV}^{ICV} \; E_{k,i}^{PV} \tag{3.2}$$

$$CST_{k,i} = CC_{k,i}^{PV} \; NC_{k,i}^{PV} + OM_{k}^{PV} \; E_{k,i}^{PV} \tag{3.3}$$

Here, the Capital Cost CC is defined, based on (2.11), as:

$$CC_{k,i}^{PV} = UC_{k}^{PV} + LbC_{k,i}^{PV} + TC_{k,i}^{PV} + LdC_{k,i}^{PV} \tag{3.4}$$

and $NC_{k,i}^{PV}$, an integer variable constructed using binary variables W_q and an assumed installation step size of 5 MW, is given by:

$$NC_{k,i}^{PV} = 5 \; \sum_{q=1}^{Q} W_q \tag{3.5}$$

The various operational, planning and financial constraints of the model are as follows:

- *Supply-Demand Balance*: The zonal power demand is met from the power generated by the conventional and solar PV sources, with the inter-zonal transmission network represented by a dc power flow model for any surplus/deficit power transfer from/to the zone as follows:

$$P_{k,i}^{Conv} + P_{k,i}^{PV} - PDE_{k,i} = \sum_{j=1}^{Z} B_{k,i,j} \; \left(\delta_{k,i} - \delta_{k,j}\right) \tag{3.6}$$

- *Conventional Energy Generation Limit*: The annual energy available from conventional sources, which are assumed to be dispatchable sources only, is constrained by the annual average capacity factor applied to the installed generation capacity as follows:

$$E_{k,i}^{Conv} \leq \; 8760 \; Cap_{k,i}^{Conv} \; CF_{i}^{Conv} \tag{3.7}$$

- *Solar PV Energy Generation Limit*: The annual energy availability from the solar PV generation, i.e., a non-dispatchable source, is specified by its installed capacity and annual average capacity factor as follows:

$$E_{k,i}^{PV} = 8760\, Cap_{k,i}^{PV}\, CF_{i}^{PV} \tag{3.8}$$

- *Transmission Line Flow Limits*: The power transfer capability between zones is limited by the maximum transfer capacity, depending on the impedances of the transmission lines, as follows:

$$B_{k,i,j}\left(\delta_{k,i} - \delta_{k,j}\right) \leq PT_{k,i,j}^{MAX} \tag{3.9}$$

- *Bus Angle Limits*: In order to ensure system stability, the power angles at the zonal buses are bounded as follows:

$$\delta_{MIN} \leq \delta_{k,i} \leq \delta_{MAX} \tag{3.10}$$

- *Annual Budget Limit*: Annual expenditure of the investor on new solar PV installations is constrained as follows:

$$\sum_{i=1}^{Z} CC_{k,i}^{PV}\, NC_{k,i}^{PV} \leq ABG_{k} \tag{3.11}$$

- *Total Budget Limit*: Total investment budget of the investor on solar PV installations is constrained as follows:

$$\sum_{k=1}^{N_{Pft}} \sum_{i=1}^{Z} \left(CC_{k,i}^{PV}\, NC_{k,i}^{PV} + OM_{k}^{PV}\, E_{k,i}^{PV}\right) \leq TBG \tag{3.12}$$

- *Dynamic Constraint on Solar PV Capacity Addition*: This ensures cumulative capacity addition updates as new solar PV installations are implemented, and can be defined by:

$$Cap_{k+1,i}^{PV} = Cap_{k,i}^{PV} + NC_{k,i}^{PV} \qquad \forall\, k = 1, 2, \cdots, (N_{Pft} - 1) \tag{3.13}$$

- *Initial Year Investment Constraint*: This constraint ensures no new solar PV capacity ad-

ditions takes place in the initial years in order to account for budgetary delays, policy changes, etc. This can be represented as follows:

$$Cap^{PV}_{k+1,i} \;=\; 0 \qquad\qquad \forall\, k = 1, 2, \cdots, DB \tag{3.14}$$

- *Terminal Year Investment Constraint*: This constraint ensures that no investment decisions are made after the planning period (N), as follows:

$$Cap^{PV}_{k+1,i} \;\leq\; Cap^{PV}_{k,i} \qquad\qquad \forall\, k \;\geq\; N_{Pft} \tag{3.15}$$

- *Solar PV Lifetime Constraint*: The following constraint ensures the decommissioning of installed solar PV capacity after completion of their useful life:

$$Cap^{PV}_{k+LT+1,i} = Cap^{PV}_{k+LT,i} - NC^{PV}_{k,i} \qquad\qquad \forall\, k = 1, 2, \cdots, (N_{Pft} - 1) \tag{3.16}$$

3.3 Application of DT Based Method to Solar PV Investment Model

In order to apply the DT-based method to the solar PV investment model and hence determine the desired sensitivities, the variables x and parameters p need to be defined in the context of the problem. From the model discussed in Section 3.2, the vector x of model variables can be defined as:

$$x = \begin{bmatrix} Cap^{PV}_{k,i} & E^{Conv}_{k,i} & E^{PV}_{k,i} & NC^{PV}_{k,i} & \delta_{k,i} \end{bmatrix}^T \tag{3.17}$$

And the vector of model parameters can be defined as:

$$\begin{aligned} p = \Big[& ABG_k \;\; B_{k,i,j} \;\; Cap^{Conv}_{k,i} \;\; CF^{Conv}_{i} \;\; CF^{PV}_{i} \;\; LbC^{PV}_{k,i} \;\; LdC^{PV}_{k,i} \;\; OM^{PV}_{k} \\ & PT^{MAX}_{k,i,j} \;\; PDE_{k,i} \;\; TBG \;\; TC^{PV}_{k,i} \;\; UC^{PV}_{k} \;\; \alpha \;\; \rho^{ICV}_{PV} \;\; \delta_{MIN} \;\; \delta_{MAX} \Big]^T \end{aligned} \tag{3.18}$$

The objective function of the optimization model given by (3.1) – (3.3) can be represented as a function $z = f(x, p)$ for the x and p defined in (3.17) and (3.18), respectively. Furthermore, assuming active and non-zero Lagrange multipliers for all inequality constraints, $g(x, p)$ can be defined as:

$$g(x,p) = \begin{bmatrix} \gamma_{1_{k,i}} \left(E^{Conv}_{k,i} - 8760\ Cap^{Conv}_{k,i}\ CF^{Conv}_{i} \right) \\ \gamma_{2_{k,i,j}} \left(B_{k,i,j}\ (\delta_{k,i} - \delta_{k,j}) - PT^{MAX}_{k,i,j} \right) \\ \gamma_{3_{k,i}}\ (\delta_{MIN} - \delta_{k,i}) \\ \gamma_{4_{k,i}}\ (\delta_{k,i} - \delta_{MAX}) \\ \gamma_{5_k} \left(\sum_{i=1}^{Z} CC^{PV}_{k,i}\ NC^{PV}_{k,i} - ABG_k \right) \\ \gamma_6 \left\{ \sum_{k=1}^{N_{Pft}} \sum_{i=1}^{Z} \left(CC^{PV}_{k,i}\ NC^{PV}_{k,i} + OM^{PV}_{k,i}\ E^{PV}_{k,i} \right) - TBG \right\} \end{bmatrix} \tag{3.19}$$

and similarly the equality constraints $h(x, p)$ can be written as:

$$h(x,p) = \begin{bmatrix} \lambda_{1_{k,i}} \left(P^{Conv}_{k,i} + P^{PV}_{k,i} - \sum_{j=1}^{Z} B_{k,i,j}\ (\delta_{k,i} - \delta_{k,j}) - PDE_{k,i} \right) \\ \lambda_{2_{k,i}} \left(E^{PV}_{k,i} - 8760\ Cap^{PV}_{k,i}\ CF^{PV}_{i} \right) \end{bmatrix} \tag{3.20}$$

First, for inactive and active zero-valued Lagrange multipliers of inequality constraints, and for zero valued Lagrange multipliers of equality constraints, the corresponding equations are removed from $g(x, p)$ and $h(x, p)$, respectively. Then, the remaining part of $g(x, p)$ is merged with the remnant of $h(x, p)$ by transforming the inequalities to equalities. The matrices U (2.48) and S (2.49) can then be determined (these were determined here using MATLAB's Symbolic Math Toolbox [72]).

The DT method provides the sensitivity indices denoted by $\xi_{DT} = d\Omega_{Pft}/dp$, as well as the sensitivities of the primal (dx/dp) and dual variables ($d\lambda/dp$ and $d\gamma/dp$) with respect to the model parameters. The computed indices $\xi^{\$}_{DT}$ are indicative of the local sensitivities of the objective function with respect to the model input parameters. Hence, for a small perturbation of the input parameter(s), the resulting change in Ω_{Pft} can be calculated using the following expression:

$$d\Omega_{Pft} = \sum_{r} \left(\frac{\partial \Omega_{Pft}}{\partial p_r} \right) dp_r \cong \sum_{r} \xi^{\$}_{DT_{p_r}} dp_r \tag{3.21}$$

The units of ξ_{DT} are \$/(unit of the parameter p_0), which can be appropriately modified to be

represented in terms of \$/(1% change in p_0). Thus, the sensitivity indices can all be transformed to the same base and scaled appropriately in order to compare and rank them as per their severity. Additionally, the dollar value of ξ_{DT} can be represented as a percentage of $\Omega_{Pft_{base}}$, i.e.,

$$\xi^{\%}_{DT} = 100\left(\frac{\xi^{\$}_{DT}}{\Omega_{Pft_{base}}}\right) \tag{3.22}$$

If a linear relationship exists between an input parameter and the output variable, the p.d.f. of the output is the same as the input p.d.f., and the mean of the input distribution generates the mean of the output distribution. In this work, the MILP model behaved linearly with respect to p.d.f.s for most parameters, with a few exceptions, as shown in Appendix A. Hence, considering that the mean of a normally distributed parameter is the base value of the parameter p_0, the mean of Ω_{Pft} from every Monte Carlo simulation output can be generally assumed to be equal to $\Omega_{Pft_{base}}$, i.e.,

$$\mu^{\$}_{\Omega_{Pft}} = \Omega_{Pft_{base}} \tag{3.23}$$

The sensitivity index computed using Monte Carlo simulation based approach, can also be represented as follows:

$$\xi^{\$}_{MC} = \frac{\sigma^{\$}_{out}}{\sigma^{\%}_{in}} = \frac{\sigma^{\$}_{\Omega_{Pft}}}{\sigma^{\%}_{p}} \tag{3.24}$$

Thus, the relationship between the sensitivity indices (2.54) and (3.24) is given by:

$$\xi^{\%}_{MC} = 100\left(\frac{\xi^{\$}_{MC}}{\mu^{\$}_{out}}\right) = 100\left(\frac{\xi^{\$}_{MC}}{\mu^{\$}_{\Omega_{Pft}}}\right) \tag{3.25}$$

Then, from (3.22) and (3.25), the following can be obtained:

$$\frac{\xi^{\%}_{MC}}{\xi^{\%}_{DT}} = \frac{\xi^{\$}_{MC}}{\xi^{\$}_{DT}}\left(\frac{\Omega_{Pft_{base}}}{\mu^{\$}_{\Omega_{Pft}}}\right) \tag{3.26}$$

Thus, using (3.23) in (3.26), the following relations are proposed:

$$\xi^{\$}_{MC} \cong \left|\xi^{\$}_{DT}\right| \tag{3.27}$$

and

$$\xi^{\%}_{MC} \cong \left|\xi^{\%}_{DT}\right| \tag{3.28}$$

3.3.1 Computation of Standard Deviation

The standard deviation of the output of a Monte Carlo simulation can be calculated using the DT-based sensitivity indices, when the inputs are normally distributed p.d.f.s and assuming a linear behavior of the model. Hence, substituting (3.22) and (3.25) in (3.28), the following relation holds:

$$\frac{\sigma^{\%}_{\Omega_{Pft}}}{\sigma^{\%}_{p}} = \xi^{\%}_{MC} \cong \left|\xi^{\%}_{DT}\right| = 100\left(\frac{\left|\xi^{\$}_{DT}\right|}{\Omega_{Pft_{base}}}\right) \tag{3.29}$$

From (2.53), substituting '*out*' with Ω_{Pft}, and (3.29), and rearranging the terms, one has:

$$100\left(\frac{\sigma^{\$}_{\Omega_{Pft}}}{\mu^{\$}_{\Omega_{Pft}}}\right) = 100\,\sigma^{\%}_{p}\left(\frac{\left|\xi^{\$}_{DT}\right|}{\Omega_{Pft_{base}}}\right) \tag{3.30}$$

Substituting (3.23) in (3.30), a relationship between the standard deviation of the output variable with the sensitivity index of the perturbed parameter can be obtained:

$$\sigma^{\$}_{\Omega_{Pft}} = \sigma^{\%}_{p}\left|\xi^{\$}_{DT}\right| \tag{3.31}$$

If more than one input parameters are perturbed, the first term of the product on the right hand side of (3.31), i.e., the standard deviation of the input parameter perturbation in percentage, can be represented by the equivalent standard deviation of the parameters perturbed using a well-known expression from multivariate normal distributions [73]. On the other hand, the second term of the product in (3.31) can be replaced by the weighted average of the sensitivity indices of the parameters that are perturbed. Hence, the computation of standard deviation of the output

using DT-based sensitivity indices, for a generic multi-parameter perturbation, can be obtained as follows:

$$\sigma^{\$}_{\Omega_{Pft}} = \sqrt{\sum_{w} \left(\sigma^{\%}_{w}\right)^2} \left(\frac{\sum\limits_{w} \sigma^{\%}_{w} \left| \xi^{\$}_{DT_w} \right|}{\sum\limits_{w} \sigma^{\%}_{w}} \right) \tag{3.32}$$

It is evident that (3.31) is the specific case of (3.32) when $w = 1$, i.e., when only one input parameter is perturbed. The relationship described in (3.32) is important, as it allows computing the standard deviation of a normally distributed output variable resulting from the input of one or more normally distributed parameter(s), without the need to carry out computationally expensive Monte Carlo simulations.

3.3.2 Application to Risk Analysis

In risk analysis, Value-at-Risk (VaR) is a measure that estimates how much a portfolio could lose because of market movements for a given probability of occurrence, which is referred to as Confidence Level (CL), of that portfolio variable [74]. VaR and CL are computed from the cumulative distribution function (c.d.f.) constructed from the p.d.f. of the output quantity. In the context of this work, the output is Ω_{Pft} and the portfolio is the normally distributed p.d.f. of Ω_{Pft}. Thus, from the c.d.f. of Ω_{Pft}, a given profit Ω_0 with a corresponding cumulative probability $CP\left(\Omega_0\right)$ yields a confidence level of $c_0 = 1 - CP\left(\Omega_0\right)$. This means that there is a $c_0\%$ likelihood that $\Omega_{Pft} \geq \Omega_0$, and the VaR from the expected profit $\mu^{\$}_{\Omega_{Pft}}$ is given by:

$$VaR = \mu^{\$}_{\Omega_{Pft}} - \Omega_0 \tag{3.33}$$

Monte Carlo simulations are typically used to compute the VaR and CL of the investment portfolio. However, this is computationally costly due to the large number of simulations required to obtain the c.d.f. of the investment portfolio. Therefore, it is demonstrated next, through mathematical derivations, that the proposed sensitivity index $\xi^{\$}_{DT}$ can be directly utilized to compute the risk parameters VaR and CL, and thus reduce the computational effort required to determine these values.

A c.d.f. of a normally distributed p.d.f. of Ω_{Pft} is shown in Figure 3.1. Although the c.d.f.

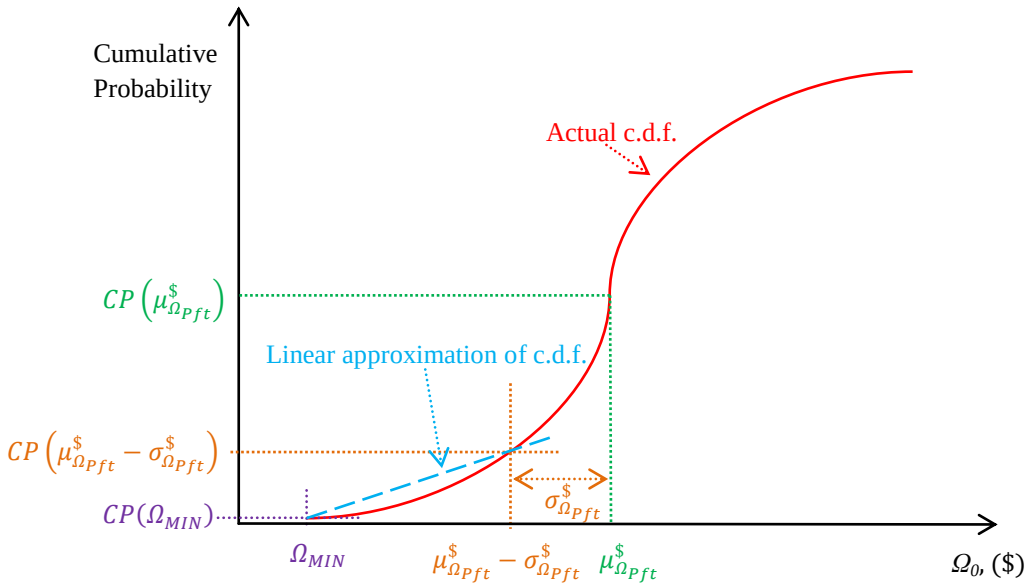

Figure 3.1: Typical c.d.f. plot of NPV of profit depicting the proposed linear approximation.

extends to the left asymptotically, it is assumed that $CP(\Omega_{MIN}) = 0$, neglecting the asymptotic nature of the curve in that region. Then, for a linear approximation of the c.d.f., $\Omega_0 \in \left[\Omega_{MIN}, \mu^{\$}_{\Omega_{Pft}} - \sigma^{\$}_{\Omega_{Pft}}\right]$ can be represented by:

$$\Omega_0 = \Omega_{MIN} + \frac{\left(\mu^{\$}_{\Omega_{Pft}} - \sigma^{\$}_{\Omega_{Pft}}\right) - \Omega_{MIN}}{CP\left(\mu^{\$}_{\Omega_{Pft}} - \sigma^{\$}_{\Omega_{Pft}}\right)}\left(1 - \frac{c_0}{100}\right) \tag{3.34}$$

A standard normal p.d.f. has $\mu = 0$ and $\sigma = 1$; hence, assuming a variable range $[-\tau, \tau]$, where $CP(-\tau) \approx 0$, a relationship between $\mu^{\$}_{\Omega}$ and Ω_{MIN} can then be obtained as follows:

$$\Omega_{MIN} = \mu^{\$}_{\Omega_{Pft}} - \tau\, \sigma^{\$}_{\Omega_{Pft}} \tag{3.35}$$

From the Standard Normal Cumulative Distribution Function Table [73], one has that for $\tau = 4$, $CP(-4) \approx 0$. The value of $\mu^{\$}_{\Omega_{Pft}} - \sigma^{\$}_{\Omega_{Pft}}$ corresponds to one standard deviation below the mean

and thus, the value of $CP\left(\mu^{\$}_{\Omega_{Pft}} - \sigma^{\$}_{\Omega_{Pft}}\right)$ can be defined as follows:

$$CP\left(\mu^{\$}_{\Omega_{Pft}} - \sigma^{\$}_{\Omega_{Pft}}\right) = CP(-1) = c_1 \tag{3.36}$$

Using the table given in [73], it follows that $c_1 = 0.1587$. Thus, replacing (3.23), (3.35) and (3.36) in (3.34) yields:

$$\Omega_0 = \Omega_{Pft_{base}} - \tau\, \sigma^{\$}_{\Omega_{Pft}} + \sigma^{\$}_{\Omega_{Pft}} \left(\frac{\tau - 1}{c_1}\right)\left(1 - \frac{c_0}{100}\right) \tag{3.37}$$

For $\tau = 4$ and $c_1 = 0.1587$, one has:

$$\Omega_0 = \Omega_{Pft_{base}} - 4\, \sigma^{\$}_{\Omega_{Pft}} + 18.904\, \sigma^{\$}_{\Omega_{Pft}} \left(1 - \frac{c_0}{100}\right) \tag{3.38}$$

The proposed equations (3.32), (3.33) and (3.38) show that, for a linear optimization problem and normal distributions, the VaR for a given CL can be closely estimated using the DT-based sensitivity analysis without actually running the computationally expensive Monte Carlo simulations.

3.4 Application to Ontario, Canada

The solar PV investment model presented in Section 3.2 is implemented for the province of Ontario, where some of the input parametric data (e.g., *LbC*, *LdC*, *TC*) are taken from [71] and extrapolated for a project life span (N_{Pft}) of 35 years (2009 – 2043). The reduced-order Ontario transmission system model and the input parameters used here are explained next.

3.4.1 Ontario Transmission System Model and Input Parameters

The simplified ten-zone transmission system model for Ontario used here is shown in Figure 3.2 [75]; this model is adequate for investment planning studies. Other parameters relevant to the transmission system, such as the maximum inter-zonal power transfer limits ($PT^{MAX}_{k,i,j}$) and the

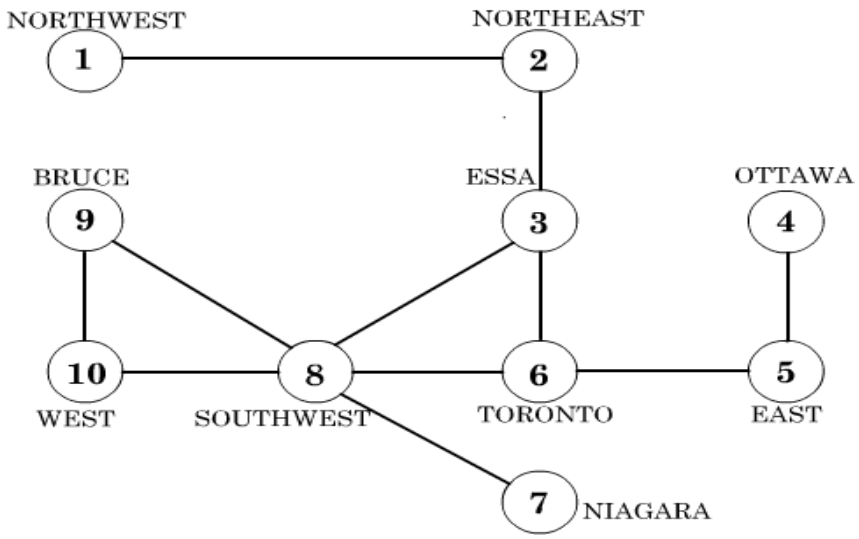

Figure 3.2: Ten-zone transmission model of Ontario [75].

Table 3.1: Maximum zonal power transfer limits of the 10-bus Ontario system [76].

Zones		$PT^{MAX}_{`2009',i,j}$	$PT^{MAX}_{`2009',j,i}$	$PT^{MAX}_{`2043',i,j}$	$PT^{MAX}_{`2043',j,i}$	Changes in
i	j	[MW]	[MW]	[MW]	[MW]	year
NW	NE	325	350	325	550	2013
NE	Essa	1400	1900	1400	2400	2017
Essa	Toronto	1000	2000	1000	2500	2017
Toronto	SW	3212		5212		2012
SW	Bruce	2560		4560		2012
Bruce	West	1940		2440		2015
Essa	SW	2488				–
Ottawa	East	1900				–
East	Toronto	9000				–
Niagara	SW	1750				–
West	SW	1560				–

transmission system resistances and reactances to compute the susceptance- or B-matrix ($B_{k,i,j}$), are obtained from [76], and shown in Tables 3.1 and 3.2, respectively.

Table 3.2: Resistances and reactances of the 10-bus Ontario transmission system [76].

Zones		Resistance [p.u.]		Reactance [p.u.]		Changes in
i	j	2009	2043	2009	2043	year
NW	NE	0.051985	0.033270	0.50737	0.32472	2013
NE	Essa	0.004032	0.003185	0.04680	0.03700	2017
Essa	Toronto	0.002352	0.001882	0.02730	0.02180	2017
Toronto	SW	0.002352	0.001458	0.02730	0.01690	2012
SW	Bruce	0.001904	0.001662	0.02210	0.01240	2012
Bruce	West	0.003024	0.002419	0.03510	0.02810	2015
Essa	SW	0.003584		0.04160		–
Ottawa	East	0.001120		0.01300		–
East	Toronto	0.003808		0.04420		–
Niagara	SW	0.002352		0.02730		–
West	SW	0.002025		0.02350		–

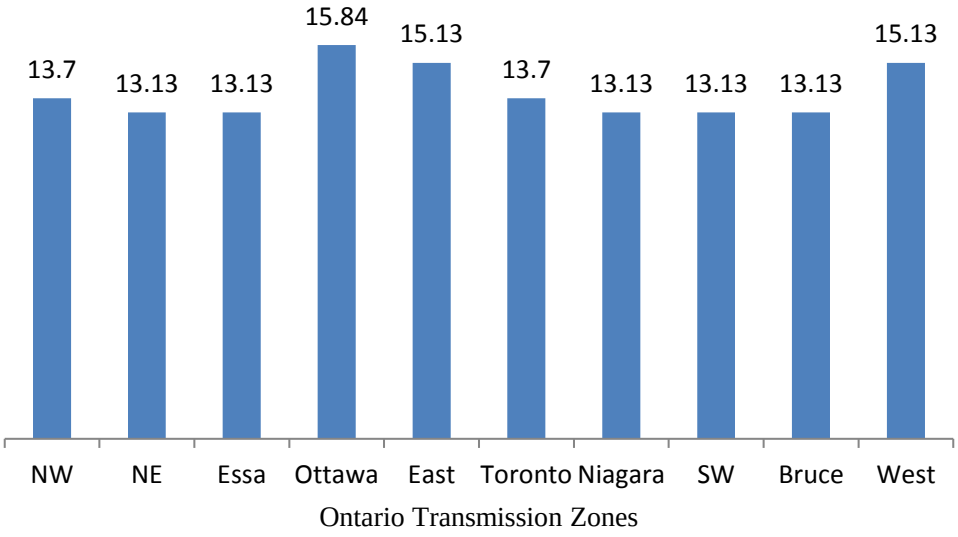

Figure 3.3: Zonal capacity factors of solar PV (CF_i^{PV}) in % [77].

The capacity factors of ground-mounted large-scale solar PV generation for the ten zones of Ontario are presented in Figure 3.3, as per [77]. The annual average capacity factors of the ex-

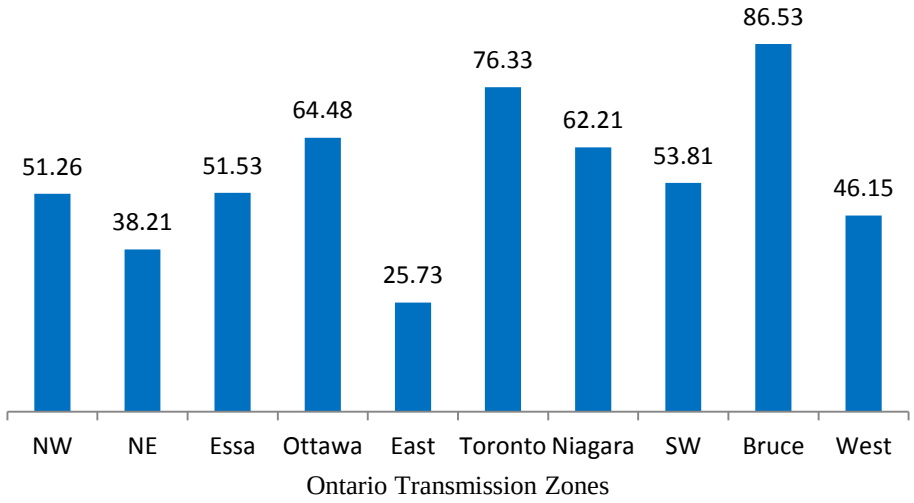

Figure 3.4: Zonal capacity factors of conventional generation (CF_i^{Conv}) in % [78].

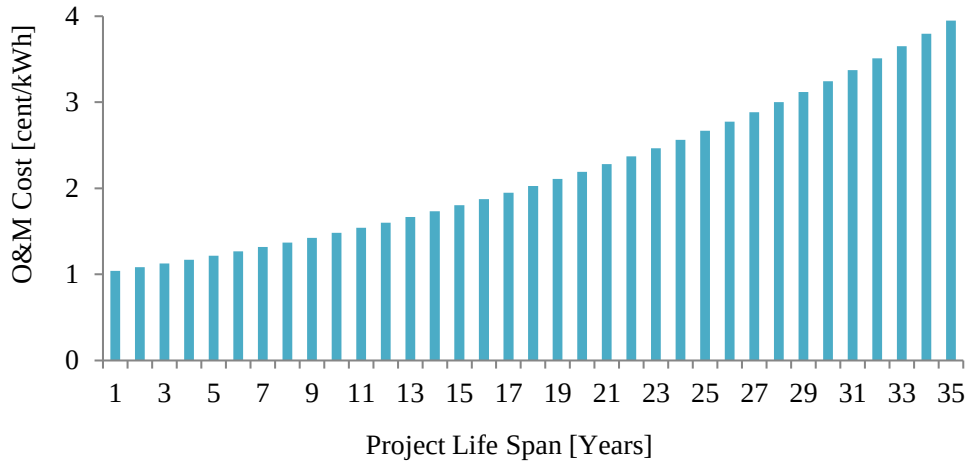

Figure 3.5: O&M cost of solar PV installations over the plan study horizon [79].

isting conventional generations are shown in Figure 3.4, which were calculated using previous 10 years generation data from the Independent Electricity System Operator (IESO) of Ontario [78].

The O&M cost of the solar PV installations is determined to be 1.267 ¢/kWh in the first year of the plan horizon for all the transmission zones in Ontario, based on [79] and the solar PV capacity factors. Figure 3.5 shows the escalation of this O&M cost over the plan study horizon

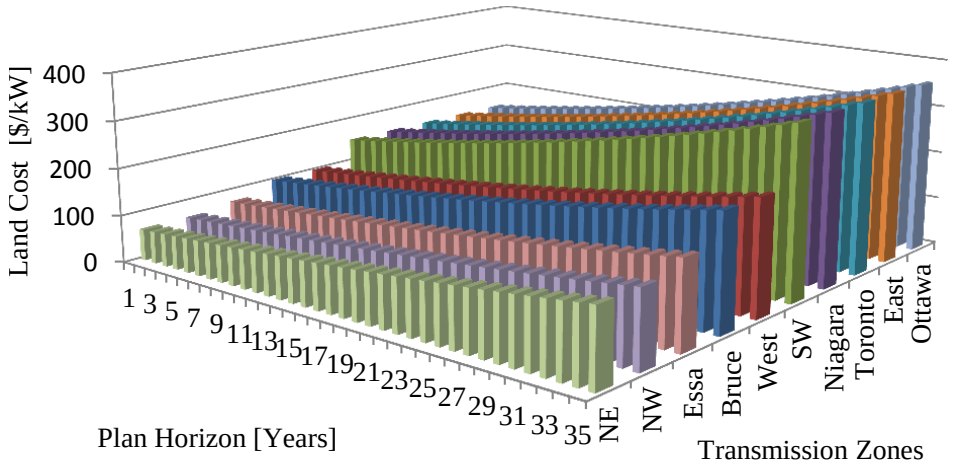

Figure 3.6: Land cost $LdC_{k,i}^{PV}$ of solar PV installations over the plan study horizon [71].

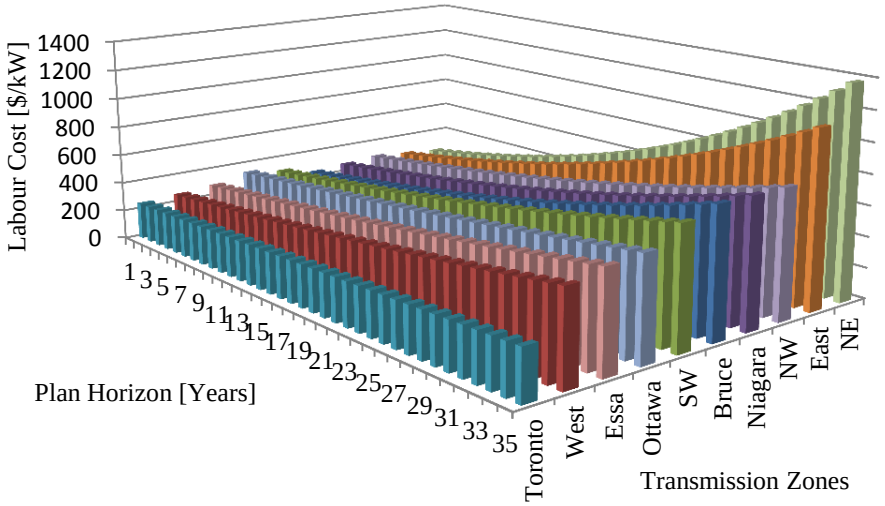

Figure 3.7: Labour cost $LbC_{k,i}^{PV}$ of solar PV installations over the plan study horizon [71].

with an assumed inflation of 4%.

The capital cost of solar PV installation comprises the land, labour, transportation and the PV unit costs. The land cost, shown in Figure 3.6 [71], reflects the cost of land required to set up the installation, and the labour cost corresponds to the wages paid to the installation and commissioning workers (see Figure 3.7 [71]). For the transportation cost, shown in Figure 3.8,

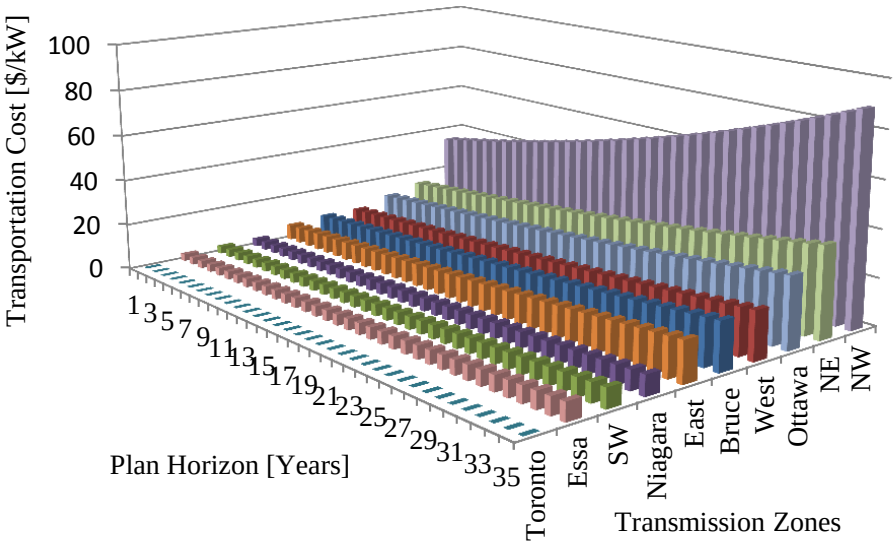

Figure 3.8: Transportation cost $TC_{k,i}^{PV}$ of solar PV units over the plan study horizon [71].

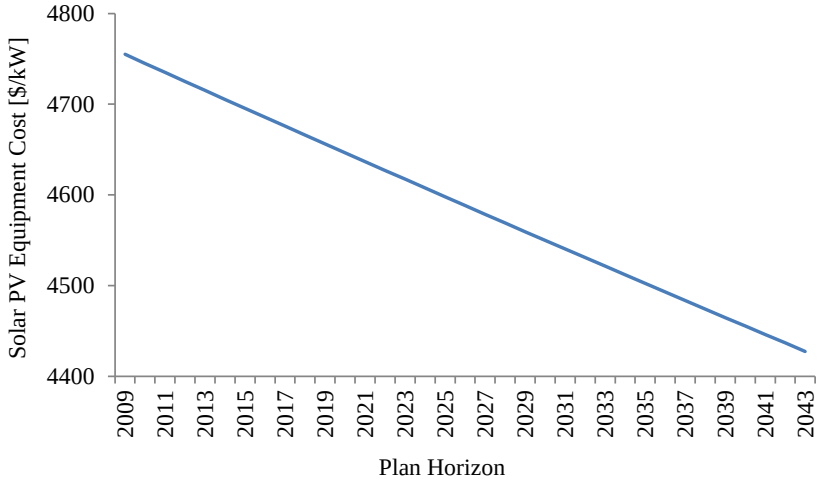

Figure 3.9: Solar PV equipment cost $UC_{k,i}^{PV}$ over the plan study horizon [79].

it is assumed that all solar PV units are purchased in the Toronto zone and transported to other zones. The equipment cost is the cost of a solar PV panel, the inverter cost, and the balance-of-system cost. Decreasing costs of solar cells and inverters are driving the cost of solar PV equipment down, as shown in Figure 3.9 [79]. Note that the equipment cost makes up the largest

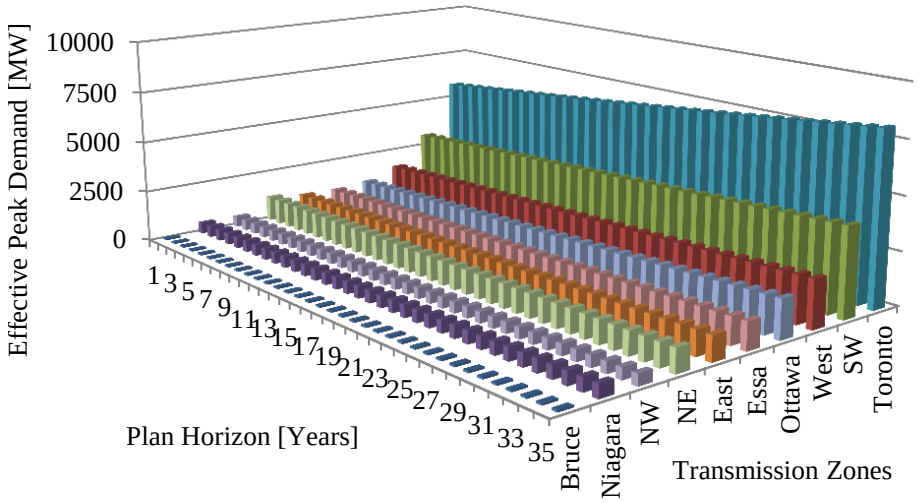

Figure 3.10: Zonal effective peak demand $PDE_{k,i}$ over the plan study horizon [78].

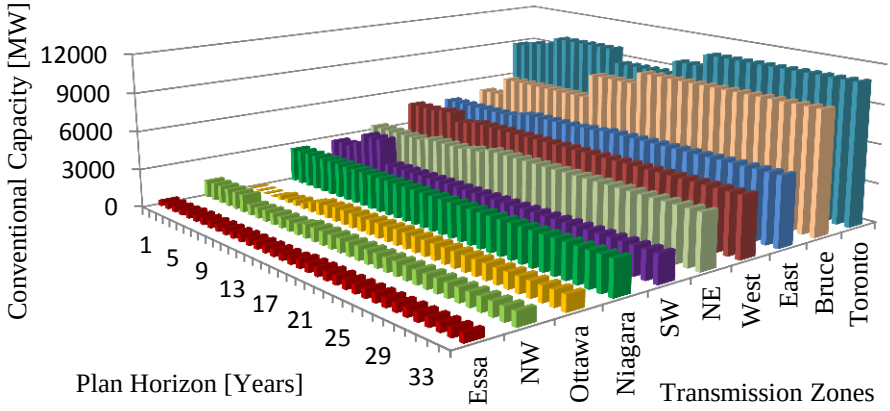

Figure 3.11: Forecast of zonal conventional generation capacity $Cap_{k,i}^{Conv}$ over the plan period.

share of the capital cost, while the transportation cost is the least.

The forecasted effective zonal peak demand over the planning horizon, shown in Figure 3.10, is computed using previous 10 years hourly load data for each zone, from [78], minus an assumed 1500 GWh/Year of energy conservation [35]. The forecasted zonal conventional generation capacity is shown in Figure 3.11, based on assumed refurbishment/shutdown of some nuclear units coupled with anticipated new installations of various types of non-solar generation capacities.

Table 3.3: Other input parametric data.

Feed-in-Tariff (ρ_{PV}^{ICV}) ¢/kWh	Discount Rate (α) %	Total Budget (TBG) Million $
44.3	8	500

Other model input parameters, relevant to the computation of sensitivity indices, are: the FIT rate or the solar PV incentive ρ_{PV}^{ICV} (prescribed by OPA [12]); the total investor's budget, and the discount rate used to compute the NPV. These are given in Table 3.3.

3.4.2 Base Case Optimization Results and Sensitivity Indices

The optimization model, described in Section 3.2 is solved using the CPLEX solver in the GAMS environment [69] [70], with a relative optimality tolerance of 0.1%. The model determines that all new solar PV generation units are to be installed in the Ottawa zone, as shown in Figure 3.12, which is consistent with the solar PV capacity factors depicted in Figure 3.3. Observe that the total new installations of solar PV are 80 MW, spread over 5 years. The resulting NPV is

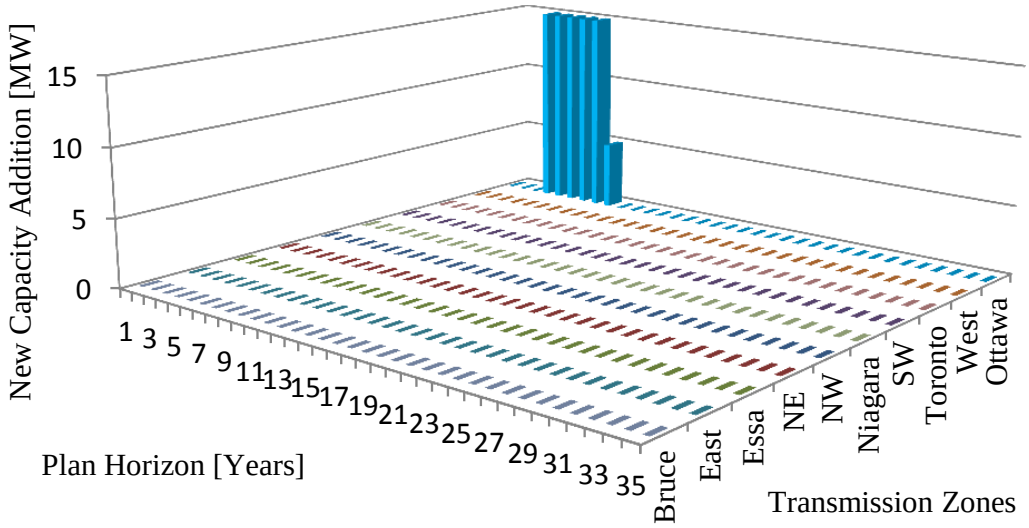

Figure 3.12: New solar PV capacity addition ($NC_{k,i}^{PV}$).

Table 3.4: Sensitivity indices of parameters using the DT based method.

Parameters	$\xi^{\$}_{DT}$	$\xi^{\%}_{DT}$
	$(\$)/(1\%p_0)$	$(\%of\Omega_{base})/(1\%p_0)$
Feed-in-Tariff	3,283,803	6.8307
Capacity Factor PV (Ottawa)	3,113,538	6.4765
Equipment Cost	-2,354,756	-4.8982
Discount Rate	-2,316,900	-4.8194
Labour Cost	-185,564	-0.3860
O& M Cost	-170,265	-0.3542
Land Cost	-85,686	-0.1782
Transportation Cost	-6786	-0.0141
Total Budget	0	0
Capacity Factor Conv. (Ottawa)	0	0
Annual Budget	0	0
Power Demand	0	0

$\Omega_{Pft_{base}}$ = \$48.074 million. The IRRs and PBPs of these new installations are 10.098% and 9 years, respectively.

The obtained optimal solution identifies both zero and non-zero Lagrange multipliers associated with both equality and inequality constraints. The constraints pertaining to non-zero Lagrange multipliers are taken into consideration for computing the sensitivities using the DT-based method; the inactive constraints and those active constraints with zero values for their Lagrange multipliers are not considered in building the U and S matrices, as mentioned in Section 2.2.1. In this example, only one set of Lagrange multipliers associated with the active constraints (3.8) is found to have non-zero values; hence, the final $h(x, p)$ relevant to (2.48) and (2.49) consists of only the set of equations associated with $\lambda_{2_{k,i}}$, as λ_1 and γ_1 to γ_6 are all zero. The matrices U (2.48) and S (2.49) are computed symbolically in MATLAB, and then the numerical values of parametric data and active Lagrange multipliers are used to compute the sensitivity indices.

The sensitivity indices obtained with the DT method are ranked as per their severity in Table 3.4. The parameter $\xi^{\$}_{DT}$ denotes the dollar amount by which $\Omega_{Pft_{base}}$ will change for a 1% increase

Table 3.5: Sensitivity indices of parameters using the FD approach.

Parameters	$\xi^{\$}_{FD}$	$\xi^{\%}_{FD}$
	($)/(1%$p_0$)	(%$of\Omega_{base}$)/(1%p_0)
Feed-in-Tariff	3,283,802	6.8307
Capacity Factor PV (Ottawa)	3,113,537	6.4765
Equipment Cost	-2,354,756	-4.8982
Discount Rate	-2,295,530	-4.7750
Labour Cost	-185,564	-0.3860
O& M Cost	-170,265	-0.3542
Land Cost	-85,686	-0.1782
Transportation Cost	-6786	-0.0141
Total Budget	0	0
Capacity Factor Conv. (Ottawa)	0	0
Annual Budget	0	0
Power Demand	0	0

in the base value of a parameter, with the initial state of parametric values being defined in Section 3.4.1, and $\xi^{\%}_{DT}$ denotes the percentage change in Ω_{Pft} for a 1% increase in the parameter. This table also includes four more parameters for which the objective function is not sensitive. Note that the sensitivity index (ξ_{DT}) corresponding to total budget (*TBG*) turned out to be zero; this is due to the fact that *TBG* appears in only one expression of the mathematical model for investment planning, inequality (3.12), which incidentally has a zero-valued Lagrange multiplier (γ_6), thereby not affecting the DT-based sensitivity values.

Table 3.5 presents the results of applying the FD method to find the "true" sensitivities, i.e., the actual change in Ω_{Pft} for a specific perturbation in an input parameter, and Table 3.6 presents the sensitivity indices computed using the Monte Carlo simulation approach. Observe that the sensitivity indices computed using DT and FD approaches are practically the same, illustrating the accuracy of the DT-based method. The sensitivity indices obtained using the Monte-Carlo-based method are also quite comparable to the absolute values of sensitivity indices obtained from the DT and FD procedures; however, this method fails to provide the correct signs, due to

Table 3.6: Sensitivity indices of parameters using Monte Carlo simulations.

Parameters	$\xi_{MC}^{\$}$	$\xi_{MC}^{\%}$
	$(\$)/(1\%\sigma_{p_0})$	$(\%of\Omega_{base})/(1\%\sigma_{p_0})$
Feed-in-Tariff	3,283,902	6.8295
Capacity Factor PV (Ottawa)	3,092,003	6.4317
Equipment Cost	2,584,392	5.3889
Discount Rate	2,315,874	4.8244
Total Budget	557,136	1.1663
Labour Cost	185,555	0.3867
O& M Cost	170,568	0.3548
Land Cost	86,539	0.1803
Transportation Cost	6785	0.0141
Capacity Factor Conv. (Ottawa)	0	0
Annual Budget	0	0
Power Demand	0	0

the fact that the sensitivities computed in this case are a ratio of the output and input standard deviations, and standard deviations always have positive values. ***From Tables 3.4 to 3.6, observe that the profit of an investor is most sensitive to the incentive rate or FIT, followed by the solar PV capacity factor in the zone of installation, i.e., Ottawa, the equipment cost, and the discount rate, in the order of reducing severity.

An important point to note is that the sensitivity indices pertaining to the total budget *TBG* are zero for ξ_{DT} and ξ_{FD}, while ξ_{MC} has a non-zero value. It has been discussed earlier regarding the effect of the absence of the associated Lagrange multiplier for *TBG*. This is reasonable as the inequality (3.12) contains the integer variable *NC*, which renders the left hand side of the inequality (the summation) to be discrete; as illustrated by the plot of Ω_{Pft} versus *TBG* perturbations in % using the FD method shown in Figure 3.13. Observe that in the vicinity of the base case solution the NPV of profit is independent of small (e.g., 1%) increments in total budget; thus, small perturbations in *TBG* fail to produce a non-zero γ_6, which is why ξ_{DT} for *TBG* is zero. On the other hand, the non-zero value of ξ_{MC} obtained using the Monte Carlo simulations

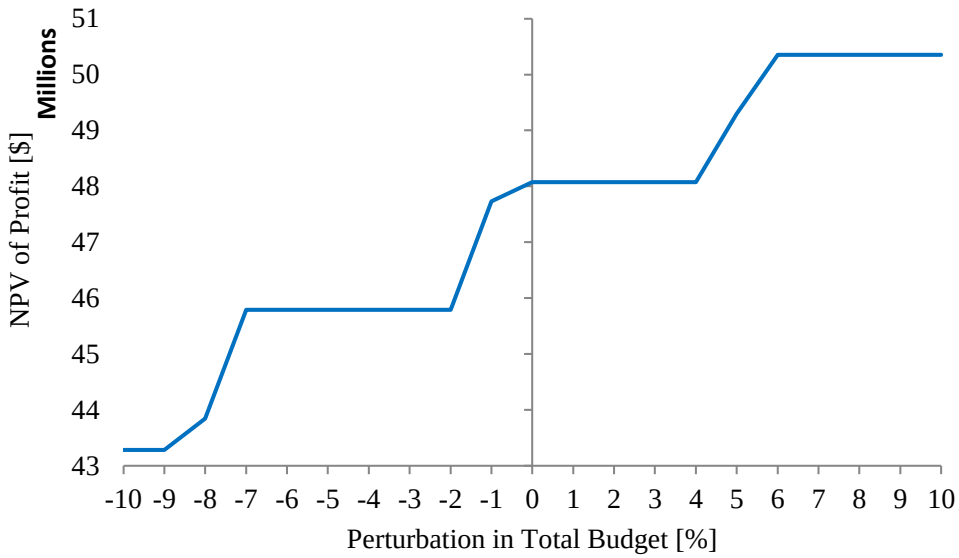

Figure 3.13: NPV of profit Ω^{Pft} vs % perturbation in total budget *TBG*, using FD method.

can be attributed to the fact that a normally distributed p.d.f. usually has a $\pm 4\sigma$ range, and thus a *TBG* perturbation in that range results in changes to Ω_{Pft}, as evident in Figure 3.13. This illustrates the non-linear nature of the optimization model, as discussed in more detail in Section 3.4.3.

The DT-based method for computing sensitivity indices is validated by calculating the percentage errors between ξ_{DT} and sensitivities computed using the other two methods, as follows:

$$Err_{DT-FD} = \frac{\xi_{DT} - \xi_{FD}}{\xi_{FD}} \times 100 \tag{3.39}$$

$$Err_{DT-MC} = \frac{|\,\xi_{DT}\,| - \xi_{MC}}{\xi_{MC}} \times 100 \tag{3.40}$$

Since the Monte Carlo simulation approach does not provide the direction of change in Ω_{Pft}, the negative sign of ξ_{DT} is removed in (3.40). Table 3.7 shows the resulting errors, demonstrating that the sensitivities obtained with the DT-based method are fairly accurate compared to the values obtained with the FD method. These values also show that, for most cases, (3.27) and (3.28) are valid; as long as the model behaves linearly with respect to the parameter changes, which is

Table 3.7: Percentage error calculations of sensitivity indices.

Parameters	Err_{DT-FD}	Err_{DT-MC}	
	Using $\xi^{\$}$ or $\xi^{\%}$	Using $\xi^{\$}$	Using $\xi^{\%}$
Feed-in-Tariff	1.0309×10^{-5}	-0.00302	0.01757
Capacity Factor PV (Ottawa)	1.1651×10^{-5}	0.69647	0.69647
Equipment Cost	-9.864×10^{-6}	-8.8855	-9.1058
Discount Rate	0.9309	0.04430	-0.1044
Labour Cost	-9.514×10^{-5}	0.00485	-0.1753
O& M Cost	-1.423×10^{-5}	-0.1776	-0.1776
Land Cost	-8.548×10^{-4}	-0.9857	-1.1645
Transportation Cost	-2.792×10^{-3}	0.01474	-0.1768

not always the case, as demonstrated by the equipment cost variations and the already discussed *TBG* variations. This issue is discussed in more details next.

It should be mentioned that the DT-based approach is computationally less expensive than the Monte Carlo simulation based approach. It is also computationally more advantageous than the FD approach, as it accurately determines all the parameter sensitivities simultaneously, for small variations of the parameters.

3.4.3 Range of Validity of DT Approach

In order to understand the range of perturbations for which the sensitivity indices computed using the DT-based method is valid, parameters are individually perturbed in a range of ±10% of their p_0 value, computing Ω_{Pft} for each case; sensitivities are then determined using the FD approach for each parameter. Figures 3.14, 3.15, and 3.16 plot the percentage errors between the computed DT and FD sensitivities. Observe that, for the parameters perturbed in Figure 3.14, the error is close to zero; thus, one can conclude that the relation between these parameters and the NPV of profit Ω_{Pft} is linear in nature. In Figure 3.15, the error lies between -50% and 10%, thus demonstrating the nonlinearity of the solar PV investment model with respect to these parameters. In Figure 3.16, note that for the capacity factor of PV at Ottawa, the error is

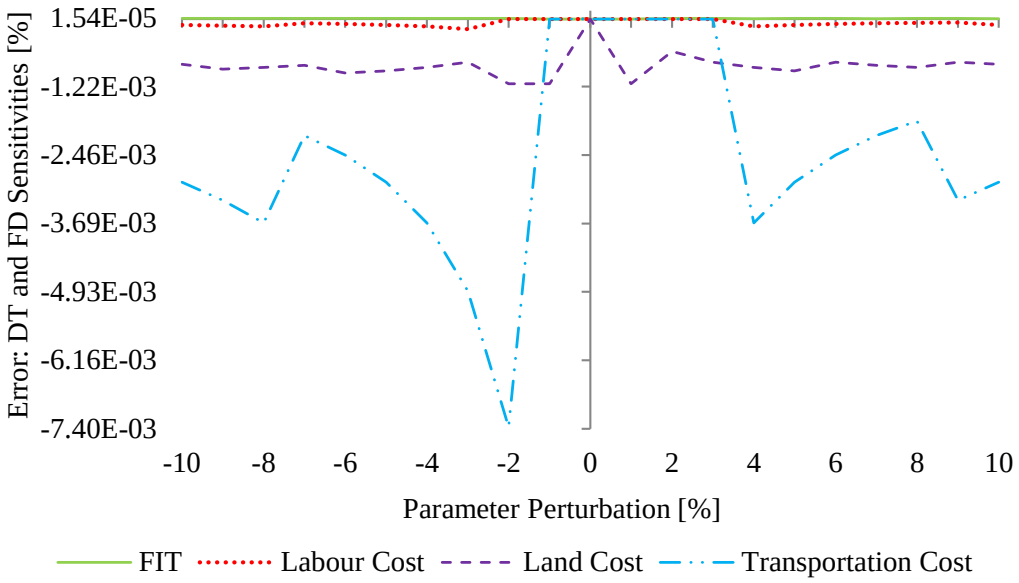

Figure 3.14: Percentage error versus range of parameter perturbation for FIT ρ_{PV}^{ICV}, Labour cost $LbC_{k,i}^{PV}$, Land cost $LdC_{k,i}^{PV}$, and Transportation cost $TC_{k,i}^{PV}$.

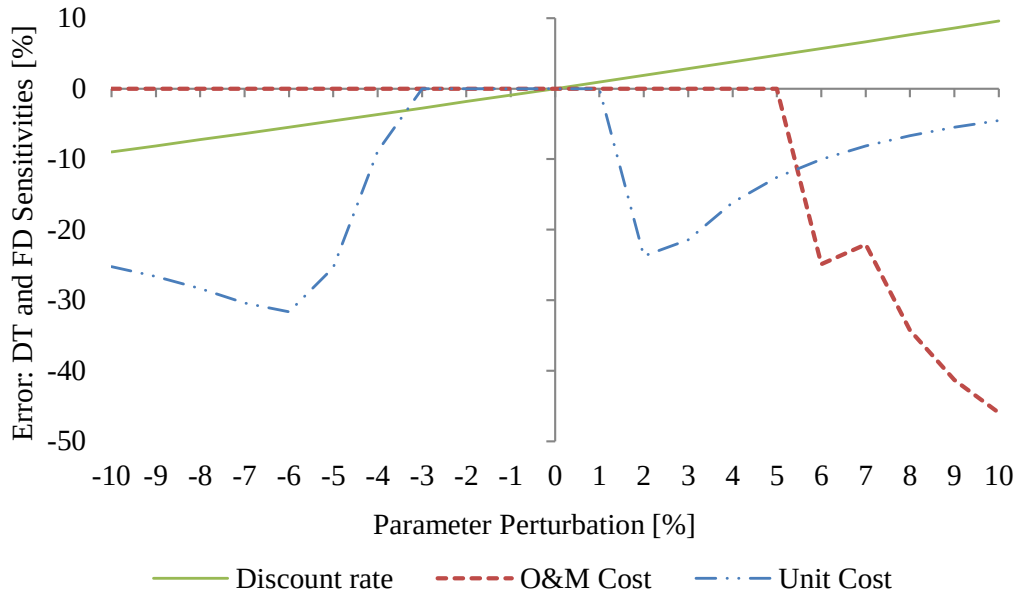

Figure 3.15: Percentage error versus range of parameter perturbation for Discount rate α, Operation and Maintenance cost OM_{k}^{PV}, and Equipment cost UC_{k}^{PV}.

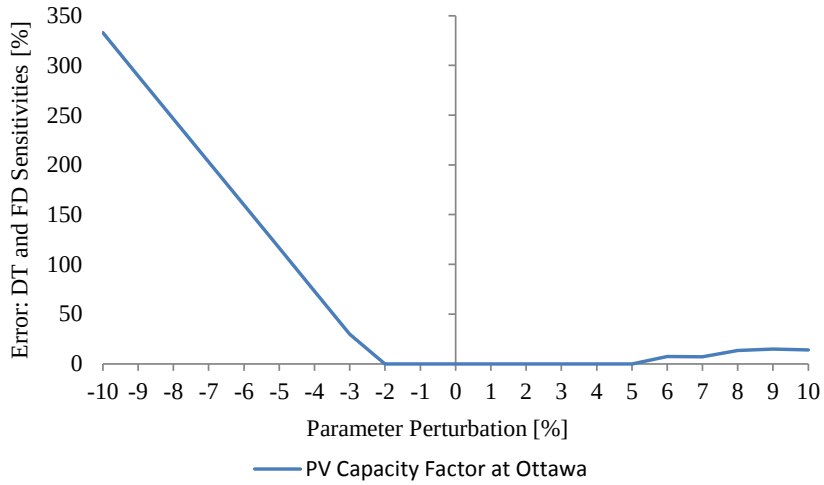

Figure 3.16: Percentage error versus range of parameter perturbation for PV capacity factor $CF^{PV}_{`Ottawa'}$ at Ottawa.

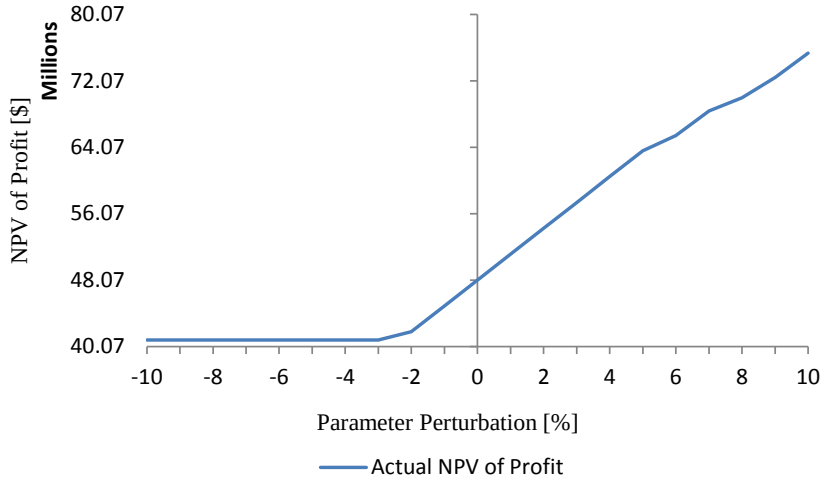

Figure 3.17: Actual NPV of profit versus range of parameter perturbation for PV capacity factor $CF^{PV}_{`Ottawa'}$ at Ottawa.

quite low for positive perturbations, but for negative perturbations below -2%, the error increases significantly. This is due to the NPV variations with respect to PV capacity factor at Ottawa, as shown in Figure 3.17, which depicts the actual Ω_{Pft} when the CF^{PV} at Ottawa is perturbed by ±10% of its base value; observe that for perturbations below -2%, the Ω_{Pft} is constant, and thus

the error depicted in Figure 3.16 increases continuously. This is because when the capacity factor of PV at Ottawa is reduced below the capacity factor value of PV of another zone, the new PV installations are shifted to that zone, and hence the Ω_{Pft} remains unchanged, creating the high percentage errors shown in Fig. 3.16.

3.4.4 Standard Deviation Computation

The standard deviation of the output variable Ω_{Pft} when any number of input parameters is perturbed with $\sigma_p^{\%}$ can be determined using (3.32). A comparison between the calculated standard deviation of Ω_{Pft} versus the actual value obtained from Monte Carlo simulations is presented in Table 3.8 (all histograms of NPV of profit Ω_{Pft}, for all parameter perturbations are presented

Table 3.8: Comparison of calculated and actual standard deviations.

Input Perturbation $\left(\sigma_p^{\%}\right)$				Actual $\sigma_{\Omega}^{\$}$	Calculated $\sigma_{\Omega}^{\$}$	Error
%						
ρ_{PV}^{ICV}	α	$CF_{`Ottawa'}^{PV}$	UC_k^{PV}	Million $	Million $	%
1	0	0	0	3.2508	3.2838	1.0151
2	0	0	0	6.5016	6.5676	1.0154
3	0	0	0	9.7524	9.8514	1.0154
0	1	0	0	2.2926	2.3169	1.0596
0	2	0	0	4.5863	4.6338	1.0348
0	3	0	0	6.8848	6.9507	0.9577
0	0	1	0	3.0566	3.1135	1.8616
0	0	2	0	5.5129	6.2271	12.955
0	0	3	0	7.4471	9.3406	25.427
1	1	0	0	3.9071	3.9603	1.3627
1	1	1	0	4.9366	5.0312	1.9152
1	1	1	1	5.5299	5.5345	0.0833
3	2	1	0	10.982	10.975	-0.0643
4	3	2	1	15.774	15.702	-0.4579

in Appendix A). Observe that the calculated $\sigma^{\$}_{\Omega_{Pft}}$ values are very close to the actual values obtained from Monte Carlo simulations, for all parameter variations not affected significantly by the non-linear nature of the model. This validates the proposed expression (3.32) for various combinations of input parameter perturbations, justifying the use of (3.38) to compute the VaR for various CLs.

3.4.5 Risk Analysis

Table 3.9 presents a comparison of the calculated Ω_0 using (3.38) versus the actual Ω_{Pft} obtained from Monte Carlo simulations (Ω_0^{MC}) for a selected set of perturbed parameters (those with high sensitivity indices), and for various values of CL. Note that the relation in (3.38) provides a more conservative estimate of Ω_0, but allows solar PV investors to adequately evaluate their risk

Table 3.9: Comparison of NPV of profit for various CLs.

Parameter Perturbed by 1%	c_0	Ω_0^{MC} Million $	Ω_0 Million $
ρ_{PV}^{ICV}	99%	40.422	35.560
	95%	42.706	38.043
	90%	43.985	41.147
	85%	44.838	44.251
α	99%	42.767	39.245
	95%	44.182	40.997
	90%	45.074	43.187
	85%	45.611	45.377
CF_{Ottawa}^{PV}	99%	40.896	36.209
	95%	42.899	38.563
	90%	44.112	41.506
	85%	44.919	44.449
UC_k^{PV}	99%	40.775	39.101
	95%	43.054	40.881
	90%	44.735	43.107
	85%	45.634	45.333

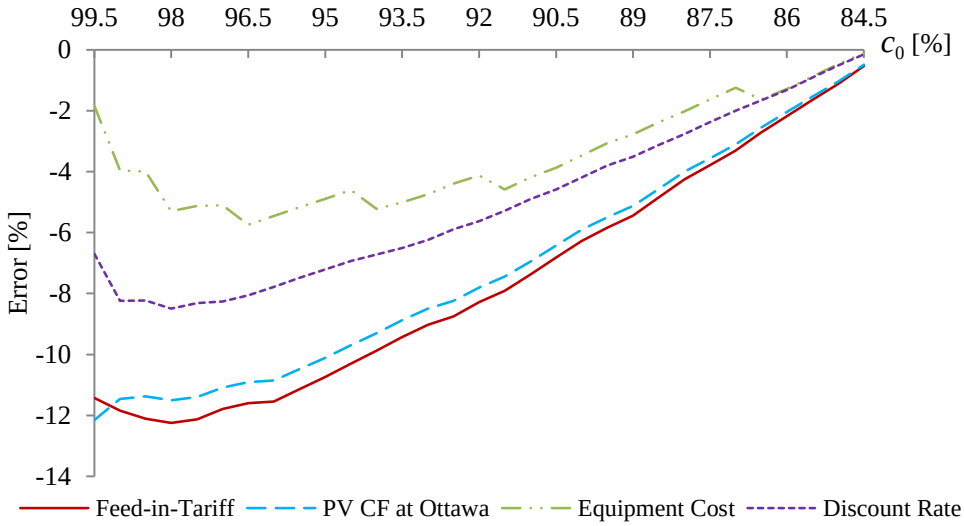

Figure 3.18: Percentage error versus CL with parameters perturbed by a 1% standard deviation.

strategies based on their VaR and the expected rate of return, and thus arrive at an appropriate decision on the investment.

The percentage errors between the Ω_0 obtained with (3.38) and the actual values Ω_0^{MC} determined from the c.d.f. plots resulting from the Monte Carlo simulations with respect to c_0 is shown in Figure 3.18 for four parameters, namely, ρ_{PV}^{ICV}, α, $UC_{k,i}^{PV}$ and CF^{PV} in Ottawa, individually perturbed by 1% standard deviation from their base values $\left(\sigma_p^{\%} = 1\%\right)$. Note that the error values lie in the range of -2% to -12% for 95% or more CL values, and improves as the CL decreases, i.e., as the risk averseness of an investor decreases.

Figure 3.19 plots the error for various CLs for the same set of parameters, simultaneously perturbed in various combinations, by 1% standard deviations from their base values. Observe that the error is higher in these cases, but are still all negative values ranging between -13% and -23% for 95% or more CL, and improves as the CL decreases. This demonstrates that the sensitivity indices computed using the DT-based method yields more conservative risk parameters for the investor, for the given solar PV model, but has significant computational advantages over the Monte Carlo simulation approach.

The input parameters are perturbed with different percentages of their base values and the

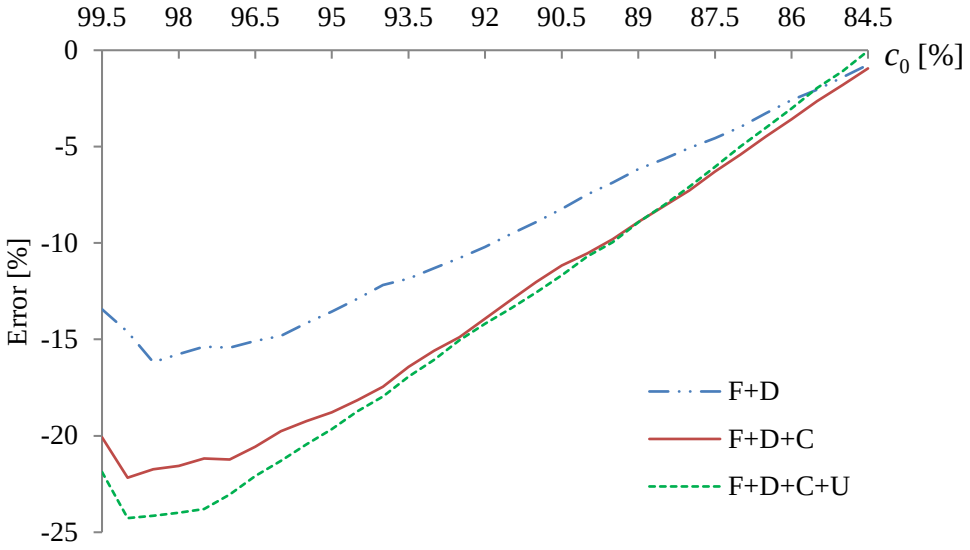

Figure 3.19: Percentage error versus CL when parameters are perturbed simultaneously by a 1% standard deviation. (F: FIT; D: Discount Rate; C: CF PV (Ottawa); U: Unit Cost)

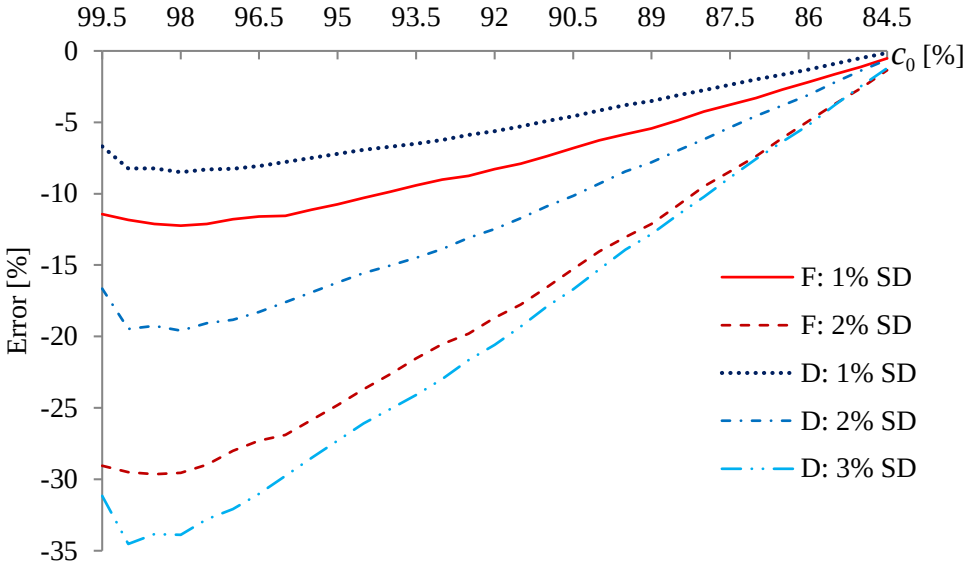

Figure 3.20: Percentage error versus CL when FIT is perturbed for various $\sigma_p^{\%}$ (F: FIT; D: Discount Rate; SD: Standard Deviation).

resulting error graphs are plotted in Figure 3.20. The figure shows the error of computing CL

when the FIT and the Discount Rate are perturbed with standard deviation of various percentages of their base values. Note that the error increases as the standard deviation of the input parameter in consideration increases.

3.5 Summary

This chapter presented the application of the DT-based method of computing sensitivity indices for a solar PV planning model from the perspective of an investor. The sensitivity indices were directly computed from the solar PV optimization model, and only involved the computation of a set of Jacobian matrices and some matrix operations. In the context of this model, the sensitivity indices represent the change in the NPV of investor's profit when model parameters such as the FIT, discount rate, total budget, etc., are varied from their respective base values, one at a time.

The results demonstrated that the sensitivity indices obtained using the DT-based method are very close to those obtained using the Monte Carlo approach, and are the same as the true sensitivity indices obtained using the FD approach. Furthermore, contrary to the Monte-Carlo-simulation-based approach for determining the sensitivity of parameters, which involves a large number of simulations of the solar PV model (in the order of thousands), this approach computes the indices directly at once, thus reducing the computational burden significantly. Moreover, the Monte Carlo simulation approach does not provide any information on the direction of change of the NPV when a parameter is perturbed, contrary to the DT-based method, which is valuable information for the investor. However, the DT-based method, like the FD method, is not able to capture the non-linear nature of the model.

A novel use of the sensitivity indices was also proposed to evaluate the investor's risk indices. Using an approximation of the cumulative distribution function of investor's profit, a linear relation was developed between the sensitivity indices and investor's profit for a certain confidence level. The proposed method to determine the risk parameters provides valuable information on investment risks for an investor, at significantly reduced computational costs, as long as the model behaves approximately linearly.

Chapter 4

Optimal Incentive Design for Targeted Penetration of Renewable Energy Sources

4.1 Introduction

In the previous chapter, a DT-based method was proposed to determine the risk indices for solar PV investment projects from the perspective of investors. In this chapter, a comprehensive GEP model is proposed from the CPA's perspective by considering all capital and O&M costs of new and existing generation plants, as well as incentives and other market price based payments made to investors. In addition, the proposed GEP model considers the incentive payments made by the CPA to LDCs to encourage energy conservation and demand reduction. Also, emissions from generation plants are considered within the proposed model via environmental penalty costs, which can be seen as an indirect incentive. Thus, the overall objective of the proposed holistic GEP is to seek a minimum overall cost considering all the above components, providing the optimal incentives that encourage integration of RES, while achieving targeted levels of RES penetration and demand reduction, and determining the optimal site, size, time, and technology of new generation capacity additions.

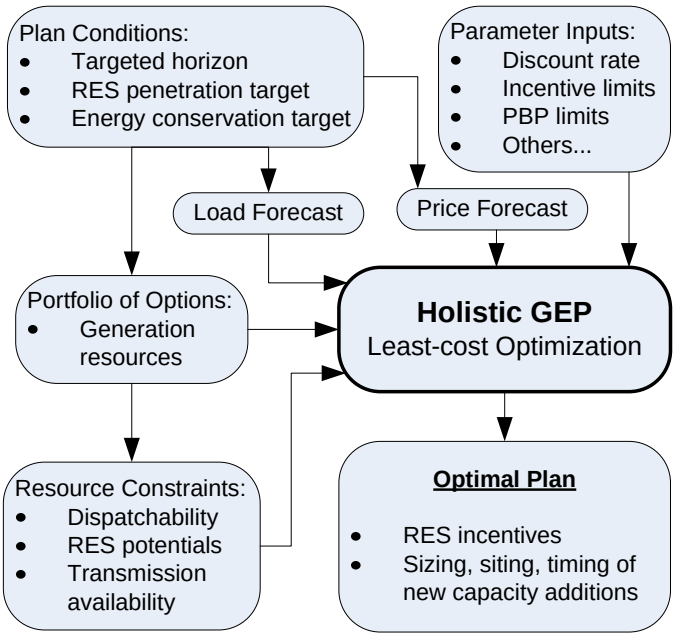

Figure 4.1: Framework of the proposed holistic GEP.

4.2 Proposed Holistic GEP Model

4.2.1 Assumptions

The framework of the proposed holistic GEP model is shown in Figure 4.1, where the main inputs and outputs of the model are highlighted. The assumptions made to develop the proposed model are the following:

- The system is modelled using several transmission zones to adequately represent the main transmission corridors, load variations in different locations, and regional availabilities of solar, wind, and/or hydro generation.
- A DC load flow model is used to determine the power flows between zones, and thus account for the main transmission system constraints and bottlenecks.
- A typical pre-specified loss factor for the transmission system is considered as in other planning studies [31], [80].

- The main input parameters that must be defined and are independent of the grid under study are: the discount rate α; cost of emission per unit energy ζ; generation reserve margin b_0; gestation period g_s; installation plan period N_1; minimum capacity factor for dispatchable sources CF_{s6}^{Min}; RES incentive rates limits ρ_{Max}^{New} and ρ_{Min}^{New}; payback-period limits ϕ^{Max} and ϕ^{Min}; and unit size of installation for new capacity additions ϑ_s.

4.2.2 Planning Objective

The objective of the GEP model (Ω_{Sys}) is to minimize the total system cost and incentive payments from the perspective of the CPA, and is given by:

$$\Omega_{Sys} = \sum_{s} \sum_{k=1}^{N_{Sys}} \sum_{i=1}^{Z} \frac{R_{s,k,i} + C_{s,k,i} + EC_{s,k,i}}{(1+\alpha)^k} + \sum_{k=1}^{N_{Sys}} \sum_{i=1}^{Z} \frac{ECP_{k,i}}{(1+\alpha)^k} \tag{4.1}$$

where R is the total payment made by the CPA to GENCOs (which in effect is their revenue), and is divided into two categories, namely, existing and new, as per:

$$R_{s,k,i} = \underbrace{R_{s1,k,i}^{Ex} + R_{s2,k,i}^{Ex} + R_{s3,k,i}^{Ex}}_{R_{s,k,i}^{Ex}} + \underbrace{R_{s1,k,i}^{New} + R_{s2,k,i}^{New} + R_{s3,k,i}^{New}}_{R_{s,k,i}^{New}} \tag{4.2}$$

These payments may be based on the market price ν^{MP} or regulated price ν^{RP} or incentives ρ, and are computed as follows:

$$R_{s,k,i}^{Ex} = \underbrace{\sum_{b=1}^{3} \nu_{k,b}^{MP} E_{s1,k,i,b}^{Ex}}_{R_{s1,k,i}^{Ex}} + \underbrace{\sum_{b=1}^{3} \nu_{s2,k}^{RP} E_{s2,k,i,b}^{Ex}}_{R_{s2,k,i}^{Ex}} + \underbrace{\rho_{s3,i}^{Ex} \sum_{b=1}^{3} E_{s3,k,i,b}^{Ex}}_{R_{s3,k,i}^{Ex}} \tag{4.3}$$

$$R_{s,k,i}^{New} = \underbrace{\sum_{b=1}^{3} \nu_{k,b}^{MP} E_{s1,k,i,b}^{New}}_{R_{s1,k,i}^{New}} + \underbrace{\sum_{b=1}^{3} \nu_{s2,k}^{RP} E_{s2,k,i,b}^{New}}_{R_{s2,k,i}^{New}} + \underbrace{\rho_{s3,i}^{New} \sum_{b=1}^{3} E_{s3,k,i,b}^{New}}_{R_{s3,k,i}^{New}} \tag{4.4}$$

where $s1 \cup s2 \cup s3 = s$, and the energy E can be written as:

$$E_{s,k,i,b} = E_{s,k,i,b}^{Ex} + E_{s,k,i,b}^{New} \tag{4.5}$$

The decision variables $\rho^{New}_{s3,i}$ in (4.4) are the zonal incentive rates for the corresponding technologies, which are determined from the model solution.

The total cost of generation C in (4.1), similar to CST in (2.2), is the sum of the costs pertaining to installation (CI), fuel (CFL), and O&M (COM) of new and existing facilities:

$$C_{s,k,i} = CI_{s,k,i} + CFL^{Ex}_{s,k,i} + CFL^{New}_{s,k,i} + COM^{Ex}_{s,k,i} + COM^{New}_{s,k,i} \tag{4.6}$$

where CI for all generation technologies are computed using:

$$CI_{s,k,i} = NC_{s,k,i}\, CC_{s,k} \tag{4.7}$$

The CFL of existing and new facilities are dependent on respective fuel prices β, and is given by:

$$CFL^{Ex}_{s,k,i} + CFL^{New}_{s,k,i} = \beta_{s,k} \left(\sum_{b=1}^{3} E^{Ex}_{s,k,i,b} + \sum_{b=1}^{3} E^{New}_{s,k,i,b} \right) \tag{4.8}$$

and the COM for existing and new technologies is given by:

$$COM^{Ex}_{s,k,i} + COM^{New}_{s,k,i} = OMF_{s,k} \left(Cap^{Ex}_{s,k,i} + Cap^{New}_{s,k,i} \right) + OMV_{s,k} \left(\sum_{b=1}^{3} E^{Ex}_{s,k,i,b} + \sum_{b=1}^{3} E^{New}_{s,k,i,b} \right) \tag{4.9}$$

where the generation capacities are obtained as follows:

$$Cap_{s,k,i} = Cap^{Ex}_{s,k,i} + Cap^{New}_{s,k,i} \tag{4.10}$$

The emission cost in (4.1), given by (EC), is obtained as follows:

$$EC_{s,k,i} = \zeta\, Em_s \sum_{b=1}^{3} E_{s,k,i,b} \tag{4.11}$$

and the incentive payments (ECP) on energy conservation (CN) and demand reduction (DR), given in (4.1), are calculated as:

$$ECP_{k,i} = a_0 \sum_{b=1}^{3} CN_{k,i,b} + \sum_{b=1}^{3} a_b DR_{k,i,b} \tag{4.12}$$

where *DR* is related to *CN* as follows:

$$CN_{k,i,b} = DR_{k,i,b}\Delta t_b \tag{4.13}$$

assuming that $a_b = a_0\Delta t_b$, since this ensures equal weight for *CN* and *DR* in *ECP*, by equating their corresponding incentive payments. The incentive rates for energy conservation (a_0) and demand reduction (a_b) are adjustable parameters which need to be tuned optimally to achieve targeted energy conservation levels, as explained in details in Section 4.3.2.

4.2.3 Model Constraints

Energy Balance

This constraint ensures zonal energy demand-supply balance and also takes into account the energy transfer between transmission zones, as follows:

$$\sum_{s5} E_{s5,k,i,b} - \sum_{j=1}^{Z} ET_{k,i,j,b} + \sum_{j=1}^{Z} ET_{k,j,i,b}(1 - LF) = \left(ED_{k,i,b} - \sum_{s4} E_{s4,k,i,b}\right) - CN_{k,i,b} \tag{4.14}$$

where $s4 \cup s5 = s$, and *ET*, a positive decision variable, is related to bus voltage angles by the dc power flow equations:

$$ET_{k,i,j,b} = B_{k,i,j}(\delta_{k,i,b} - \delta_{k,j,b})\Delta t_b \tag{4.15}$$

Power Transfer and Bus Angle Limits

The following limits ensure the operational security of the transmission system, as follows:

$$ET_{k,i,j,b} \leq PT_{k,i,j}^{Max}\Delta t_b \tag{4.16}$$

$$\delta^{Min} \leq \delta_{k,i,t} \leq \delta^{Max}. \tag{4.17}$$

Adequacy Limit

The following constraint ensures that the proposed GEP considers the system reliability by guaranteeing that a specified generation reserve margin (GRM), as defined in [59], is maintained in the system, while taking into account the peak demand reduction resulting from energy conservation measures, and where b_0 (GRM) is a given percentage of peak demand:

$$\sum_{s}\sum_{i=1}^{Z} Cap_{s,k,i} \geq (1 + b_0)\sum_{i=1}^{Z} PD_{k,i} - \sum_{i=1}^{Z} DR_{k,i,\text{“3”}} \tag{4.18}$$

Dynamic Constraint on Capacity Addition

This is incorporated as follows:

$$Cap^{New}_{s,k+1,i} = NC_{s,k,i} + Cap^{New}_{s,k,i} \tag{4.19}$$

where the timing for new installations are bounded by g_s and N_1 as follows:

$$NC_{s,k,i} = 0 \;\forall\; k = 1, \ldots, g_s, (N_1 + 1), \ldots, N \text{ for } N_1 > g_s \tag{4.20}$$

Here, it is assumed that, if a given capacity is commissioned in year k, the total investment and installation takes place in year *k–1*, instead of being distributed over the typical gestation period g_s. Since commissioning takes g_s years from the initiation of the plan, (4.20) is used to defer the commissioning by a minimum of g_s years, as shown in Figure 4.2; and N_1 is assumed to be the year in the planning horizon after which there is no new installations.

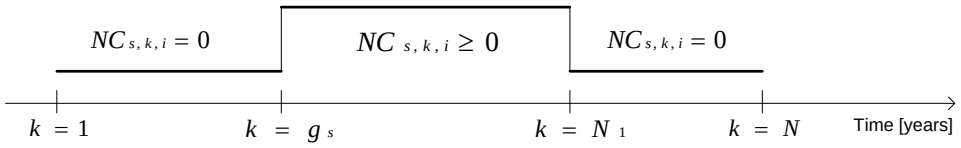

Figure 4.2: Dynamic new capacity additions.

Energy Dispatchability Constraint

The annual maximum energy generation capability of dispatchable sources is given by:

$$\sum_{b=1}^{3} E_{s6,k,i,b} \leq 8760\ CF_{s6} Cap_{s6,k,i} \tag{4.21}$$

while, for non-dispatchable sources, the annual energy generation should satisfy the following:

$$\sum_{b=1}^{3} E_{s7,k,i,b} = 8760\ CF_{s7,i} Cap_{s7,k,i} \tag{4.22}$$

where $s6 \cup s7 = s$. Note that (4.22) is an equality constraint, and provides an appropriate representation of non-dispatchable RES in the plan, as these sources do not have the flexibility to adjust their generation and will generate as per their assumed annual capacity factor, whereas non-dispatchable sources in (4.21) have the flexibility to adjust their generation as required.

Power and Minimum Energy Generation Limits

The following constraint is imposed on existing dispatchable capacities, so that the new plan does not shut them down before their usual end of life, in favour of less costly alternatives:

$$\sum_{b=1}^{3} E^{Ex}_{s6,k,i,b} \geq 8760\ CF^{Min}_{s6} Cap^{Ex}_{s6,k,i} \tag{4.23}$$

And the power generated at different time blocks is limited by the available capacity as follows:

$$E_{s,k,i,b}/\Delta t_b \leq Cap_{s,k,i} \tag{4.24}$$

In addition, the price regulated capacities have a minimum power generation limit (ψ) at base load, given by:

$$E_{s2,k,i,b}/\Delta t_b \geq \psi_{s2}\ Cap_{s2,k,i} \tag{4.25}$$

Discounted Pay-Back-Period (PBP) Constraint

The following constraint ensures that the PBP is bounded by specified periods, with a lower limit imposed so that the incentives are not too high:

$$\phi_{s3,i}^{Min} \leq \phi_{s3,i} \leq \phi_{s3,i}^{Max} \tag{4.26}$$

Here, ϕ is computed using the following non-linear equation:

$$\phi_{s3,i}\left[\left\{\sum_{k=1}^{N_{Sys}} \frac{R_{s3,k,i}^{New} - \left(COM_{s3,k,i}^{New} + CFL_{s3,k,i}^{New}\right)}{(1+\alpha)^k}\right\}\theta\right] = \sum_{k=1}^{N_{Sys}} \frac{CI_{s3,k,i}}{(1+\alpha)^k} \tag{4.27}$$

where the right hand side of (4.27) is the NPV of installation costs, and the left hand side is the product of PBP and levelized cash flow, with the latter being distributed evenly over the planning horizon N from the NPV of cash flow, using a capital recovery factor θ.

Integer Constraint

Binary variables are used to obtain integer solutions for the new capacity additions as follows:

$$NC_{s,k,i} = \sum_{q=1}^{Q_s} \vartheta_s W_{s,k,i,q} \tag{4.28}$$

RES Penetration Target

This is achieved as follows:

$$\sum_{s8}\sum_{i=1}^{Z} Cap_{s8,k,i} \geq \varpi \sum_{s}\sum_{i=1}^{Z} Cap_{s,k,i} \quad for \quad k = N_1 \tag{4.29}$$

If the target applies to incentive based technologies only, then *s8* will be replaced by *s3* and ϖ by ϖ^{s3}.

Energy and Power Potentials

Annual energy generation potential or zonal new capacity addition potential, as applicable, are given by:

$$\sum_{i=1}^{Z} \sum_{b=1}^{3} E_{s,k,i,b} \leq \Upsilon_{s,k} \tag{4.30}$$

$$\sum_{k=1}^{N_{Sys}} NC_{s,k,i} \leq \Gamma_{s,i} \tag{4.31}$$

Equations (4.1) to (4.29) describe the nonlinear mathematical optimization model (MINLP) of the holistic GEP, with nonlinearities in (4.4) and (4.27) only. Constraints (4.30) and (4.31) are included in the optimization model only when applicable.

4.2.4 Model Linearization

The linearization technique described in Section 2.4.1 is applied to the proposed holistic GEP model to transform it into an MILP problem, and thus allow for simpler and well-tested solution approaches.

Optimal RES Incentives

The nonlinear part of (4.4) can be rewritten as:

$$R^{New}_{s3,k,i} = \rho^{New}_{s3,i} \sum_{b=1}^{3} E^{New}_{s3,k,i,b} \tag{4.32}$$

Thus, the nonlinearity can be removed by the linearization approach as follows:

$$R^{New}_{s3,k,i} \leq \rho^{New}_{Max} \sum_{b=1}^{3} E^{New}_{s3,k,i,b} \tag{4.33}$$

$$R^{New}_{s3,k,i} \geq \rho^{New}_{Min} \sum_{b=1}^{3} E^{New}_{s3,k,i,b} \tag{4.34}$$

Hence, replacing (4.4) by the following:

$$R^{New}_{s,k,i} = \sum_{b=1}^{3} \nu^{MP}_{k,b} E^{New}_{s1,k,i,b} + \sum_{b=1}^{3} \nu^{RP}_{s2,k} E^{New}_{s2,k,i,b} + R^{New}_{s3,k,i} \tag{4.35}$$

together with (4.33) and (4.34), removes the nonlinearity.

The zonal values of $\rho^{New}_{s3,i}$ for the incentive-driven sources can later be calculated from the model solution using:

$$\rho^{New}_{s3,i} \left(\sum_{k=1}^{N_{Sys}} \sum_{b=1}^{3} E^{New}_{s3,k,i,b} \right) = \sum_{k=1}^{N_{Sys}} R^{New}_{s3,k,i} \tag{4.36}$$

and the province-wide values of ρ^{New}_{s3} can later be computed as follows:

$$\rho^{New}_{s3} \left(\sum_{k=1}^{N_{Sys}} \sum_{i=1}^{Z} \sum_{b=1}^{3} E^{New}_{s3,k,i,b} \right) = \sum_{k=1}^{N_{Sys}} \sum_{i=1}^{Z} R^{New}_{s3,k,i} \tag{4.37}$$

Pay-Back Period

The PBP computation is linearized by replacing (4.26) and (4.27) with:

$$\sum_{k=1}^{N_{Sys}} \frac{CI_{s3,k,i}}{(1+\alpha)^k} \leq \phi^{Max}_{s3,i} \left(\sum_{k=1}^{N_{Sys}} \frac{R^{New}_{s3,k,i} - \left(COM^{New}_{s3,k,i} + CFL^{New}_{s3,k,i} \right)}{(1+\alpha)^k} \right) \theta \tag{4.38}$$

$$\sum_{k=1}^{N_{Sys}} \frac{CI_{s3,k,i}}{(1+\alpha)^k} \geq \phi^{Min}_{s3,i} \left(\sum_{k=1}^{N_{Sys}} \frac{R^{New}_{s3,k,i} - \left(COM^{New}_{s3,k,i} + CFL^{New}_{s3,k,i} \right)}{(1+\alpha)^k} \right) \theta \tag{4.39}$$

Then, ϕ can later be computed from the optimization solution using (4.27).

The final linearized holistic GEP model in MILP form thus comprises equations (4.1) to (4.3), (4.5) to (4.25), (4.28), (4.29), (4.33) to (4.35), (4.38) and (4.39), with (4.30) and (4.31) being included when applicable, as shown in Figure 4.3.

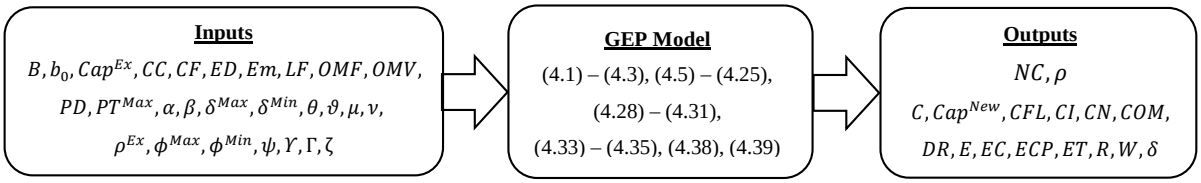

Figure 4.3: Inputs and output variables and equations of the proposed GEP model.

4.3 Application to Ontario, Canada

The holistic GEP model is implemented for the province of Ontario, Canada, with a plan horizon (N_{Sys}) of 25 years, i.e., 2011 to 2035. A simplified ten-zone transmission system model for Ontario is used, as shown in Figure 3.2 [75], where the relevant transmission data ($PT^{Max}_{k,i,j}$, $B_{k,i,j}$) is given in Tables 3.1 and 3.2 [76], along with an assumed transmission loss factor (LF) of 5%.

The set of market price based technologies (*s1*) are COAL, GAS, OIL, and some hydro units (HNR). Similarly, some hydro and nuclear generators receiving regulated prices (HR and NR, respectively) and nuclear generators with contracted prices (NCP) form the set *s2*. The incentive-driven technologies (*s3*) are biomass (BIO), ground-mounted PV (GPV), rooftop PV (RPV), wind onshore (WON) and wind offshore (WOF) generation. Furthermore, only RPV is considered to be a distribution connected resource (*s4*), and all types of wind and solar generation are considered non-dispatchable (*s6*).

4.3.1 Input Parameters

The base-line generation capacities, i.e., the capacity in the system at the start of the planning horizon, and how it changes over the plan period, are shown in Figure 4.4 [35], [78], which depicts the shutdown of coal based plants in 2014, as per the IPSP [35], with the objective of reducing emissions; the end-of-life shutdown of one NR generation facility in 2020 is also shown (Pickering, in TORONTO zone). It is further assumed that other existing technologies will not reach their end of life during the plan horizon.

The capital cost CC for all technologies considered in the GEP model is the equipment cost (UC) portion only in (2.11), neglecting the labour (LbC), land (LdC), and transportation (TC)

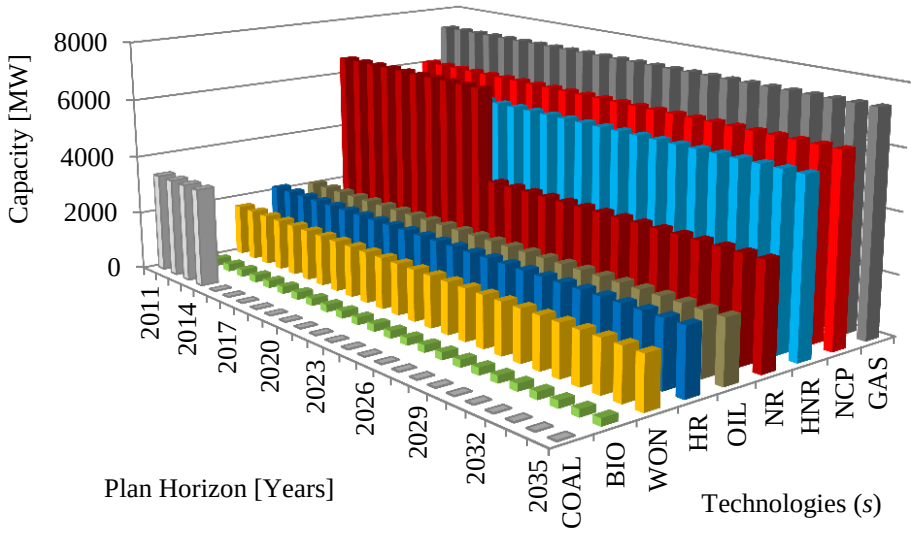

Figure 4.4: Base-line capacities and their continuity over the plan horizon [35], [78].

Table 4.1: Cost components of generation technologies and CO_2 emission [81].

s	$CC_{s,1}$		$O\&M$		Em_s
	Cost [$/kW]	Increment [%]	$OMF_{s,1}$ [$/kW]	$OMV_{s,1}$ [$/MWh]	[Kg of eqCO$_2$ per MWh]
BIO	3859	-0.18	100.55	5.0	107
COAL	3804	-0.14	49.29	6.39	1100
GAS	820	-0.16	6.84	12.29	610
GPV	4755	-0.21	16.7	0	58
HNR, HR	2347	-0.07	14.27	2.55	17.5
NR, NCP	5335	-0.18	88.75	2.04	13.4
OIL	1347	-0.15	30.25	6.45	850
RPV	6050	-0.21	26.04	0	58
WON	2437	-0.11	28.07	0	19
WOF	5974	-0.15	53.33	0	14

costs. The *CC* and the O&M cost (*OMV*, *OMF*) data for the first year is shown in Table 4.1 [81]. The annual increments in *CC* are calculated using last 10-year data [81], [82], while for O&M costs, the annual increment is assumed to be 4% (inflation rate). Table 4.1 also includes the

Table 4.2: Zonal capacity factors and potentials of non-dispatchable sources.

i	GPV		RPV		WON		WOF	
	CF_i [%]	Γ_i [MW]	CF_i [%]	Γ_i [MW]	CF_i [%]	Γ_i [MW]	CF_i [%]	Γ_i [MW]
NW	13.70	130	14.27	7	29.21	107	34.62	0
NE	13.13	203	13.70	12	33.40	935	38.83	1495
ESSA	13.13	218	13.70	15	32.16	0	37.57	0
OTTAWA	15.84	21	15.98	19	30.92	0	0	0
EAST	15.13	167	15.70	24	34.36	0	40.04	0
TORONTO	13.70	30	13.98	104	31.40	0	35.70	0
NIAGARA	13.13	129	13.70	9	24.22	0	28.18	0
SW	13.13	462	13.70	50	26.91	200	31.31	2030
BRUCE	13.13	173	13.70	2	36.05	0	41.53	405
WEST	15.13	464	15.70	23	36.97	33	42.63	1945
ONTARIO	-	**1997**	-	**265**	-	**1275**	-	**5875**

$eq\mathrm{CO}_2$ emission per unit energy produced [83].

Capacity factors of all non-dispatchable resources, i.e., solar PV and wind, computed from [77] and [78] respectively, are shown in Table 4.2, which also includes the zonal power generation potentials ($\Gamma_{s,i}$) for these technologies. The GPV generation potential is computed by assuming the zonal land availability and considering a 5 kWh/m^2 energy density. For RPV, the number of households in each zone is estimated based on [84], and it is assumed that a maximum of 1% of them will have installed rooftop panels. It is further assumed that the average rated capacity of rooftop panels is 5 kW. The potential for wind generation is based on the most favourable sites available [35]. The maximum value of CF_i attainable by dispatchable sources are assumed to be 100% for all except BIO (70%), HNR (85%), and HR (90%), based on last 10-years data from [78], while a CF^{Min} is imposed for existing capacities based on data available at the IESO [78], resulting in minimum averages of 30% for BIO, COAL and HNR, and 20% for GAS and OIL. Additionally, for HR, NCP and NR, a minimum generation (ψ) of 60% at all times is assumed.

The average annual electricity market price is computed using price duration curves of Hourly

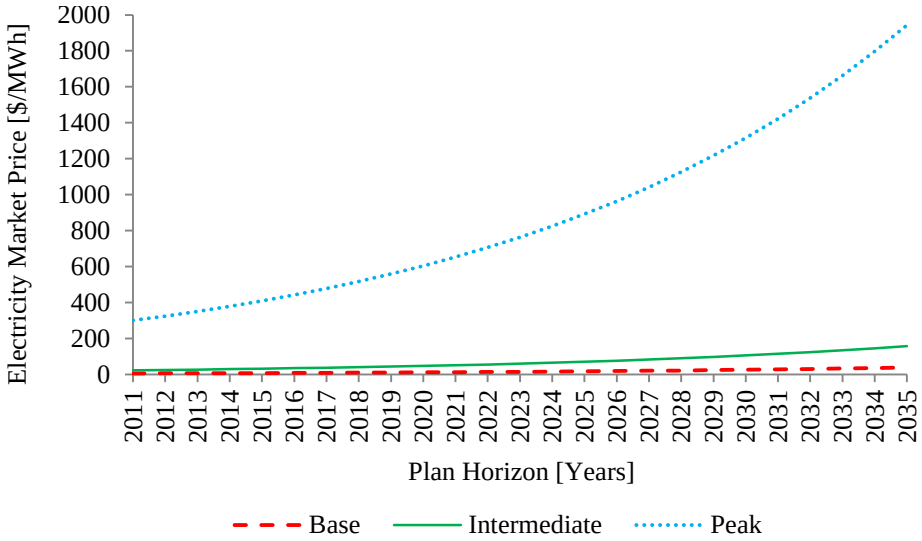

Figure 4.5: Long-term market-price ν^{MP} estimates [78].

Ontario Energy Price (HOEP) [78], yielding $\nu^{MP}_{1,b}$ = [5.08 22.61 299.54] \$/MWh and corresponding growth rates of 8.8%, 8.4% and 8.1% for the respective time blocks, as depicted in Figure 4.5. It is to be noted that the peak market prices are expected to increase and reach significantly high values in the coming years as compared to the base and intermediate prices.

The FIT rates offered by the OPA in 2009 are the existing incentives (ρ^{Ex}) used for BIO (151.29 \$/MWh), GPV (443 \$/MWh), RPV (672.25 \$/MWh), WON (135 \$/MWh), and WOF (190 \$/MWh) [12]. Regulated prices (ν^{RP}) of HR (35 \$/MWh), NR (55 \$/MWh) and NCP (60 \$/MWh) are from [85], [86]. Additionally, all the regulated/contract prices are assumed to have an annual growth rate equal to the base (b = 1) growth rate of the HOEP, i.e., 8.8%.

The annual fuel cost (β_k) for COAL, OIL and GAS is taken from [81], shown in Figure 4.6, and it is assumed to be 12 \$/MWh for BIO [87], 7.5 \$/MWh for NR and NCP [88], and zero for other technologies.

The IPSP forecasts a demand growth rate over the period 2007–2027 for base (23%), intermediate (38%) and peak (21%) load [35]. Using this information, and the zonal energy and power demands for 2011 [78], the annual growth rates are obtained and depicted in Table 4.3, where *PD* growth rate is assumed to be the same as the peak energy growth rate. The IPSP also

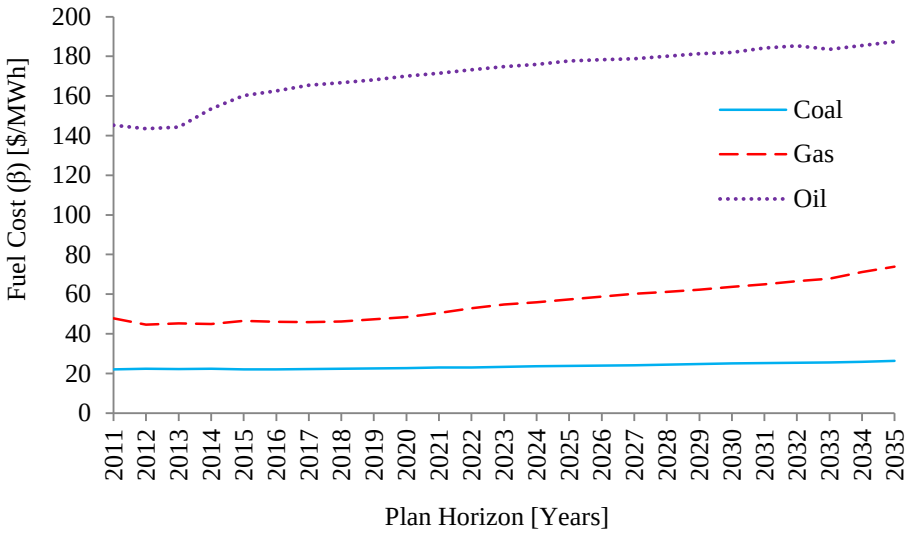

Figure 4.6: Long-term fuel cost β estimates for fossil fuel sources [81].

Table 4.3: Zonal energy and power demand and their annual growth rates.

i	$ED_{1,i,b}$ [GWh]			Growth Rate [%]			$PD_{1,i}$
	Base	Int.	Peak	Base	Int.	Peak	[MW]
NW	3066	1298	62	0.05	0.26	0.18	728
NE	7139	3265	126	−0.28	−0.36	−0.27	1710
ESSA	4888	3350	201	0.86	1.41	0.93	1612
OTTAWA	6412	3110	272	0.93	1.74	1.55	1874
EAST	5772	2771	227	0.56	0.99	0.47	1647
TORONTO	33585	16133	1692	1.11	1.73	1.02	10285
NIAGARA	3101	1433	172	0.56	0.88	0.51	970
SW	18930	8198	562	1.11	1.7	0.89	4873
BRUCE	131	534	46	0.48	0.85	0.63	210
WEST	9408	4538	474	1.05	1.47	0.99	2886

specifies a target of 1500 GWh of Ontario-wide energy conservation per year, with 10,700 MW of total capacity target for *s3* technologies by 2018, and 15,700 MW of *s8* technologies by 2025. Hence, (4.29) in the GEP model is redefined as:

Table 4.4: Generation input parameters assumed for the GEP model.

s	g_s [years]	CF_{s6} [%]	CF_{s6}^{Min} [%]	ϑ_s [MW]
BIO	3	70	30	1
COAL	N	100	30	0
GAS	2	100	20	20
HNR	4	85	30	1
HR	4	90	60	50
NCP	6	100	60	500
NR	6	100	60	500
GPV	2	Not Applicable		1
RPV	1			1
WON	3			1
WOF	4			5

Table 4.5: Additional input parameters assumed for the GEP model.

b_0	LF	N	N_1	α	ψ_{s2}	δ^{Max}
10%	5%	25 years	15 years	8%	60%	$+\pi$
$\phi_{s3,i}^{Max}$	$\phi_{s3,i}^{Min}$	ζ		ρ_{Max}^{New}	ρ_{Min}^{New}	δ^{Min}
10 years	2 years	\$100/ton of $eq\mathrm{CO}_2$		\$1000/MWh	\$1/MWh	$-\pi$

$$\sum_{s3}\sum_{i=1}^{Z} Cap_{s3,\text{“2018”},i} \geq 10,700 \tag{4.40}$$

$$\sum_{s8}\sum_{i=1}^{Z} Cap_{s8,\text{“2025”},i} \geq 15,700 \tag{4.41}$$

The duration of load blocks for the base ($b = 1$), intermediate ($b = 2$) and peak ($b = 3$) are estimated from [78] to be 43%, 51% and 6% of 8760 hrs, respectively. (Zonal load duration curves are shown in Appendix B.) Other relevant input parameters are the discount rate $\alpha = 8\%$, GRM $b_0 = 10\%$, and emission penalty $\zeta = 100$ \$/ton of $eq\mathrm{CO}_2$. A summary of all assumed main input parameters required for the model are given in Tables 4.4 and 4.5.

4.3.2 Base Case Scenario

Selection of Energy Conservation Incentive Rate

The proposed holistic GEP model is solved using CPLEX [69] in the GAMS environment [70]. The initial task is to determine the appropriate value of a_0 for a given energy conservation target. Thus, Figure 4.7 shows the effect of varying a_0 on attaining the desired energy conservation target. The results demonstrate that for $1 \leq a_0 \leq 35$ \$/MWh, 100% of the targeted energy conservation is achieved even when the targets and discounted PBPs vary. By increasing a_0 above 35 \$/MWh, the plan fails to achieve the targeted level of annual energy conservation, since from the planner's perspective, energy generation and supply becomes cheaper than the incentive payment.

The energy conservation target *CN* of the base case scenario (*Case–0*) is varied from 0 to 3000 GWh/year, i.e., from no conservation to twice the desired target. Figures 4.8 and 4.9 show that variations in a_0 has no significant effect on new *s3* installations NC_{s3} or their corresponding incentives ρ_{s3}^{New}, respectively. This is important for the central planner, as it renders the deci-

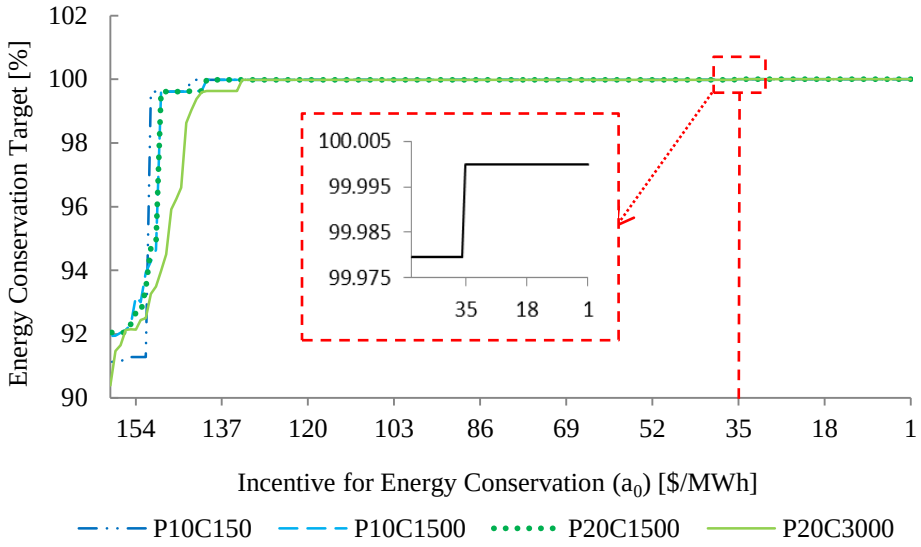

Figure 4.7: Energy conservation incentives (P10C150 means PBP limit ϕ^{Max} = 10 years, and conservation target *CN* = 150 GWh/year).

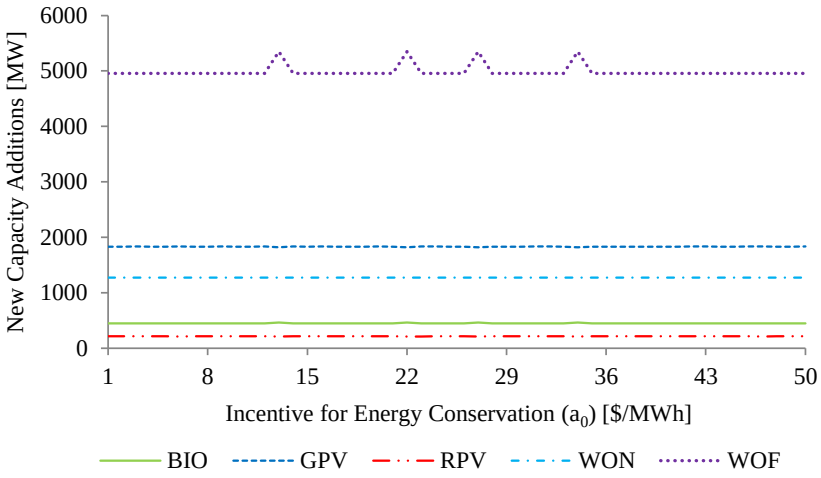

Figure 4.8: Effect of a_0 on new *s3* capacity additions NC_{s3}.

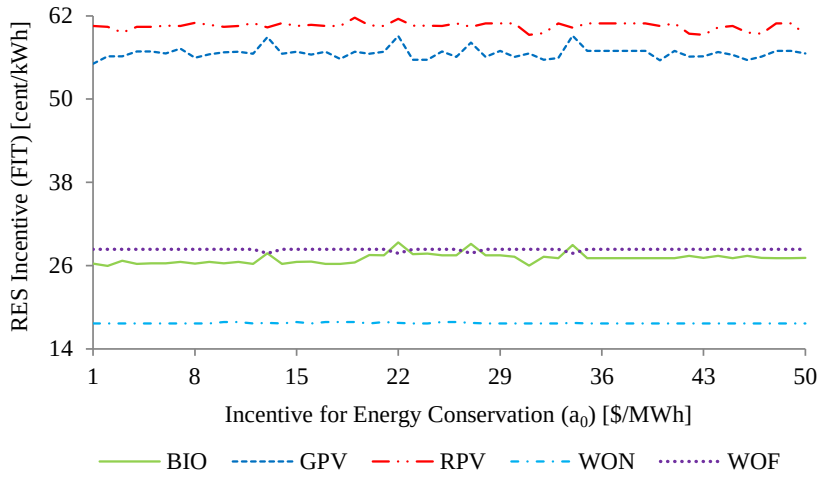

Figure 4.9: Effect of a_0 on incentives for new *s3* capacity additions ρ_{s3}^{New}.

sion making on a_0 basically independent from the optimal decision on ρ_{s3}^{New}. Therefore, a_0 = 35 $/MWh is selected for all the studies reported in this thesis, so that LDCs are encouraged to implement energy conservation. On the other hand, new installations of GAS declined steadily (see Figure 4.10a) for an increasing energy conservation target, signifying a reduction in the peak serving GAS plants, as the *CN* measures incorporated in this GEP model reduces the peak demand. It is also found (see Figure 4.10b) that the total system costs and payments, i.e., Ω_{Sys},

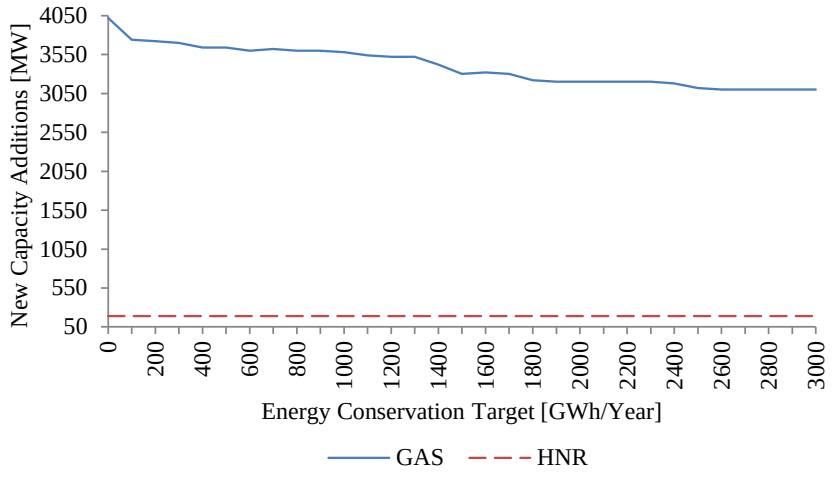

(a) NC_{s1} vs. CN

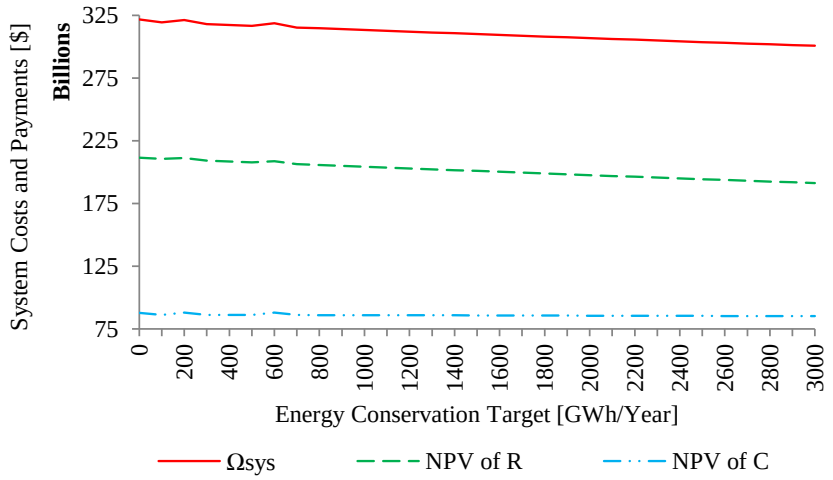

(b) Costs and Payments vs. CN

Figure 4.10: Effect of variation in energy conservation target (CN) on new capacity additions (NC_{s1}) and NPV of system costs and payments, with ϕ^{Max} = 10 years.

reduces by $21 billion, along with a similar reduction in the NPV of R, while the NPV of cost of generation (C) drops by nearly $4 billion, which gets nullified by the incentive payments made to LDCs for introducing conservation. Thus, Figure 4.10 suggests that adoption of conservation measures is not only beneficial for the LDCs (receives incentives) and GENCOs (cost reduction), but also less costly from the system planner's point of view, which may as well result in a

reduction in the consumers' electricity bill.

The Holistic Plan and Optimal Incentive Design

The holistic plan results are based on an energy conservation target of 1500 GWh/year and ϕ^{Max} = 10 years. Figure 4.11 presents the optimal generation capacity plan obtained from the proposed holistic GEP model. Note that the main capacity additions are from wind (WON and WOF) and GAS technologies with small support from BIO, PV and HNR. The effective peak demand *PD* in Figure 4.11 is essentially the right-hand-side of (4.18), and corresponds to the annual Ontario demand with specified GRM, minus the demand reduction target. Similarly, the optimal annual energy supply-demand balance is shown in Figure 4.12, where the effective energy demand is the actual provincial energy demand minus of the energy conservation achieved. Observe that the optimal energy supply mix results in a reduced contribution from nuclear generation in order to accommodate energy generation from non-dispatchable resources.

The holistic GEP solution suggests, as shown in Tables 4.6 and 4.7, that only incentive driven and market price based technologies are economically viable for future installations. Table 4.7 shows the optimal incentive rates with respective IRR for *s3* technologies, along with the sizing,

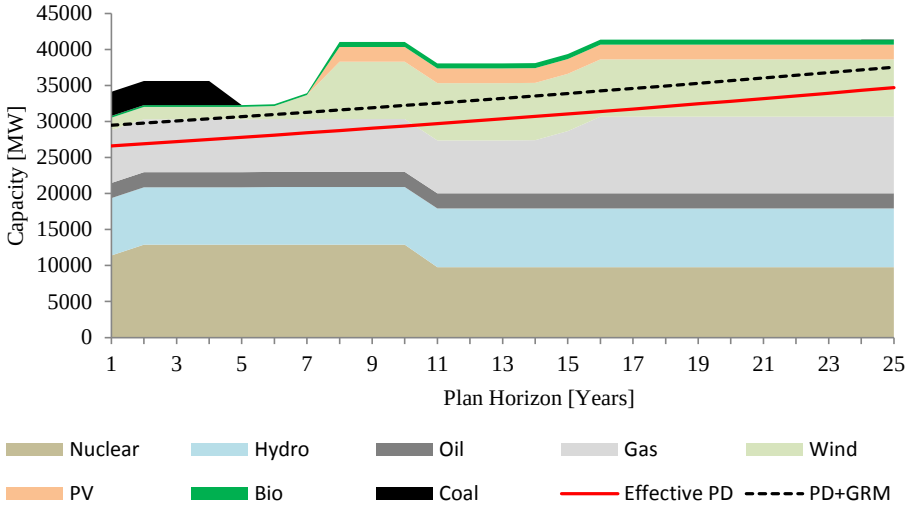

Figure 4.11: Optimal generation capacity plan to supply the effective peak demand.

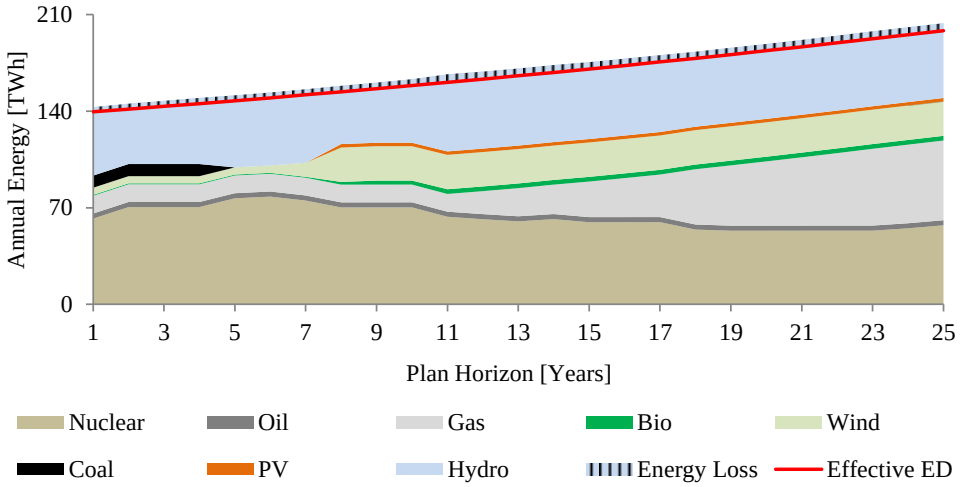

Figure 4.12: Energy supply-demand balance including energy conservation.

Table 4.6: Size (NC), site (i), time (k) and PBP (ϕ) of new ν^{MP}–based Technologies.

s1	$i\rightarrow$	ESSA	OTTAWA			EAST	TORONTO		NIAGARA	SW
GAS	k	-	13	14	15	-	14	15	-	-
	NC [MW]		40	260	1000		1000	1000		
	ϕ [years]		2				2			
HNR	k	10	5			10	-		10	10
	NC [MW]	39	41			85			16	9
	ϕ [years]	6	4			5			9	7

siting and timing of their new installations. It should be noted that the provincial ρ_{s3}^{New} are higher than ρ_{s3}^{Ex}, which indicates that the existing incentives have higher PBPs and, consequently, lower IRRs than the proposed ones. Also, from Figure 4.12), it can be observed that energy generation from gas increases continuously since the installation of new capacities in year 13, which is also reflected in their very small PBPs, as shown in Table 4.6.

It is observed from the GEP solution that the total capacity of *s3* technologies increased from 1975 MW in 2011 to the target of 10,700 MW in 2035, and the penetration of incentive-based technologies reached 25.87% from a mere 5.79%. Consequently, in the case of *s8* technologies (*s3* group plus hydro), the penetration changed from 29.15% (9939 MW) to 45.59% (18,854 MW), exceeding the target *s8* penetration of 15,700 MW.

Table 4.7: Provincial and zonal incentives (ρ^{New}) and IRRs, with optimal sizing (*NC*), siting (*i*) and timing (*k*) of new capacity additions for *s3* technologies.

s3	*i*→	NW	NE	ESSA	OTTAWA	EAST	TORONTO	NIAGARA	SW	BRUCE	WEST	**ONTARIO**
BIO	*k*	-	-	7	7	7	7	-	7	-	-	**7**
	NC [MW]			200	15	150	25		58			**448**
	ρ^{New} [¢/kWh]			27.60	18.20	26.86	27.77		28.08			**27.10**
	IRR [%]			22.03	14.65	24.29	25.24		21.57			**22.66**
GPV	*k*	7	7	7	7	7	7	7	7	5 7	7	**5,7**
	NC [MW]	129	202	217	20	167	29	129	461	16 1	463	**1834**
	ρ^{New} [¢/kWh]	62.54	56.96	53.48	55.49	57.60	62.57	64.80	56.96	48.38	50.49	**55.75**
	IRR [%]	14.90	12.65	11.68	15.35	15.20	14.90	14.78	12.65	10.22	12.99	**13.21**
RPV	*k*	7	7	7	7	7	7	6 7	7	-	-	**6,7**
	NC [MW]	1	1	14	18	24	103	1 2	49			**213**
	ρ^{New} [¢/kWh]	69.59	71.08	61.29	51.83	55.54	59.25	70.28	62.78			**59.25**
	IRR [%]	13.18	12.96	10.68	10.40	11.15	10.40	12.66 12.68	10.95			**10.14**
WON	*k*	7	7	-	-	-	-	-	7	-	5	**5,7**
	NC [MW]	107	935						200		33	**1275**
	ρ^{New} [¢/kWh]	18.78	17.07						21.75		12.17	**17.65**
	IRR [%]	17.62	18.45						19.03		13.84	**18.51**
WOF	*k*	-	7	-	-	-	-	-	5 6 7	7	6 7	**5,6,7**
	NC [MW]		995						30 995 995	405	540 995	**4955**
	ρ^{New} [¢/kWh]		27.10						33.47	25.72	24.70	**28.33**
	IRR [%]		13.21						13.25 13.38 13.33	13.67	13.45 13.41	**13.39**

4.3.3 Case Studies

Presence/Absence of Targets

The following case studies are set up, in addition to base case (Case0), to examine the effect of inclusion or exclusion of plan targets on the GEP results:

1. No energy conservation target.
2. No capacity target for *s3* technologies.
3. No capacity target for RES (*s8*) technologies.
4. No capacity or energy conservation targets, i.e., business-as-usual (BAU) case.

Figure 4.13 shows that minimum emissions occur in Case0, increasing gradually as the targets are progressively removed (from Case1 to Case3), and reaching maximum when both targets are excluded from the GEP model (Case4), thereby confirming the need for introduction of RES and energy conservation. A comparison of the optimal costs and payments, i.e., *R*, *C*, *EC* and

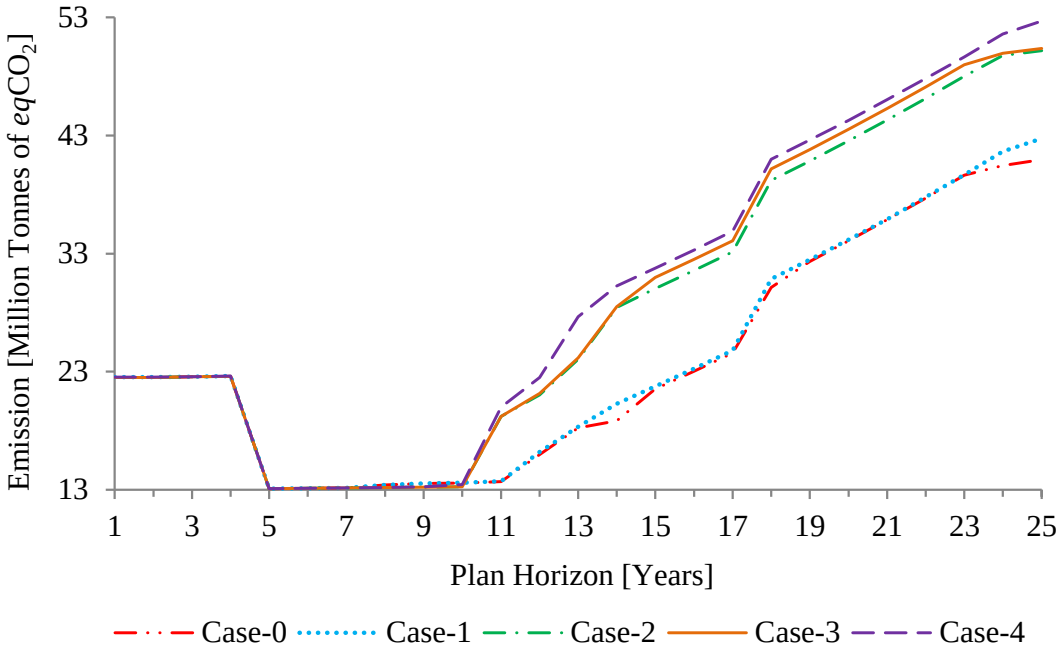

Figure 4.13: Variation in annual emission from all technologies.

Table 4.8: Capacity additions, PBPs, incentives and costs for all case studies.

		Case Studies				
		Case0	Case1	Case2	Case3	Case4
GAS	*NC* [MW]	3300	3860	6320	6340	6960
	ϕ [years]	2	2	2	2	2
HNR	*NC* [MW]	190	190	2148	190	190
	ϕ [years]	4	4	21	4	4
HR	*NC* [MW]	-	-	1900	-	-
	ϕ [years]	-	-	7	-	-
BIO	*NC* [MW]	448	448	-	-	-
	ρ^{New} [¢/kWh]	27.10	26.48	-	-	-
GPV	*NC* [MW]	1834	1825	-	-	-
	ρ^{New} [¢/kWh]	55.75	54.48	-	-	-
RPV	*NC* [MW]	213	217	-	-	4
	ρ^{New} [¢/kWh]	59.25	64.89	-	-	52.90
WON	*NC* [MW]	1275	1275	1275	1275	1275
	ρ^{New} [¢/kWh]	17.65	17.49	15.85	15.85	18.06
WOF	*NC* [MW]	4955	4960	440	-	-
	ρ^{New} [¢/kWh]	28.33	28.98	28.82	-	-
Excess capacity [%]		21.18	22.82	20.79	8.26	10.09
NPV of *R* [Billion $]		200.95	211.31	198.16	198.56	208.98
NPV of *C* [Billion $]		85.85	86.39	67.21	63.20	64.36
NPV of *EC* [Billion $]		22.08	22.25	25.12	25.34	25.86
NPV of *ECP* [Billion $]		1.12	0	1.12	1.12	0
Ω_{Sys} [Billion $]		310	319.95	291.61	288.22	298.68

ECP, depicted in Table 4.8, shows that Case0 is not the cheapest option from the CPA's point of view; it also indicates that forceful integration of RES using incentives is more expensive than the BAU (Case4) scenario. The difference in the plan cost (Ω_{Sys}) is not only due to the relatively higher than market-price values of the incentives, but also due to the excess capacity addition decisions (with respect to *PD*) made in cases with RES capacity targets, due to the relatively low RES capacity factors.

Variation in RES Penetration Targets

Since RES based generation technologies are categorized in two sets, given by *s3* and *s8*, their penetration targets are varied separately here. The total installed capacity of *s3* technologies in 2011 is 1975 MW; thus, *s3* penetration is varied from 2000 MW upwards to the maximum capacity that can return a feasible GEP solution. The corresponding new capacity additions are shown in Figure 4.14, demonstrating that offshore wind is the most economic choice from the CPA's perspective among *s3* technologies after onshore wind. Observe that onshore wind achieves its maximum installation potential of 1275 MW (see Table 4.2) for any given RES target, and that *s3* technologies are introduced in the order WON, WOF, GPV, BIO, and RPV, since WON has already reached its penetration potential. Note that WOF provides the major share of the RES target, and GPV and RPV installations (1990 MW and 261 MW, respectively) approach their given capacity addition potentials as the *s3* target increases. Since hydro is not included in *s3* technologies, it is not sensitive to the variation in *s3* targets. The variation in optimal incentives resulting from the variation in RES targets is shown in Figure 4.15, demonstrating that increase in *s3* penetration targets do not have a significant effect on their incentives.

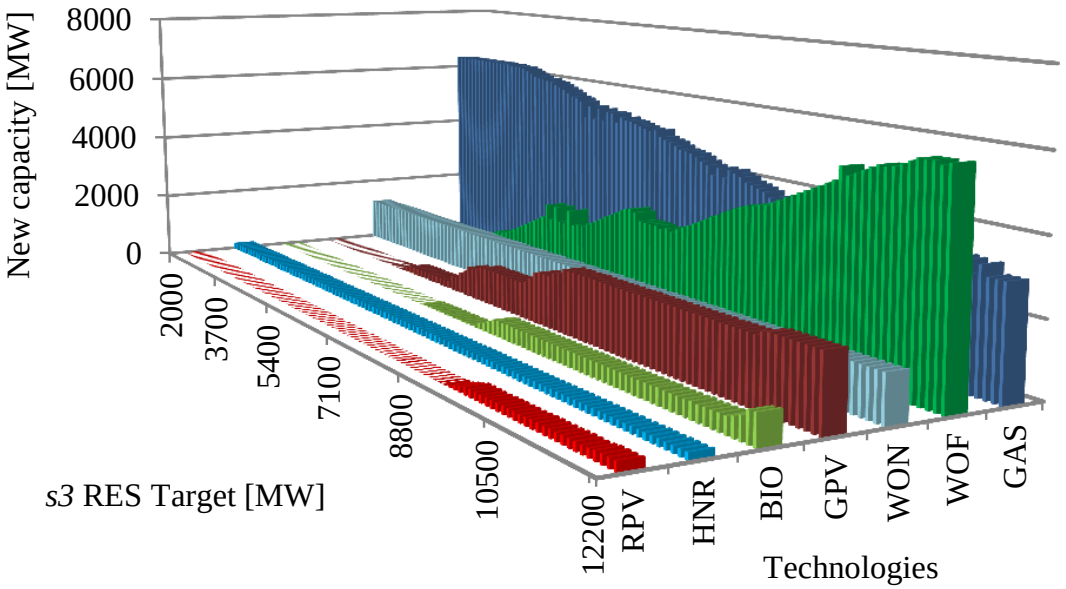

Figure 4.14: Effect of variation in *s3* RES targets on new capacity additions *NC*.

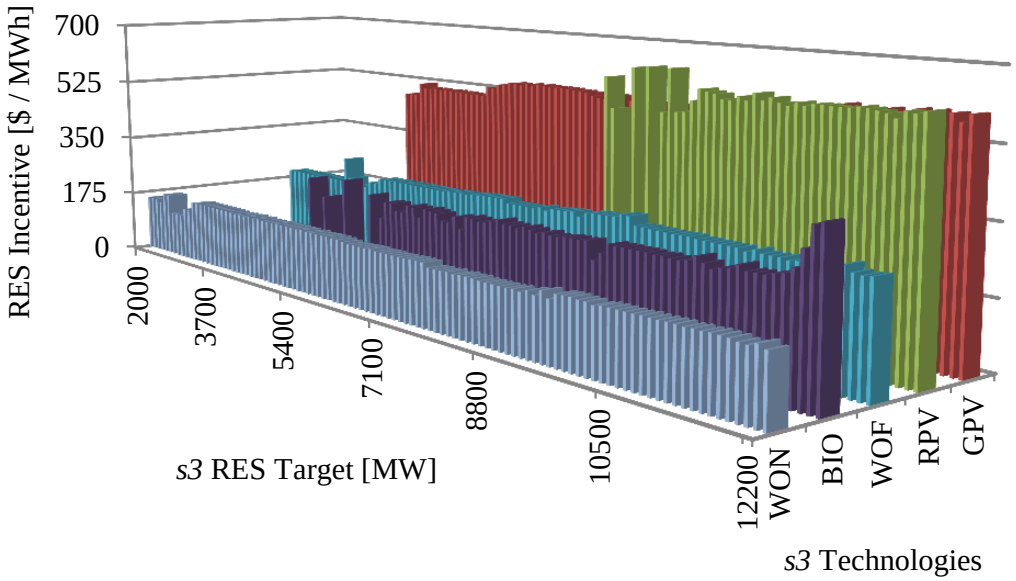

Figure 4.15: Optimal RES incentives for variation in *s3* RES targets.

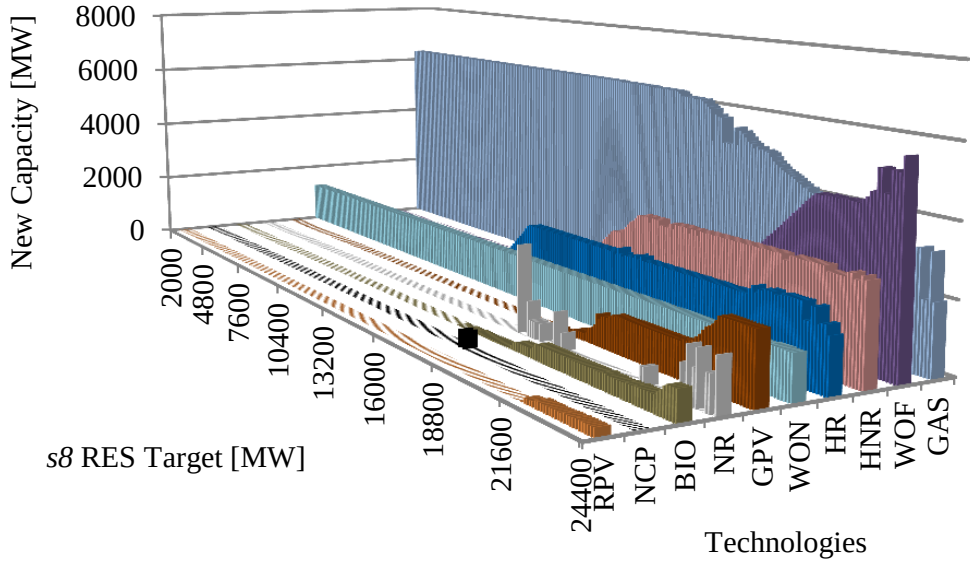

Figure 4.16: New capacity additions for variation in *s8* RES targets.

When the penetration target of *s8* technologies, which include *s3* and hydro, are varied, the resultant variations in new capacity additions and optimal incentives are shown in Figures 4.16

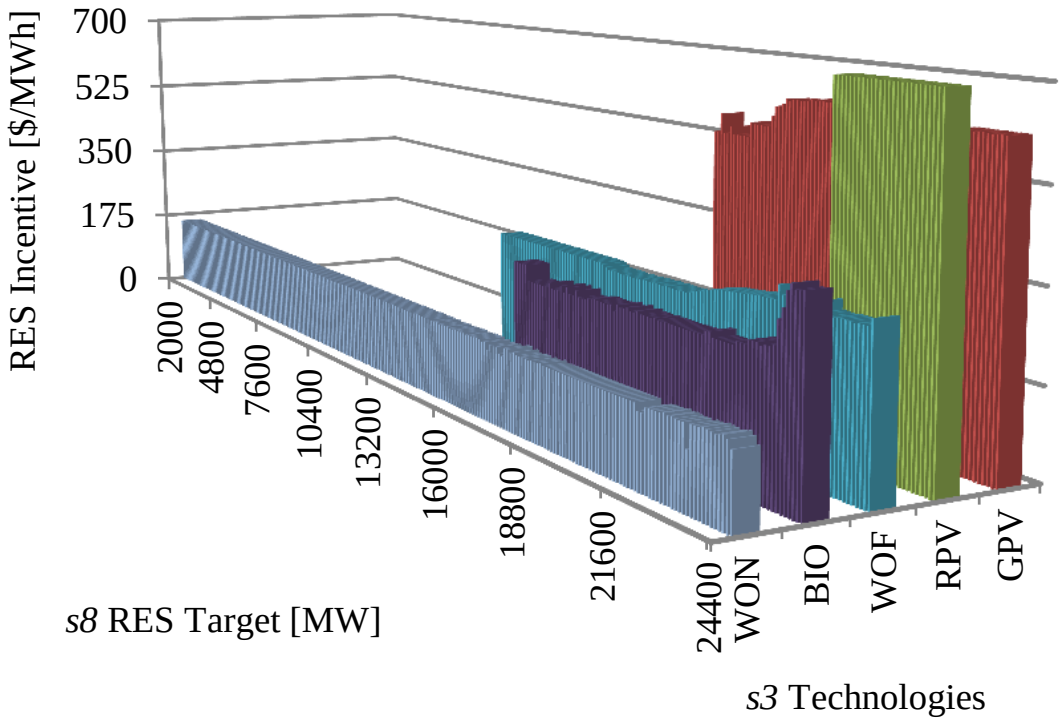

Figure 4.17: Optimal RES incentives for variation in *s8* RES targets.

and 4.17, respectively. Comparing Figures 4.14 and 4.16, a significant increase in new capacity additions of HNR and the introduction of HR is observed, which is due to the fact that the per unit capital cost of hydro is lower than *s3* technologies (see Table 4.1), with similar low rate of carbon emission. Observe that the bulk of RES installations still consists of WOF (Figure 4.16), because, along with BIO, GPV, and RPV, hydro (HNR and HR) also reaches their capacity addition potentials. Comparison of Figures 4.15 and 4.17 show that the optimal incentives for *s3* technologies are affected significantly when hydro is included in the RES penetration target, as installations of *s3* technologies get delayed in time due to hydro being a cheaper option.

Variation in the Maximum PBP of Incentive Driven Technologies

The maximum PBP ϕ^{Max} of incentive driven *s3* technologies was considered to be 10 years in the Base Case (Case0); hence, to study its impact on the optimal GEP, this is varied here from

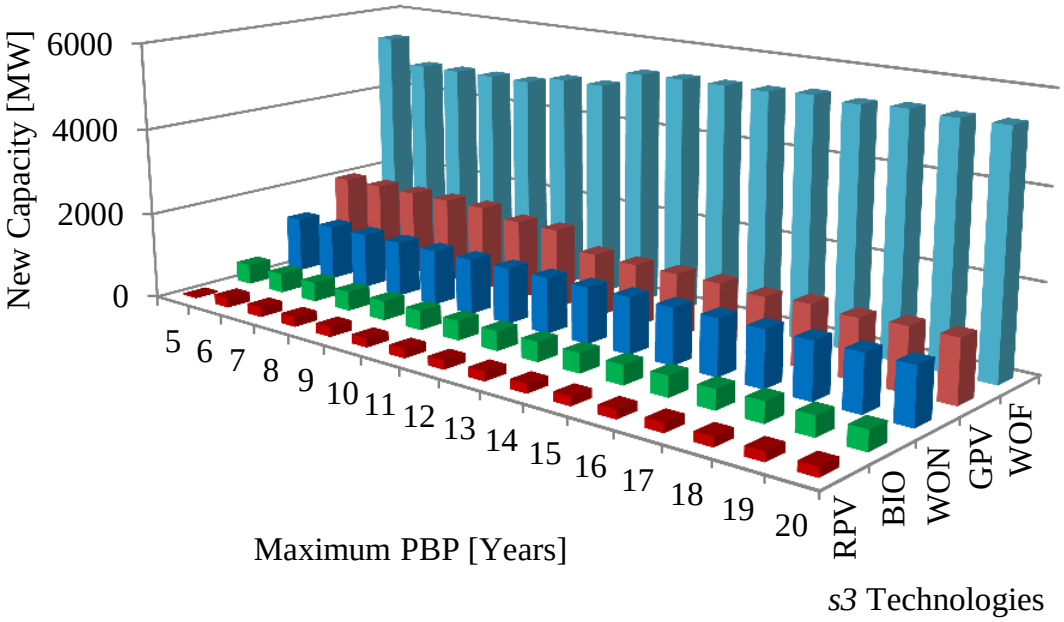

Figure 4.18: Effect of varying ϕ^{Max} on new capacity additions NC_{s3}.

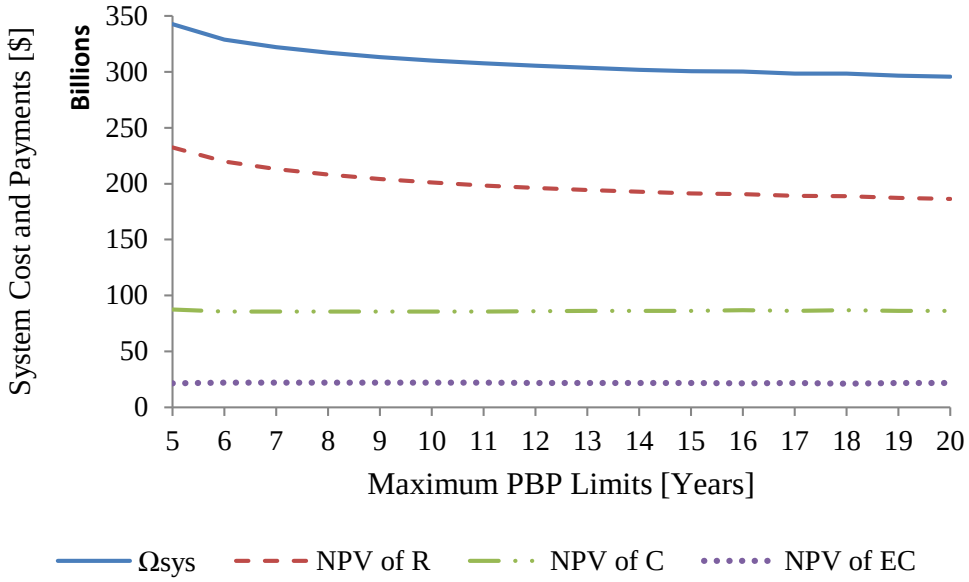

Figure 4.19: Effect of varying ϕ^{Max} on the NPV of system costs and payments.

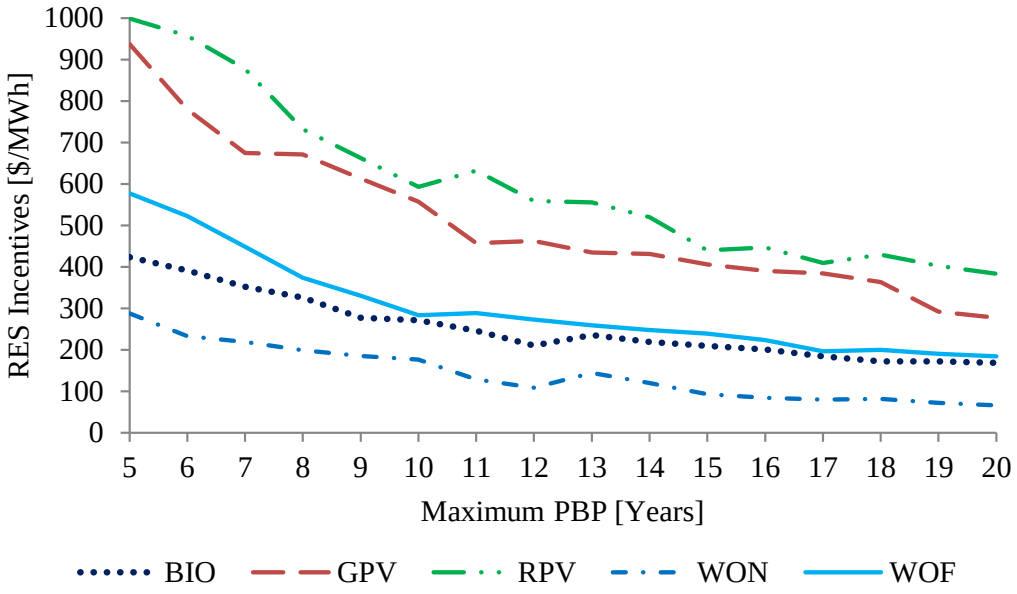

Figure 4.20: Effect on optimal RES incentives for variation in ϕ^{Max} of *s3* technologies.

5 to 20 years. Figures 4.18 and 4.19 show the effect of varying ϕ^{Max} on new capacity additions of *s3* technologies and the corresponding NPV of system costs and payments, respectively. Note that ϕ^{Max} has little effect on capacities of new *s3* technology installations, and thus has almost no effect on the costs of generation. Only the system payments (NPV of R) are reduced, signifying that there is a reduction in the optimal incentives obtained for *s3* technologies.

Figure 4.20 shows the variation in the RES incentives due to variations in their corresponding ϕ^{Max}, demonstrating that ϕ^{Max} is a key factor in determining the optimal incentives. It is interesting to note that the values of maximum PBP ϕ^{Max}_{s3} corresponding approximately to Ontario's existing RES incentives (ρ^{Ex}_{s3}) are 23, 13, 11, 11, and 17 years for BIO, GPV, RPV, WON, and WOF, respectively.

Variation in Fossil-fuel Prices

Fossil-fuels GAS and OIL are assumed here to have high and low price growths, as shown in Figure 4.21. Hence, the following four cases can be defined by combining these price variations:

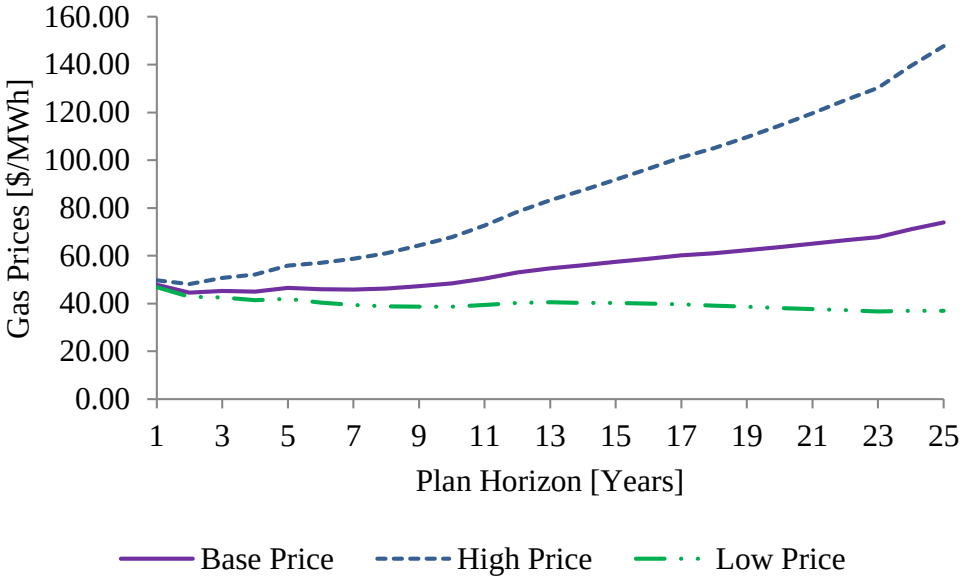

(a)

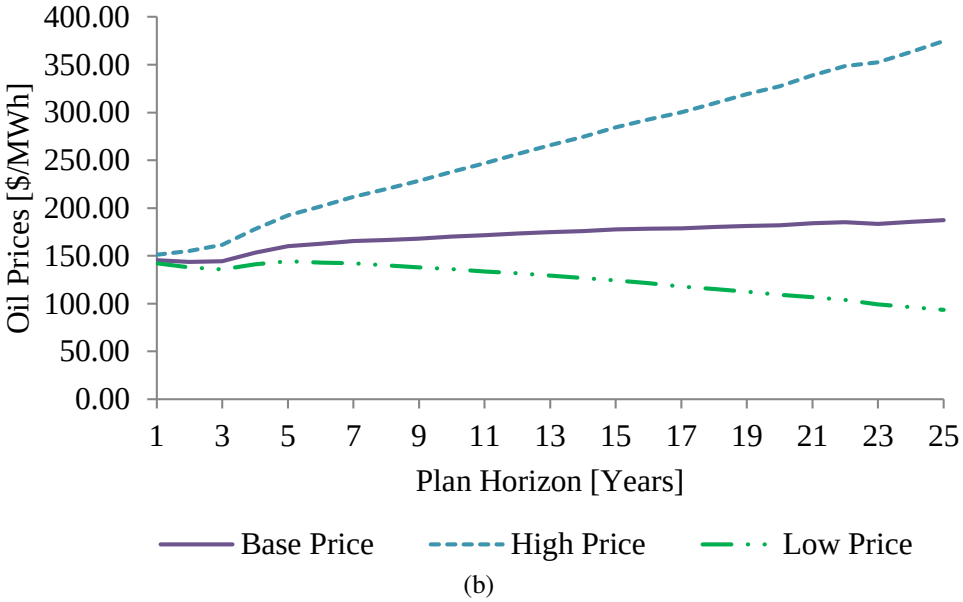

(b)

Figure 4.21: Assumed high and low fuel price growths of (a) GAS and (b) OIL with respect to base prices [81].

Table 4.9: Effect of fossil-fuel price variations on new capacity additions and RES incentives.

		Case0				Case4			
		HGHO	HGLO	LGHO	LGLO	HGHO	HGLO	LGHO	LGLO
Total planned capacity additions [MW]	BIO	448	448	448	465	0	0	0	0
	GPV	1489	1486	1990	1990	1	1	0	0
	RPV	233	217	217	208	4	4	4	4
	WON	1275	1275	1275	1275	1275	1275	1275	1275
	WOF	5280	5300	4795	4790	0	0	0	0
	GAS	2560	1520	3700	3000	6960	6940	6960	6960
	HNR	190	190	190	190	190	190	190	190
RES incentives [¢/kWh]	BIO	276.58	276.93	269.19	276.87	–	–	–	–
	GPV	575.55	583.50	572.61	580.07	508.53	508.53	–	–
	RPV	605.49	605.47	605.93	602.90	529.02	529.02	529.02	529.02
	WON	179.12	177.56	176.48	176.48	181.89	181.89	180.63	180.63
	WOF	280.47	280.51	289.50	284.77	–	–	–	–

- *HGHO*: High prices for both GAS and OIL.
- *HGLO*: High price for GAS and low price for OIL.
- *LGHO*: Low price for GAS and high price for OIL.
- *LGLO*: Low prices for both GAS and OIL.

These are then applied to the Base case (Case0) and BAU (Case4) scenarios, yielding Table 4.9 to show the effect of these fossil-fuel price scenarios on the outcome of the GEP. Note that there is almost no effect of fossil-fuel price variations on the optimal RES incentives determined by the GEP. With respect to new capacity additions, observe that OIL remains totally absent in all the studied cases, as previously noted for the Base Case and BAU scenarios (Table 4.8), from the set of technologies selected for new installations. This can be attributed to the fact that the high price of OIL renders this technology more expensive than offshore wind and solar PV.

Table 4.10: Effect of fossil-fuel price variations on energy generation over the plan horizon.

Total energy [TWh]	BIO	GPV	RPV	WOF	GAS	HNR	HR	NCP	NR	OIL
Case0–HGHO	62.50	32.00	5.23	319.10	598.10	919.82	390.21	881.12	760.61	91.98
Case0–HGLO	62.43	31.94	4.86	320.25	530.14	919.85	390.18	885.12	760.60	158.89
Case0–LGHO	63.76	43.41	4.88	283.82	717.92	914.95	382.98	848.43	702.43	91.98
Case0–LGLO	63.92	43.41	4.68	283.53	712.03	915.75	382.79	848.35	699.80	102.46
Case0 (Base)	63.32	40.22	4.79	295.26	687.05	916.22	384.83	855.24	717.94	91.98

Table 4.11: Effect of fossil-fuel price variations on emissions and system costs and payments.

	Case0 (Base Case)				Case0	Case4 (BAU)
	HGHO	HGLO	LGHO	LGLO		
Ω_{Sys} [Billion \$]	319	315	309	305	310	299
NPV of R [Billion \$]	204	204	200	200	201	209
NPV of C [Billion \$]	92.8	88.1	85.3	81.5	85.8	64.4
Emissions [million tonne of $eq\text{CO}_2$]	208	210	226	227	221	259

The effect that price variations of OIL and GAS has on the total energy generation over the plan horizon by a particular technology is shown in Table 4.10. Observe that for both high and base oil prices, the energy generation from OIL is forced to its lowest limit, based on its minimum capacity factor of 20%, with the variations in energy generation from OIL and GAS being supplemented by WOF and NR. It should be mentioned that the energy generation over the plan horizon for COAL and WON are 35.18 and 194.44 TWh, respectively, for all the cases, and thus are not included in Table 4.10.

The variations in energy generation from fossil-fuel-based technologies have a significant effect on system costs and payments and the total emission over the plan horizon, as shown in Table 4.11. Note that reductions in the fuel-prices of OIL and GAS result in decreased system costs and payments, but the total emissions over the plan horizon increase, as expected from the energy values of fossil-fuel-based generation capacities in Table 4.10.

4.3.4 Uncertainty Analysis

A Monte Carlo simulation procedure was carried out and the results are presented here, to examine the effect of uncertainties in solar and wind generation availabilities on plan decisions. Thus, the annual average *CF*s of GPV, RPV, WON, and WOF for each zone are perturbed simultaneously, considering a normal distribution with standard deviations of 20% for each, and means corresponding to the deterministic values previously used. Note that this results in significant broad range of variations in *CF*s, as shown in Table 4.12.

The results of Monte Carlo simulations are shown in Table 4.13, which includes the range, standard deviation, mean, and percentage standard deviation of the probability density function of target output variables *NC* and ρ^{New}; the table also includes the NPV of costs and payments and total emissions. Observe that the percentage standard deviations of plan costs and payments (R, C, EC, and Ω_{Sys}) are low, as depicted in Figure 4.22, showing that significant *CF* variations do not have a large impact on the system costs and payments. Note as well that the *CF* variations have little effect on the resulting capacity addition or optimal incentive design for BIO (see Figure 4.23a). Thus, one can conclude that the uncertainties in solar and wind energy availability affect

Table 4.12: Range of solar and wind zonal *CF* perturbations.

$CF_{s,i}$ [%]	GPV		RPV		WON		WOF	
	Min.	Max.	Min.	Max.	Min.	Max.	Min.	Max.
NW	5.79	23.24	5.59	25.32	8.23	49.89	6.86	51.80
NE	4.35	22.76	3.85	21.66	14.21	55.78	6.69	55.35
ESSA	5.31	23.04	4.63	23.46	11.00	53.47	11.66	53.28
OTTAWA	6.26	27.82	6.00	27.09	8.71	59.94	0.00	0.00
EAST	5.45	25.31	2.90	28.21	9.44	57.55	10.05	57.76
TORONTO	4.59	22.18	4.23	23.12	8.37	56.72	9.81	53.08
NIAGARA	4.16	21.99	3.55	22.29	8.29	42.75	8.82	41.27
SW	4.95	21.58	3.73	23.27	5.97	47.06	9.83	46.44
BRUCE	4.45	21.59	1.31	23.39	11.22	60.99	9.52	60.15
WEST	5.39	26.96	6.05	26.05	13.48	61.37	11.85	62.14

Table 4.13: Main output variables of Monte Carlo simulations.

		Minimum Value	Standard Deviation	Expected (Mean)	Maximum Value	Percent Std. Dev. [%]
Total planned capacity additions [MW]	BIO	447	7.78	452.26	589	1.72
	GPV	1242	185.10	2064.62	2806	8.96
	RPV	18	35.92	216.74	261	16.57
	WON	1275	8.19×10^{-14}	1275	1275	6.42×10^{-15}
	WOF	4015	207.59	4733.54	5505	4.39
	GAS	3000	322.39	4421.15	6000	7.29
	HNR	190	1.75×10^{-13}	190	190	1.0×10^{-13}
RES incentives [¢/kWh]	BIO	21.54	0.53	26.89	32.69	1.97
	GPV	44.95	4.22	57.60	72.92	7.32
	RPV	43.09	5.45	59.89	87.47	9.10
	WON	12.73	2.25	17.75	29.31	12.69
	WOF	22.48	3.19	31.69	44.91	10.06
NPV of R [Billion $]		196.01	8.64	199.38	202.49	0.433
NPV of C [Billion $]		84.01	0.74	86.78	91.01	0.849
NPV of EC [Billion $]		22.33	0.40	23.74	24.99	1.68
Ω_{Sys} [Billion $]		304.66	1.69	311.02	316.52	0.543

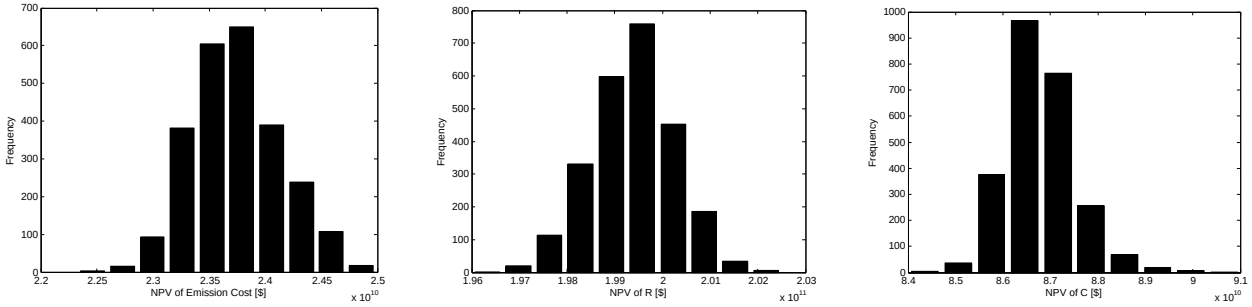

(a) NPV of EC. (b) NPV of R. (c) NPV of C.

Figure 4.22: Histograms of system costs and payments from Monte Carlo simulations.

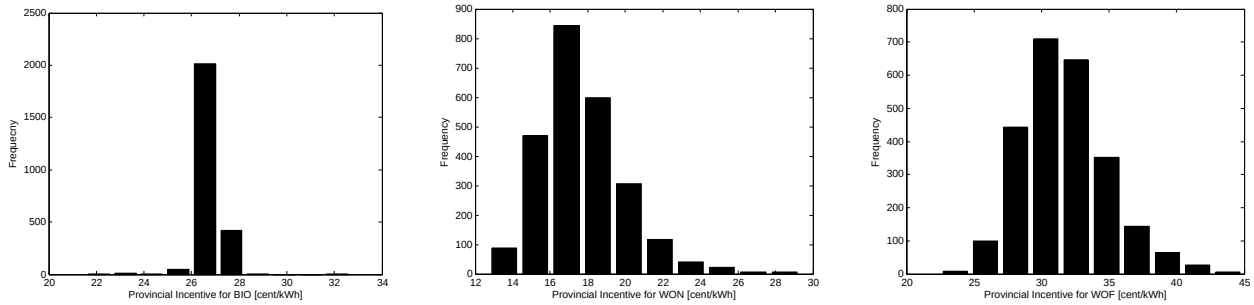

(a) Incentive for BIO. (b) Incentive for WON. (c) Incentive for WOF.

Figure 4.23: Histograms of RES incentives for bio and wind generation from Monte Carlo simulations.

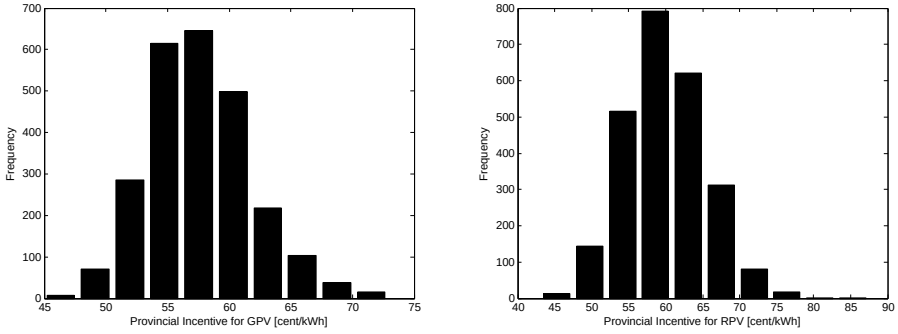

(a) GPV (b) RPV

Figure 4.24: Histograms of solar PV incentives from Monte Carlo simulations.

the capacity addition and incentive design for mostly solar and wind technologies. Observe also that WON capacity additions remain unaltered at its maximum province-wide potential, not decreasing at lower capacity factors, and thereby establishing itself as a techno-economically proven RES. On the other hand, the optimal incentive design for WON varies with a log-normal distribution (see Figure 4.23b), indicating that for lower CF values, high incentive rates are required to maintain the same amount of capacity additions. Finally, note that capacity additions of PV technologies, particularly RPV, vary significantly with changes in their CFs, as shown in Figure 4.24. (The rest of the histograms pertaining to this Monte Carlo simulation are given in Appendix C.)

4.4 Summary

This chapter presented the mathematical model of a novel holistic GEP problem that is designed to determine the optimal incentives for targeted penetration of RES, considering optimally chosen incentives for energy conservation, while determining the optimal site, size, and time of new capacity additions. The proposed GEP model was designed to be used by a CPA, such as a regulator or a regional planning authority, to minimize the costs for GENCOs while minimizing the CPA's payments to GENCOs and LDCs, thereby considering both GENCOs' profits and system costs. Furthermore, GENCO's investment constraints were considered by including a maximum limit on the PBP of RES investments.

The proposed GEP approach was applied to a model of Ontario's grid with realistic data, and the results obtained are similar to the existing incentives, demonstrating the feasibility and usefulness of the approach. An array of case studies was presented for this practical grid to aide in understanding the sensitivities of the model outcome with respect to some important input parameter variations. Finally, a Monte Carlo simulation procedure was presented to show the effect of solar and wind generation uncertainties on the optimal plan outcome of the proposed GEP model in the case of Ontario, with the results demonstrating that solar and wind capacity factor variations affect the new capacity additions and corresponding incentives of solar and wind only, and not other RES.

Chapter 5

Conclusions

5.1 Summary

The research presented in this thesis has focused on the integration of RES in the generation planning procedure; in particular, determining the parameter sensitivities and risk indices from a solar PV investor's perspective, and determining the optimal incentive rates for RES from the perspective of a CPA. The main content of this thesis is summarized next.

Chapter 1 presented the motivation behind this research, discussing the capacity expansion planning problem from both central planner's and investor's perspectives, while considering energy conservation and emissions. A critical literature review of related works on traditional GEP, investor oriented and centralized planning, considering RES integration, and IRP was presented, to determine and justify the main research objectives proposed in this chapter.

The background topics relevant to the proposed research were presented in Chapter 2. Thus, mathematical modeling related to capacity planning considering investor's and planner's perspective, and sensitivity analysis procedures using DT, FD, and Monte Carlo simulation approaches were discussed. A brief overview of investment risk assessment tools, mathematical programming, and a linearization technique used in this research, were also presented in this chapter.

Chapter 3 discussed the novel application of various approaches of the computation of sensitivity indices for a solar PV investment planning model, with the sensitivities representing the change in the NPV of investor's profit with respect to changes in model parameters such as RES incentives or FIT, discount rate, equipment cost, and total budget. A new application of the DT-based sensitivity indices to determine the risk parameters of an investment planning model was presented in this chapter. The results of applying the techniques proposed in this chapter to a detailed investment model for Ontario demonstrated that the DT-based approach computes sensitivity indices accurately for a small perturbation in the model parameters one at a time, as the values were the same with the "true" sensitivities obtained using the FD approach, and were very close to those obtained using Monte Carlo simulations, at low computational costs. The computation of investment risk parameters in the same Ontario model demonstrated that the proposed mathematical formulations provide fairly accurate standard deviations, and more conservative VaR values.

In Chapter 4, a novel holistic GEP model was proposed to determine the optimal RES incentive rates to be offered to GENCOs, along with the incentives for LDCs' energy conservation, in order to achieve desired renewable penetration targets. The application of the proposed model to the Ontario grid, based on available realistic data, demonstrated the feasibility and benefits of the developed model. The results showed the importance of proper incentive design for RES penetration and energy conservation, indicating that the determined optimal incentives for various RES technologies were insensitive to most input parameter variations, except the ones directly related to the technology under consideration. This work is an important step toward designing suitable incentives and targets for RES capacity penetration and energy conservation to achieve reduced emissions at minimal system costs, demonstrating that energy conservation and optimal RES incentives are uncorrelated, thus allowing the system planner to select the corresponding desired targets independently.

5.2 Contributions

The main contributions of the research presented in this thesis are the following:

- A novel mathematical formulation has been proposed to compute the standard deviation of the output of an optimization model using DT-based sensitivity indices, for a set of normally distributed input parameters of the model. The relation can compute the standard deviations fairly accurately, particularly for input parameters that are linearly related to the output.
- A new mathematical formulation has been proposed to evaluate the risks of an investment portfolio for a given confidence level, based on the standard deviations obtained from the proposed DT-based sensitivity indices.
- A novel holistic GEP framework has been proposed to determine the optimal incentive rates for RES integration and energy conservation. The holistic GEP model amalgamates, for the first time, cost minimization of GENCOs with minimization of CPA's payments to GENCOs and LDCs, while also considering cost of emissions; this ensures that the designed RES incentives are optimal, accounting for both GENCOs' investment constraints and system costs. The GEP model determines the optimal sizing, siting, and timing of new capacity additions, simultaneously with the optimal RES incentives, considering both RES penetration and energy conservation targets.
- Application of all the proposed formulas and models to the Ontario grid, based on realistic data, obtains relevant results such as investment risks, and RES and energy conservation incentives and targets for Ontario investors and the OPA.

The main contents and contributions of Chapter 3 have been published in the IEEE Transactions on Sustainable Energy [89], and the contents and contributions of Chapter 4 have been accepted for publication to the IEEE Transactions in Sustainable Energy [90].

5.3 Future Work

Some possible future directions for the presented research are the following:

- An investment planning model for a prospective investor examining a combination of solar and wind generation portfolios, followed by sensitivity and risk analyses of the investment, is an important issue that should to be investigated.
- The proposed GEP model needs to be augmented by a better representation of spinning reserve requirements within the GRM. This will help better address the variations in RES generations, and capture adequacy and reliability aspects in a more comprehensive manner.
- A sensitivity analysis of the holistic GEP model should be performed using the DT-based approach, which may provide important information regarding the relationship and behaviour of the input and output variables of the model.
- The proposed GEP model could be modified to consider the stochastic nature of variables, so as to capture the uncertainties of various model parameters, in particular capacity factors, load and price forecasts, cost components of different technologies, and renewable energy resource potentials.

APPENDICES

Appendix A

Results of Monte Carlo Simulations applied to the Solar PV Investment Model

Probability distributions of perturbed input parameters and the corresponding histograms of Ω_{Pft}, used for the Monte Carlo Simulation results presented in Chapter 3, are shown here. The labour (*LbC*), land (*LdC*), and transportation (*TC*) costs are perturbed with the help of a multiplier, which has a mean value $\mu = 1$ and a standard deviation $\sigma = 0.01$. This ensures that the different zonal values of these parameters vary collectively for the whole province of Ontario instead of varying individually for different zones.

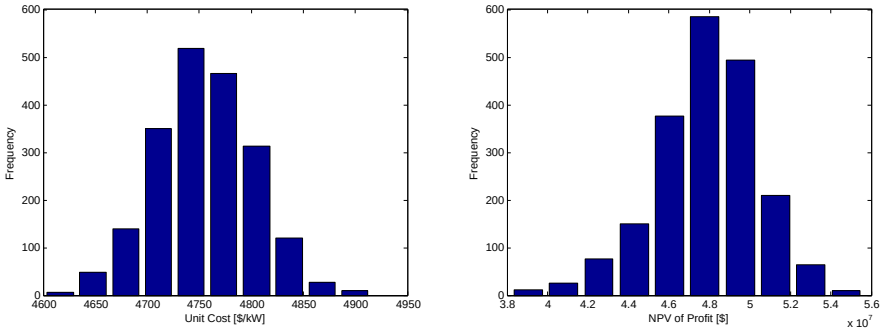

(a) Input (b) Output

Figure A.1: Perturbing UC_k^{PV} with σ=1% and resulting Ω_{Pft}: Table 3.6.

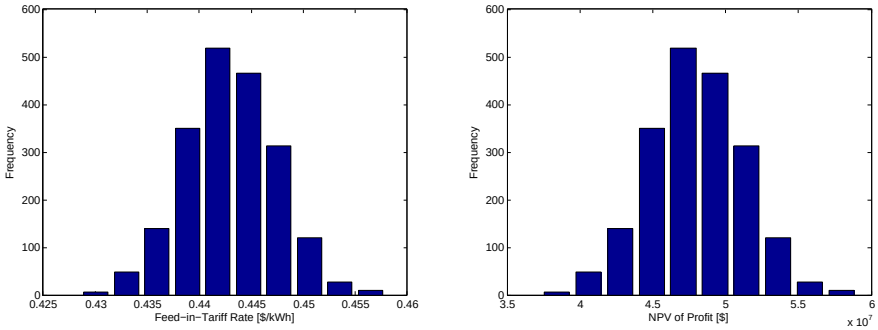

(a) Input (b) Output

Figure A.2: Perturbing ρ_{PV}^{ICV} with σ=1% and resulting Ω_{Pft}: Tables 3.6 and 3.8.

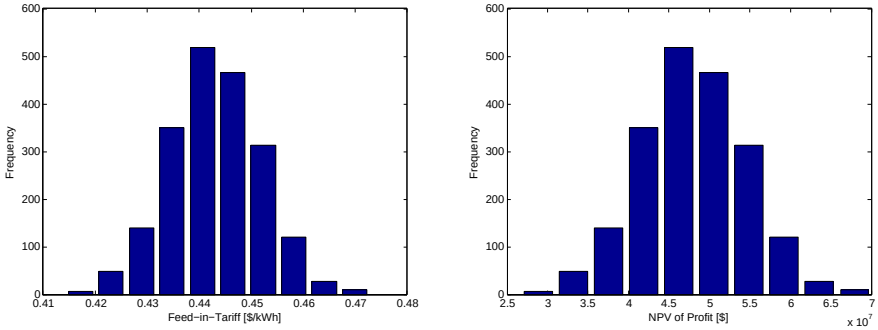

(a) Input (b) Output

Figure A.3: Perturbing ρ_{PV}^{ICV} with σ=2% and resulting Ω_{Pft}: Table 3.8.

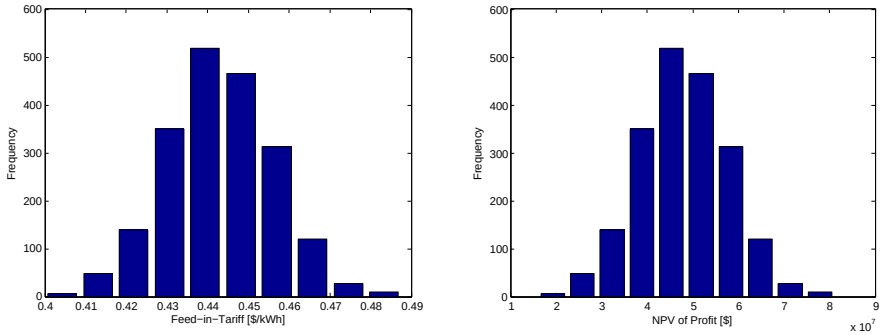

(a) Input (b) Output

Figure A.4: Perturbing ρ_{PV}^{ICV} with σ=3% and resulting Ω_{Pft}: Table 3.8.

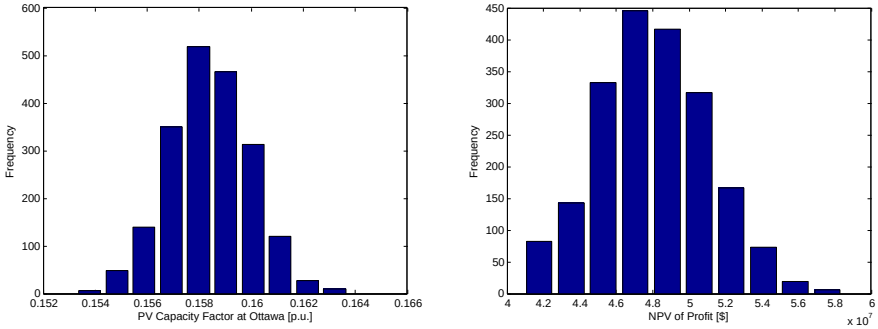

(a) Input (b) Output

Figure A.5: Perturbing CF^{PV}_{Ottawa} with σ=1% and resulting Ω_{Pft}: Tables 3.6 and 3.8.

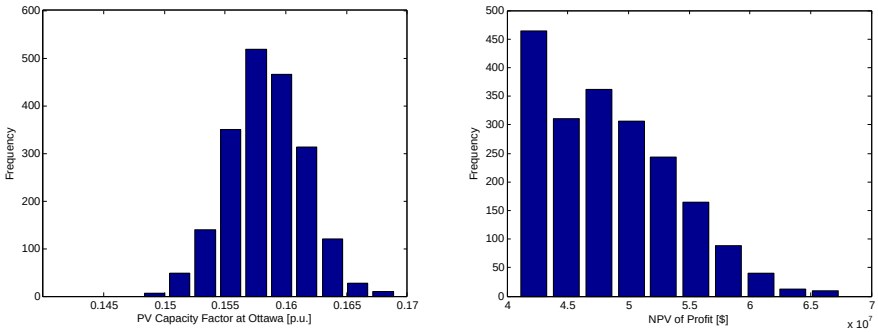

(a) Input (b) Output

Figure A.6: Perturbing CF^{PV}_{Ottawa} with σ=2% and resulting Ω_{Pft}: Table 3.8.

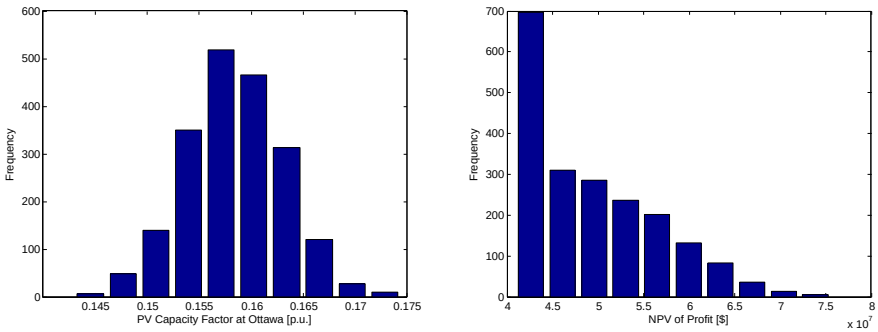

(a) Input (b) Output

Figure A.7: Perturbing CF^{PV}_{Ottawa} with σ=3% and resulting Ω_{Pft}: Table 3.8.

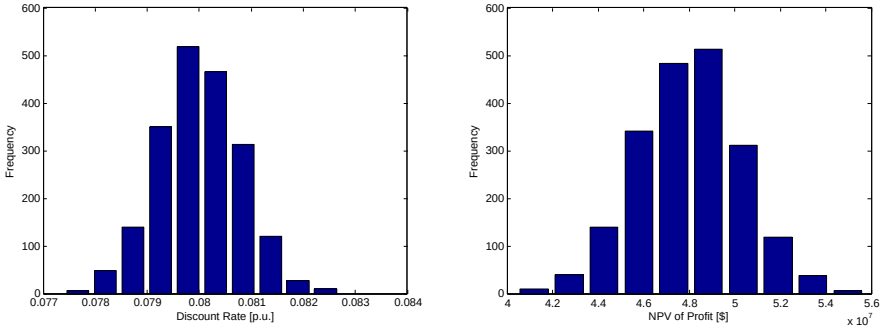

(a) Input (b) Output

Figure A.8: Perturbing α with σ=1% and resulting Ω_{Pft}: Tables 3.6 and 3.8.

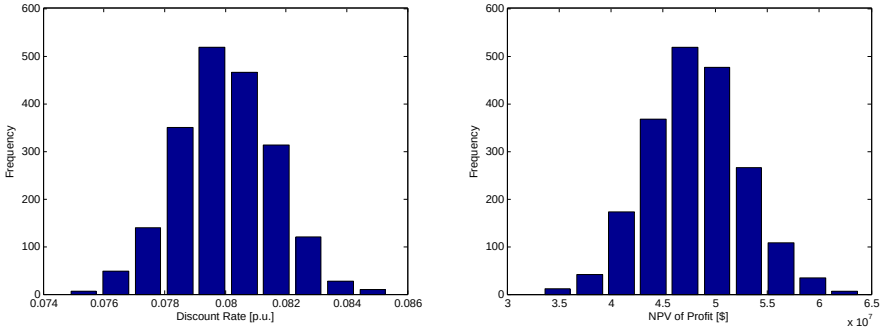

(a) Input (b) Output

Figure A.9: Perturbing α with σ=2% and resulting Ω_{Pft}: Table 3.8.

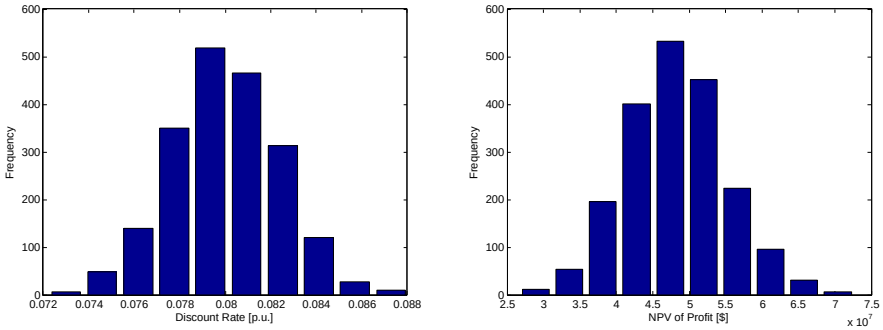

(a) Input (b) Output

Figure A.10: Perturbing α with σ=3% and resulting Ω_{Pft}: Table 3.8.

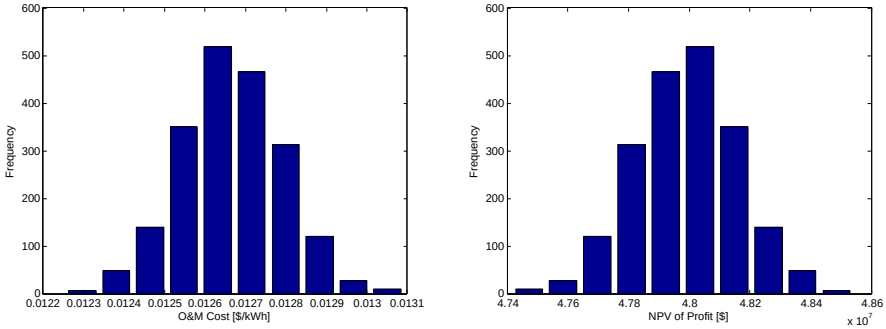

(a) Input (b) Output

Figure A.11: Perturbing OM_k^{PV} with σ=1% and resulting Ω_{Pft}: Table 3.6.

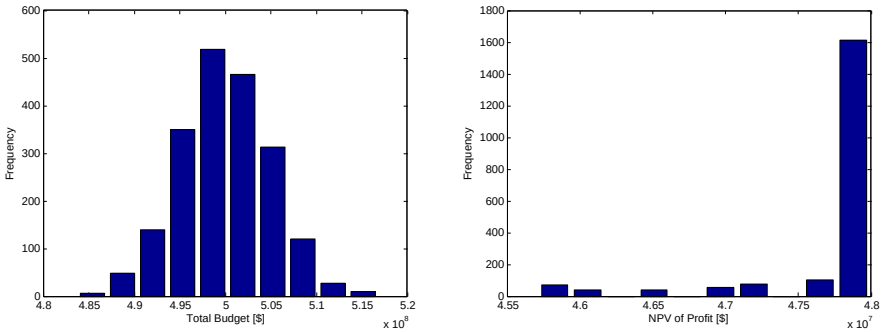

(a) Input (b) Output

Figure A.12: Perturbing *TBG* with σ=1% and resulting Ω_{Pft}: Table 3.6.

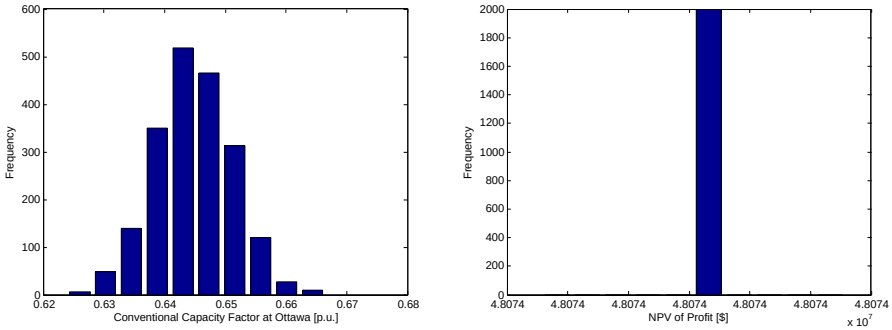

(a) Input (b) Output

Figure A.13: Perturbing CF_{Ottawa}^{Conv} with σ=1% and resulting Ω_{Pft}: Table 3.6.

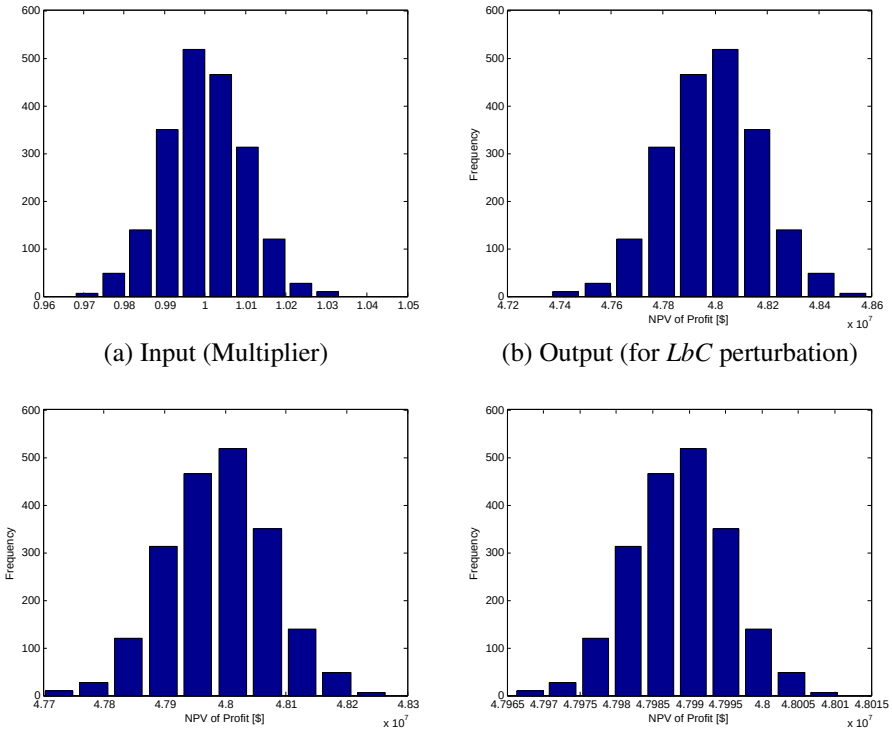

(a) Input (Multiplier) (b) Output (for *LbC* perturbation)

(c) Output (for *LdC* perturbation) (d) Output (for *TC* perturbation)

Figure A.14: Perturbing $LbC_{k,i}^{PV}$, $LdC_{k,i}^{PV}$, and $TC_{k,i}^{PV}$ using a multiplier with σ=1% and resulting Ω_{Pft}: Table 3.6.

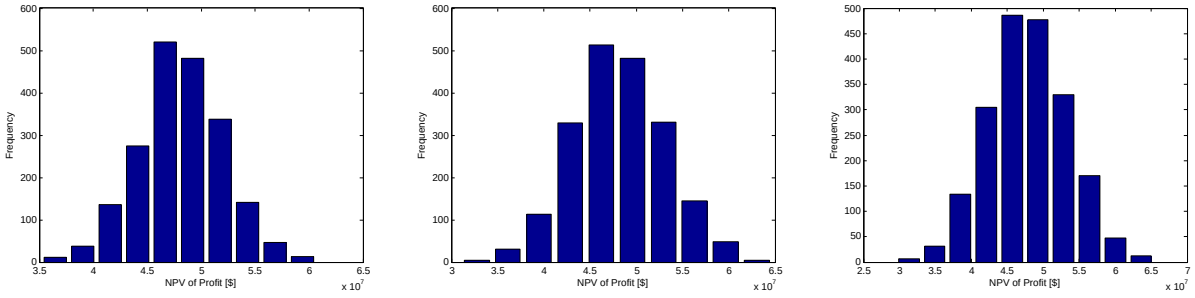

(a) Input ($\rho_{PV}^{ICV} + \alpha$) (b) Input ($\rho_{PV}^{ICV} + \alpha + CF_{Ottawa}^{PV}$) (c) Input ($\rho_{PV}^{ICV} + \alpha + CF_{Ottawa}^{PV} + UC_{k}^{PV}$)

Figure A.15: Resulting probability distribution of Ω_{Pft} for various combinations of ρ_{PV}^{ICV}, α, CF_{Ottawa}^{PV}, and UC_{k}^{PV} perturbed with individual σ=1%: Table 3.8.

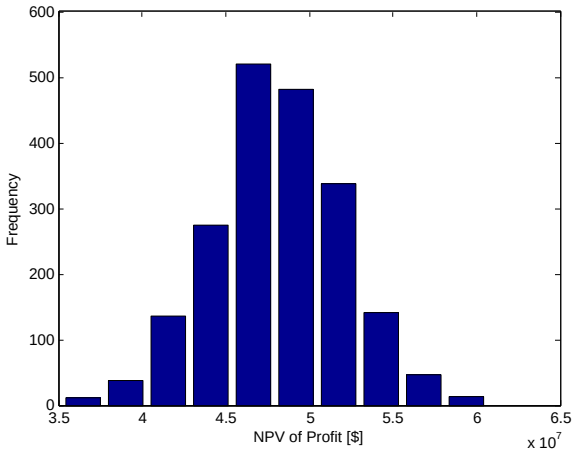

(a) Input ($\sigma^{\rho_{PV}^{ICV}}$=3%, σ^{α}=2%, $\sigma^{CF_{Ottawa}^{PV}}$=1%)

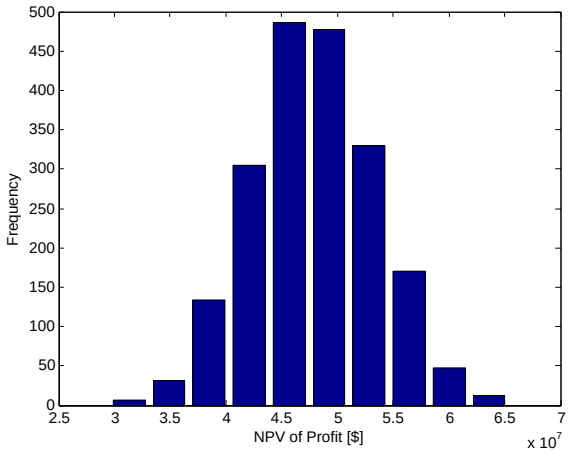

(b) Input ($\sigma^{\rho_{PV}^{ICV}}$=4%, σ^{α}=3%, $\sigma^{CF_{Ottawa}^{PV}}$=2%, $\sigma^{UC_k^{PV}}$=1%)

Figure A.16: Resulting probability distribution of Ω_{Pft} for various combinations of ρ_{PV}^{ICV}, α, CF_{Ottawa}^{PV}, and UC_k^{PV} perturbed with different σ values: Table 3.8.

Appendix B

Zonal Load Forecasts for Ontario, Canada

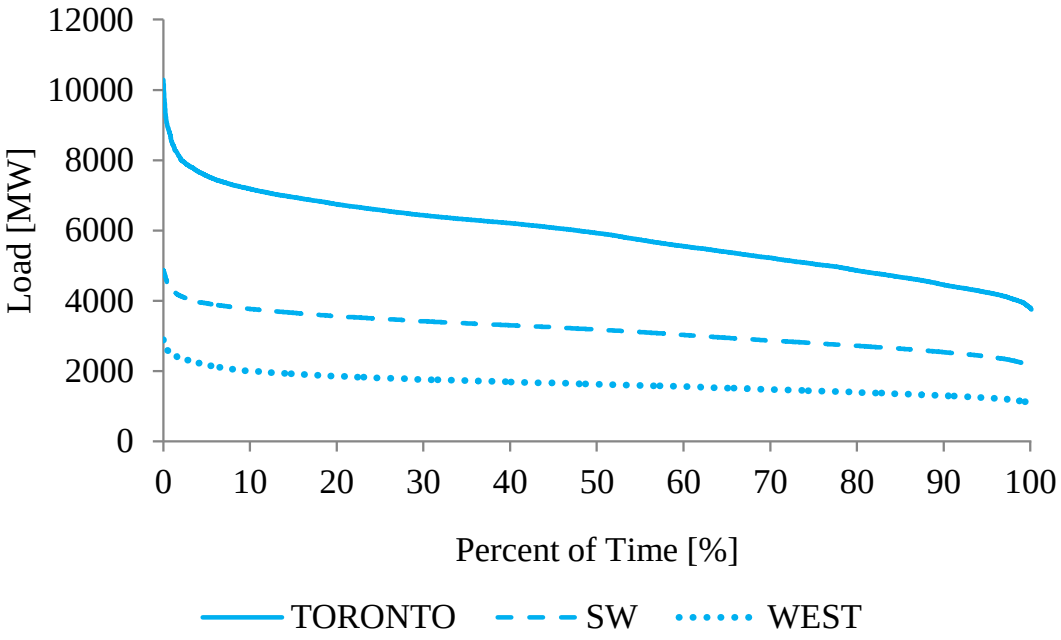

Figure B.1: Actual load duration curves in 2011 for the highly loaded zones.

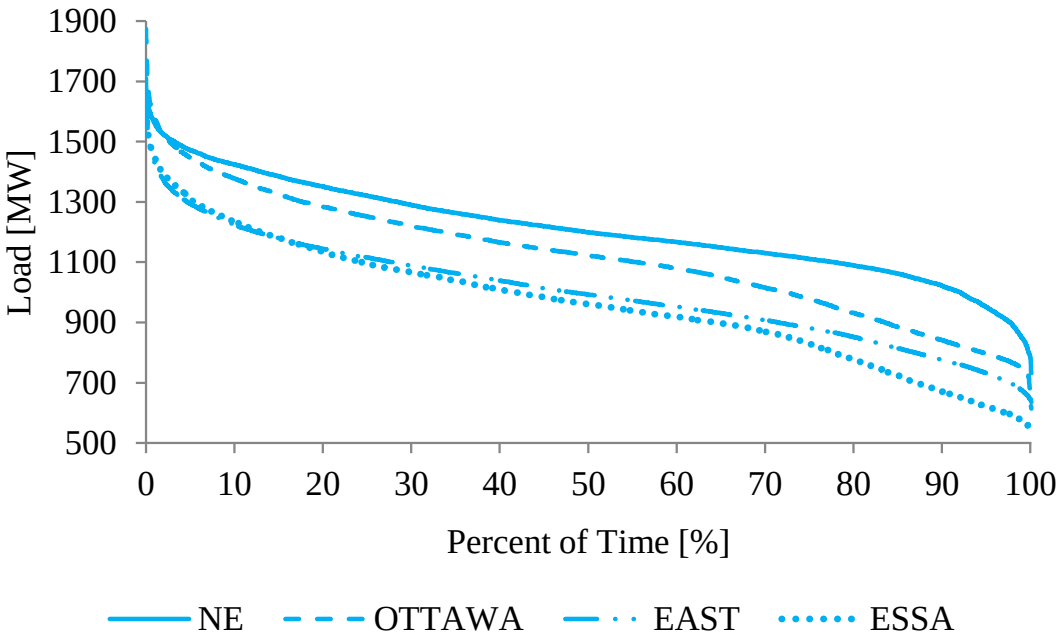

Figure B.2: Actual load duration curves in 2011 for the medium loaded zones.

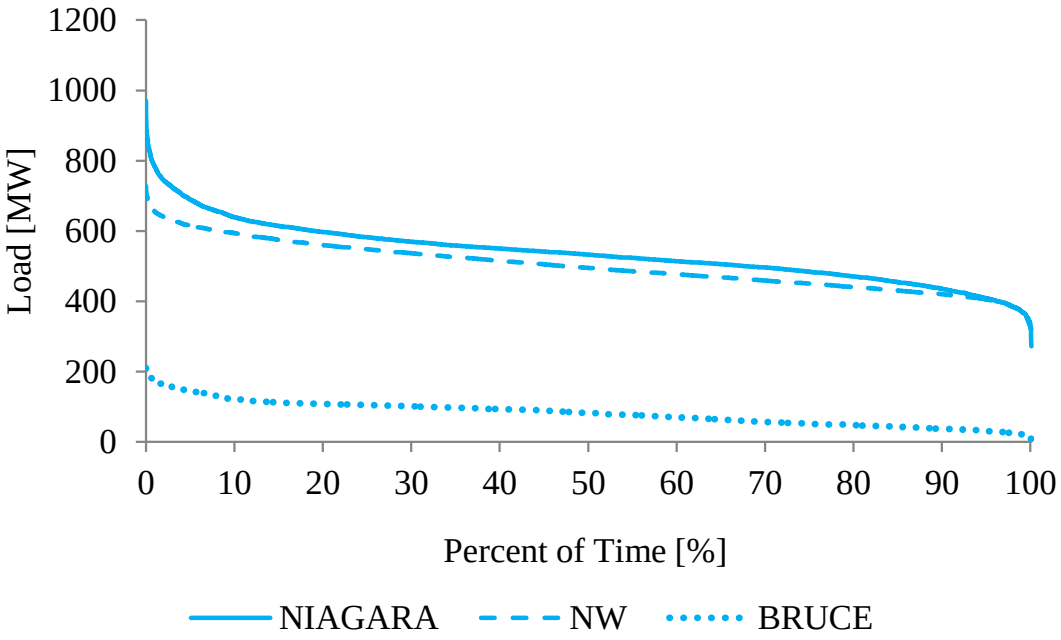

Figure B.3: Actual load duration curves in 2011 for the lightly loaded zones.

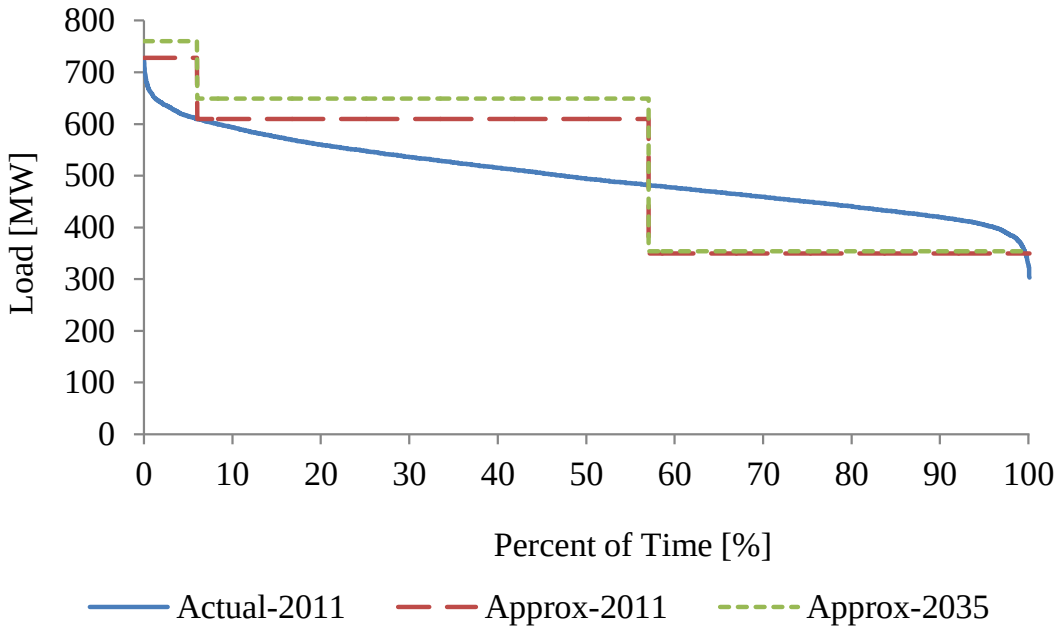

Figure B.4: Load forecast for the NW zone.

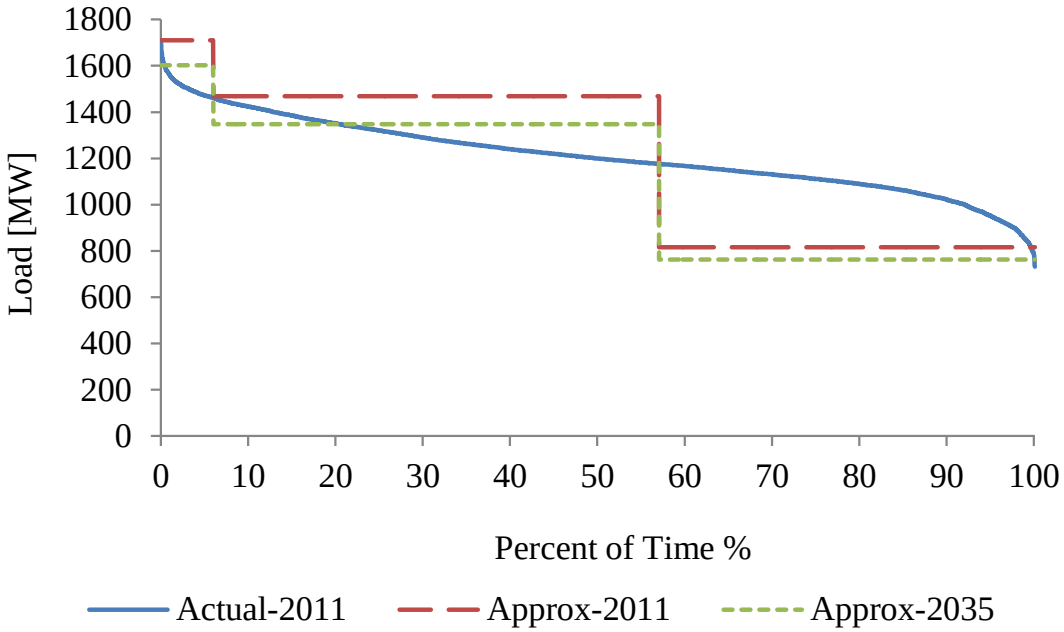

Figure B.5: Load forecast for the NE zone.

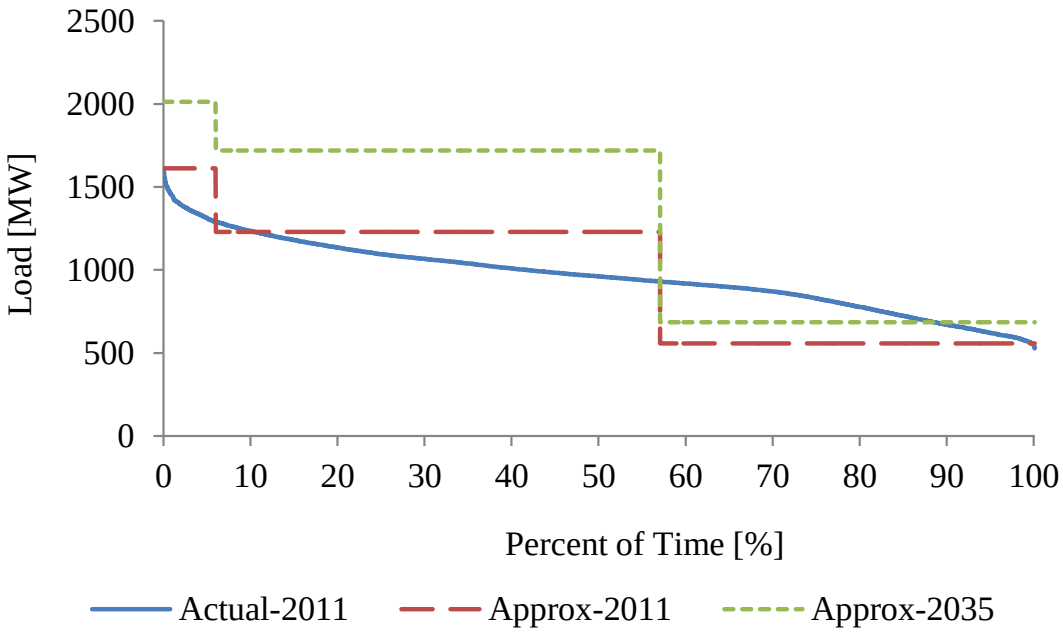

Figure B.6: Load forecast for the ESSA zone.

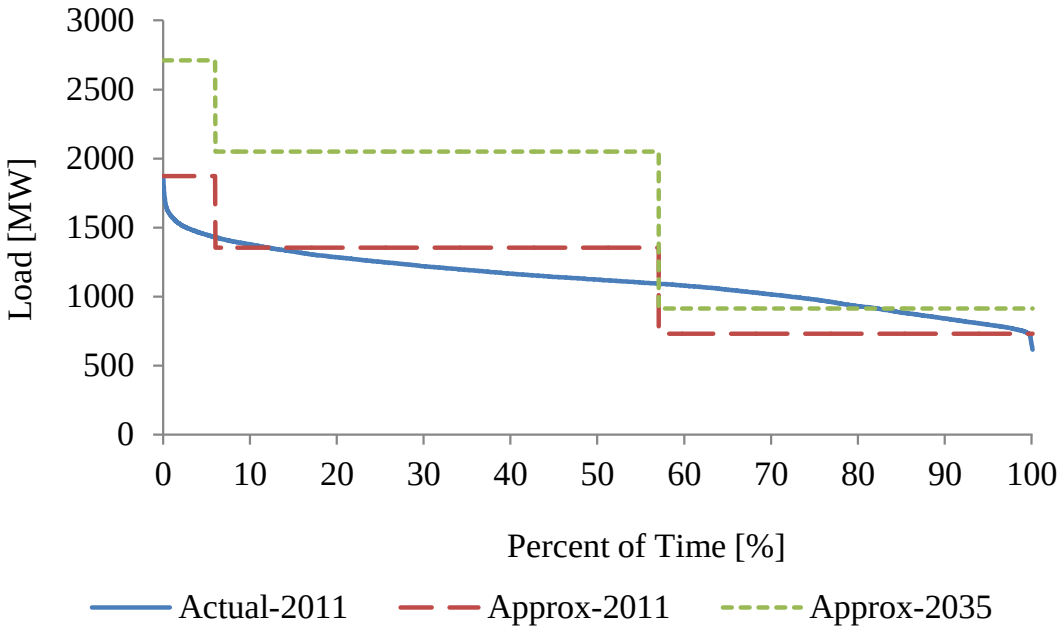

Figure B.7: Load forecast for the OTTAWA zone.

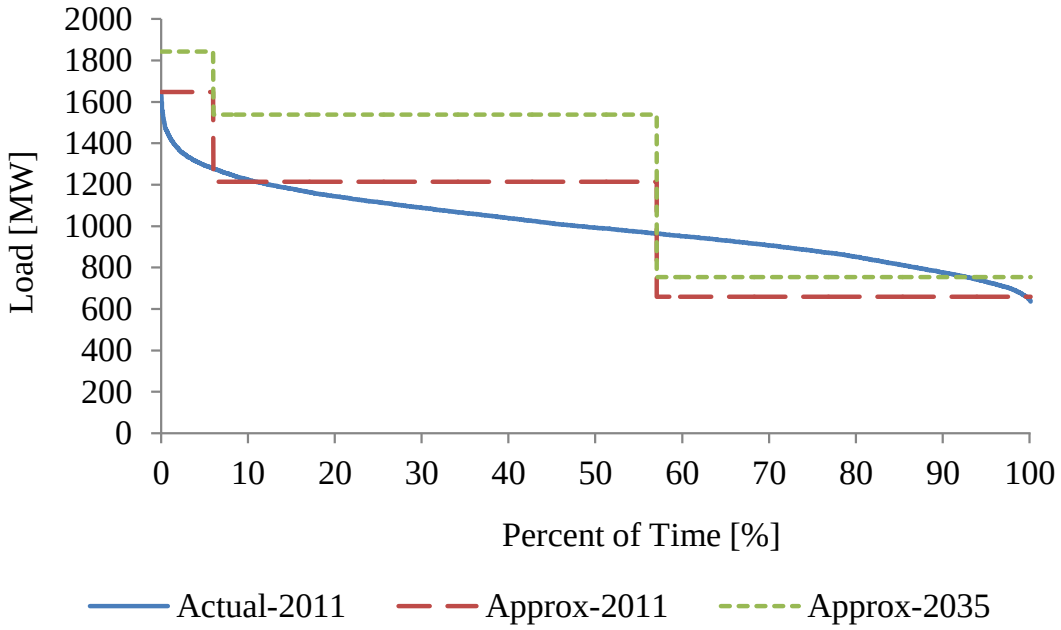

Figure B.8: Load forecast for the EAST zone.

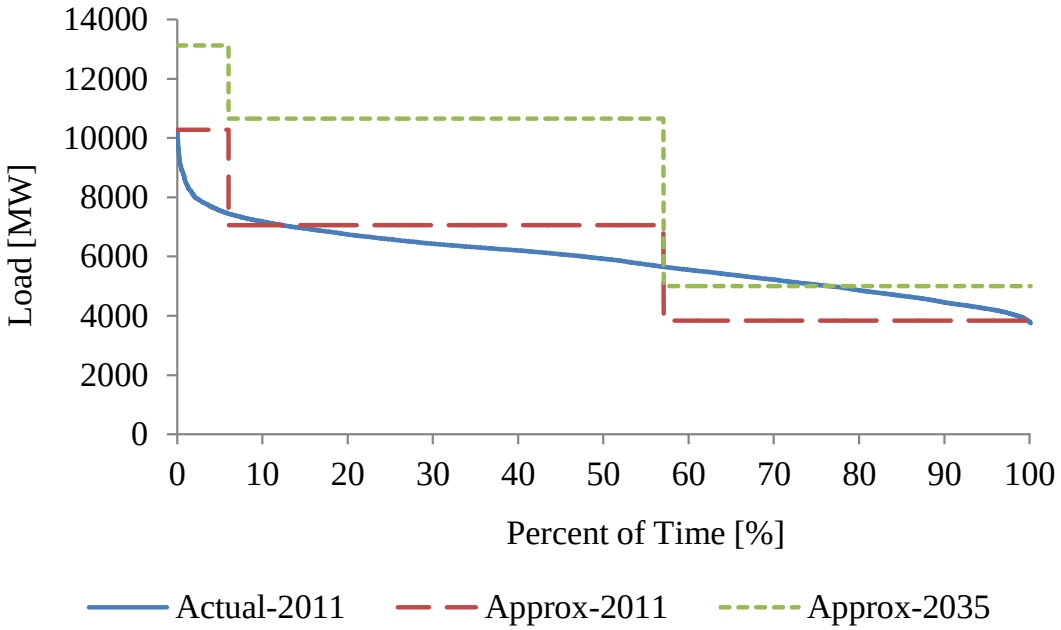

Figure B.9: Load forecast for the TORONTO zone.

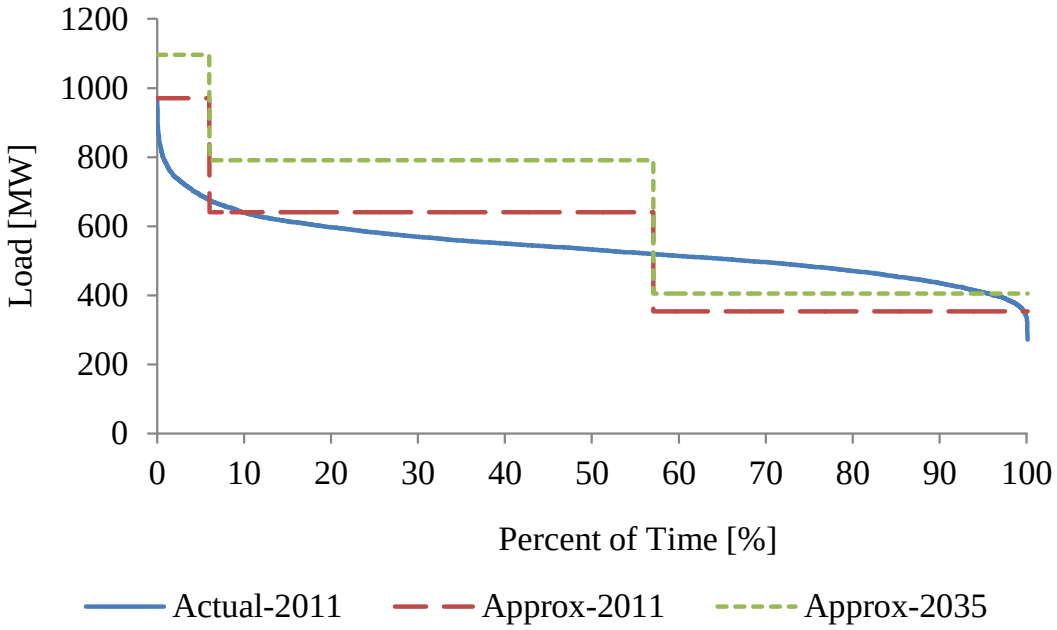

Figure B.10: Load forecast for the NIAGARA zone.

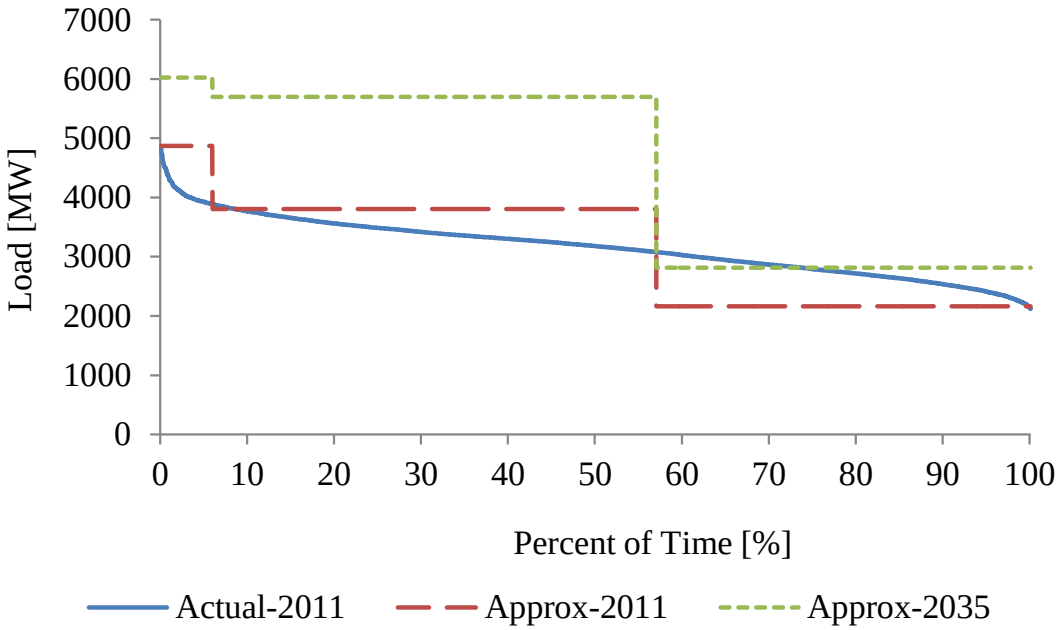

Figure B.11: Load forecast for the SW zone.

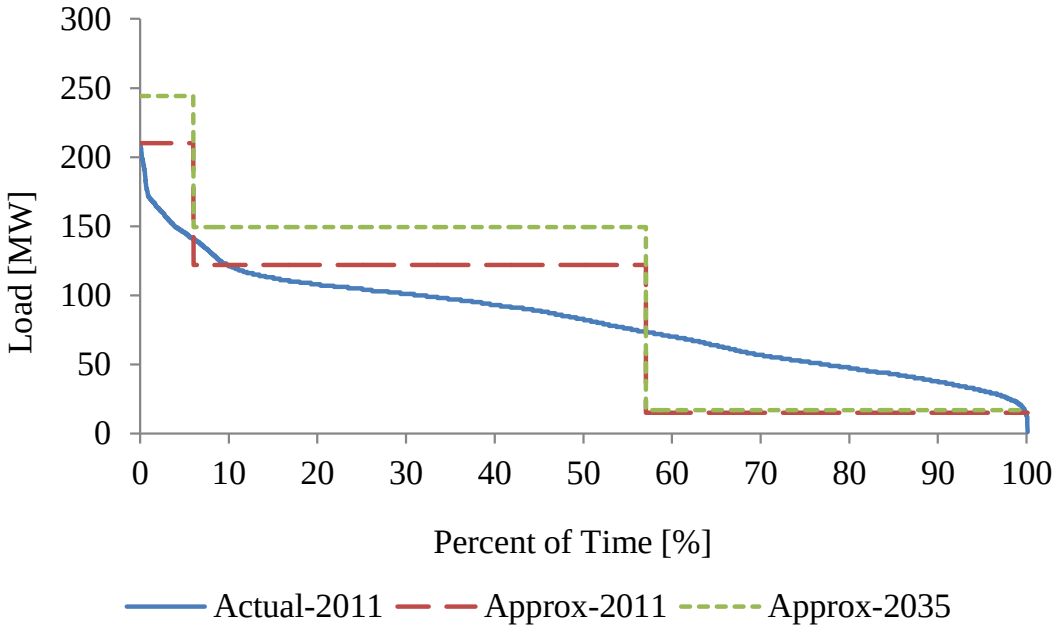

Figure B.12: Load forecast for the BRUCE zone.

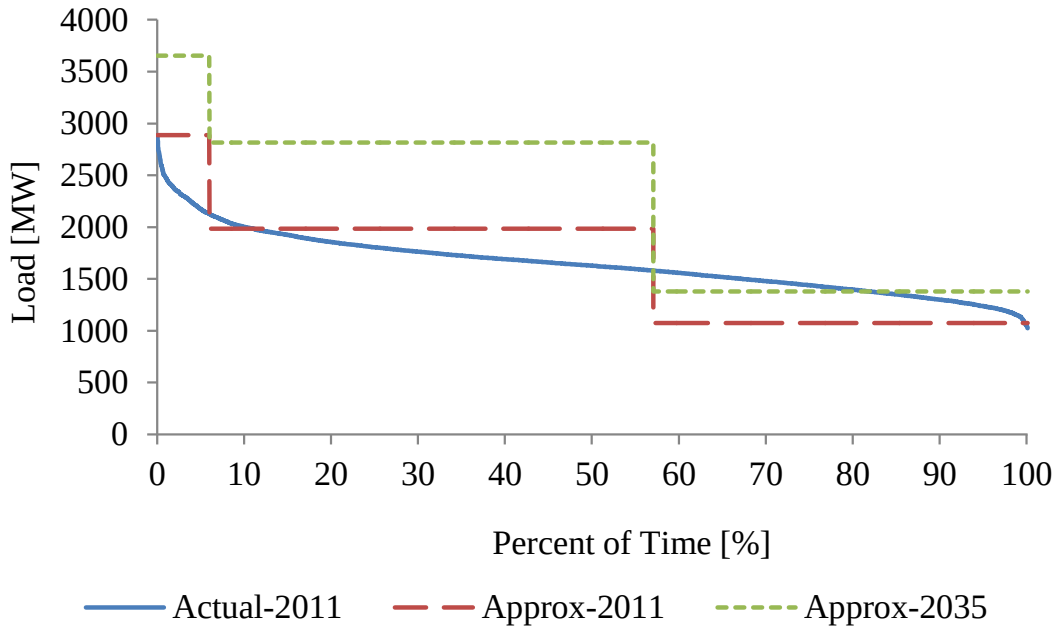

Figure B.13: Load forecast for the WEST zone.

Appendix C

Effect of Solar and Wind Capacity Factor Uncertainties on the Holistic GEP

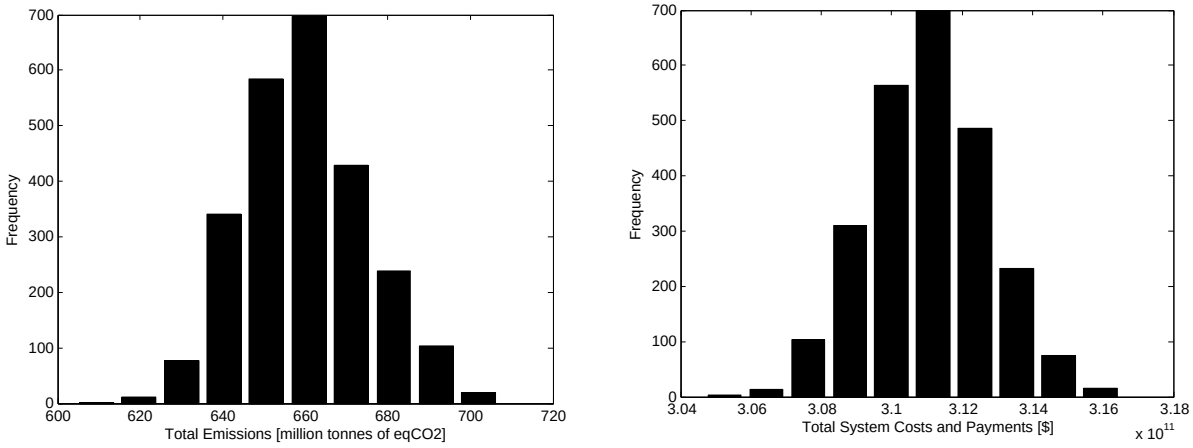

(a) (b)

Figure C.1: Resulting (a) Total emissions and (b) System costs and payments variations.

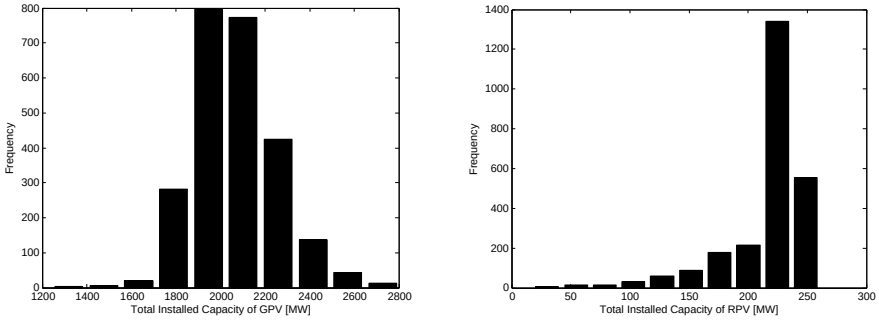

(a) GPV (b) RPV

Figure C.2: Resulting new capacity additions *NC* of solar PV.

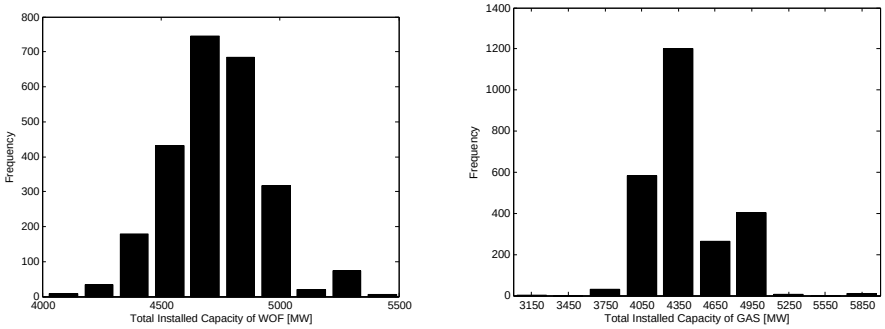

(a) WOF (b) GAS

Figure C.3: Resulting new capacity additions *NC* of (a) offshore wind and (b) gas.

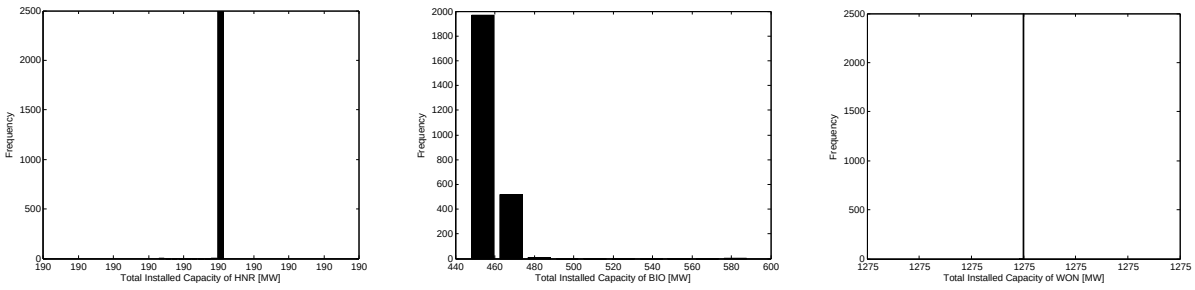

(a) (b) (c)

Figure C.4: Perturbing solar and wind *CF*s with σ=20% and resulting *NC* of (a) WOF and (b) GAS.

References

[1] "Coping with the Energy Challenge: The IEC's role from 2010 to 2030," International Electrotechnical Commission, Switzerland, White Paper, 2010. [Online]. Available: www.iec.ch/smartenergy/pdf/white_paper_Ires.pdf

[2] "Trends in Photovoltaic Applications 2010," International Energy Agency Photovoltaic Power System Programme, IEA PVPS Survey Report, 2010. [Online]. Available: http://iea-pvps.org/

[3] "PV Status Report 2013," European Commission, Joint Research Centre, Institute of Energy and Transport, JRC Scientific and Policy Report, 2013, accessed: 2 Jan. 2014. [Online]. Available: http://re.jrc.ec.europa.eu/refsys/

[4] "Trends in Photovoltaic Applications 2013," International Energy Agency Photovoltaic Power System Programme, IEA PVPS Survey Report, 2013. [Online]. Available: http://iea-pvps.org/

[5] P. Luukkonen, P. Bateman, J. Hiscock, Y. Poissant, D. Howard, and L. Dignard-Bailey, "National Survey Report of PV Power Applications in Canada: 2012," International Energy Agency Photovoltaic Power System Programme, IEA PVPS Survey Report, 2013. [Online]. Available: http://iea-pvps.org/

[6] "World Energy Perspective: Cost of Energy Technologies," World Energy Council, Tech. Rep., 2013. [Online]. Available: http://www.worldenergy.org/wp-content/uploads/2013/09/WEC_J1143_CostofTECHNOLOGIES_021013_WEB_Final.pdf

[7] "WWEA Quarterly Bulletin: Issue 3/4 - 2013," World Wind Energy Association, Tech. Rep., 2013, Accessed: 24 Feb. 2014. [Online]. Available: http://www.wwindea.org/webimages/WWEA_Bulletin-ISSUE_3_4_2013.pdf

[8] "Global Wind Statistics 2013," Global Wind Energy Council, Tech. Rep., 2013, Accessed: 25 Feb. 2014. [Online]. Available: http://www.gwec.net/wp-context/uploads/2014/02/GWEC-PRstats-2013_EN.pdf

[9] M. Rosano, "On with the Wind: Wind Energy in Canada Timeline," *Canadian Geographic Magazine*, Jun. 2009, Accessed: 26 Feb. 2014. [Online]. Available: http://www.canadiangeographic.ca/magazine/jun09/wind_power_timeline.asp

[10] "Wind by the Numbers: Economic Benefits of Wind Energy," Canadian Wind Energy Association, Tech. Rep., 2013, Accessed: 26 Feb. 2014. [Online]. Available: http://www.canwea.ca/pdf/canwea-factsheet-economic-web-final.pdf

[11] "Renewables 2013: Global Status Report," Renewable Energy Policy Network for the 21st Century (REN21), Tech. Rep., 2013. [Online]. Available: www.ren21.net/Portals/0/documents/Resources/GSR/2013/GSR2013_highres.pdf

[12] "FIT and microFIT Program," Ontario Power Authority. [Online]. Available: http://fit.powerauthority.on.ca

[13] L. Dignard-Bailey and J. Ayoub, "Canada Photovoltaic Technology Status and Prospects: Canadian Annual Report 2010," Natural Resources Canada, NRCan Report, 2010. [Online]. Available: http://canmetenergy-canmetenergie.nrcan-rncan.gc.ca/

[14] "The Support of Electricity from Renewable Energy Sources," Commission of the European Communities, Brussels, Commission Staff Working Document, 2008. [Online]. Available: ec.europa.eu/energy/climate_actions/doc/2008_res_working_document_en.pdf

[15] "Deploying Renewables: Principles for Effective Policies," International Energy Agency (IEA), Tech. Rep., 2008. [Online]. Available: www.iea.org/publications/freepublications/publication/DeployingRenewable2008.pdf

[16] "Feed-in-Tariff for grid-connected solar power systems." [Online]. Available: www.energymatters.com.au/government-rebates/feedintariff.php

[17] "FITs and Stops: Spain's new Renewable Energy plot twist & what it all means," 2012. [Online]. Available: www.e3analytics.ca/wp-content/uploads/2012/05/Analytical_Brief_Vol4_Issue1.pdf

[18] "New Feed-in Tariff levels for large-scale solar and anaerobic digestion announced today," 2011. [Online]. Available: https://www.gov.uk/government/news/

[19] C. Böhringer, T. F. Rutherford, N. J. Rivers, and R. Wigle, "Green Jobs and Renewable Electricity Policies: Employment Impacts of Ontario's Feed-in-Tariff," *The B.E. Journal of Economic Analysis and Policy*, vol. 12, no. 1, 2012, Article 25. [Online]. Available: http://www.ie.uottawa.ca/dl181&display

[20] B. Sharp, "Ontario Electricity Price Increase Forecast: December 2011 to December 2016," Aegent Energy Advisors Inc., Report submitted to Ontario Energy Board, 2012.

[21] D. D. Dewees, "What is Happening to Ontario Electricity Prices," Sustainable Prosperity, Background Report, 2012. [Online]. Available: http://sustainableprosperity.ca/dl764

[22] L. K. Kirchmayer, A. G. Mellor, J. F. O'Mara, and J. R. Stevenson, "An Investigation of the Economic Size of Steam-Electric Generating Units," *AIEE Trans. Power Apparatus and Systems, Part III.*, vol. 74, no. 3, pp. 600–614, Jan. 1955.

[23] R. J. Fitzpatrick and J. W. Gallagher, "Determination of an Optimized Generator Expansion Pattern," *AIEE Trans. Power Apparatus and Systems, Part III.*, vol. 80, no. 3, pp. 1052–1057, Apr. 1961.

[24] K. M. Dale, "Dynamic-programming Approach to the Selection and Timing of Generation-plant Additions," *Proc. IEE*, vol. 113, no. 5, pp. 803–811, May 1966.

[25] J. Zhu and M.-Y. Chow, "A Review of Emerging Techniques on Generation Expansion Planning," *IEEE Trans. Power Syst.*, vol. 12, no. 4, pp. 1722–1728, 1997.

[26] P. H. Henault, R. B. Eastvedt, J. Peschon, and L. P. Hajdu, "Power System Long-Term Planning in the Presence of Uncertainty," *IEEE Trans. Power App. Syst.*, vol. PAS-89, no. 1, pp. 156–164, Jan. 1970.

[27] M. Caramanis, "Investment Decisions and Long-Term Planning Under Electricity Spot Pricing," *IEEE Trans. Power App. Syst.*, vol. PAS-101, no. 12, pp. 4640–4648, 1982.

[28] Y. Kaya and H. Asano, "Electric Power System Planning under Time-Of-Use Rates," *IEEE Trans. Power Syst.*, vol. 4, no. 3, pp. 943–949, Aug. 1989.

[29] A. K. David, Y. Q. He, and P. N. Fernando, "Private Investment in Power and Deviations from the Least Cost Expansion Plan," *IEE Proc. - Gener. Transm. Distrib.*, vol. 142, no. 3, pp. 269–276, 1995.

[30] J.-B. Park, Y.-M. Park, J.-R. Won, and K. Lee, "An Improved Genetic Algorithm for Generation Expansion Planning," *IEEE Trans. Power Syst.*, vol. 15, no. 3, pp. 916–922, Aug 2000.

[31] S. A. McCusker, B. F. Hobbs, and J. Yuandong, "Distributed Utility Planning Using Probabilistic Production Costing and Generalized Benders Decomposition," *IEEE Trans. Power Syst.*, vol. 17, no. 2, pp. 497–505, May 2002.

[32] J. L. C. Meza, M. B. Yildirim, and A. S. M. Masud, "A Model for the Multiperiod Multiobjective Power Generation Expansion Problem," *IEEE Trans. Power Syst.*, vol. 22, no. 2, pp. 871–878, 2007.

[33] J. H. Roh, M. Shahidehpour, and Y. Fu, "Security-Constrained Resource Planning in Electricity Markets," *IEEE Trans. Power Syst.*, vol. 22, no. 2, pp. 812–820, 2007.

[34] M. Sunderkotter and C. Weber, "Valuing Fuel Diversification in Power Generation Capacity Planning," *Energy Economics*, 2012.

[35] "Integrated Power System Plan," Ontario Power Authority, 2007. [Online]. Available: http://www.powerauthority.on.ca/integrated-power-system-plan

[36] A. Botterud and M. Korps, "A Stochastic Dynamic Model for Optimal Timing of Investments in new Generation Capacity in Restructured Power Systems," *International Journal of Electrical Power & Energy Systems*, vol. 29, no. 2, pp. 163–174, 2007.

[37] S. Wong, K. Bhattacharya, and J. D. Fuller, "Long-Term Effects of Feed-In Tariffs and Carbon Taxes on Distribution Systems," *IEEE Trans. Power Syst.*, vol. 25, no. 3, pp. 1241–1253, Aug. 2010.

[38] S. Wong, K. Bhattacharya, and J. D. Fuller, "Coordination of Investor-Owned DG Capacity Growth in Distribution Systems," *IEEE Trans. Power Syst.*, vol. 25, no. 3, pp. 1375–1383, Aug 2010.

[39] D. Talavera, G. Nofuentes, and J. Aguilera, "The Internal Rate of Return of Photovoltaic Grid-connected Systems: A Comprehensive Sensitivity Analysis," *Renewable Energy*, vol. 35, no. 1, pp. 101–111, 2010.

[40] W. Muneer, K. Bhattacharya, and C. A. Cañizares, "Large-Scale Solar PV Investment Models, Tools, and Analysis: The Ontario Case," *IEEE Trans. Power Syst.*, vol. 26, no. 4, pp. 2547–2555, Nov. 2011.

[41] J. Sterling, J. McLaren, M. Taylor, and K. Cory, "Treatment of Solar Generation in Electric Utility Resource Planning," National Renewable Energy Laboratory (NREL), Tech. Rep., Oct. 2013. [Online]. Available: http://www.nrel.gov/analysis/re_futures/

[42] M. M. Hand, J. M. Reilly, G. Porro, S. Baldwin, T. Mai, M. Meshek, E. DeMeo, D. Arent, and D. Sandor, "Renewable Electricity Futures Study," National Renewable Energy Laboratory (NREL), Tech. Rep., 2012. [Online]. Available: http://www.nrel.gov/analysis/re_futures/

[43] M. Madrigal and K. Porter, *Operating and Planning Electricity Grids with Variable Renewable Generation*. The World Bank, 2013. [Online]. Available: http://elibrary.worldbank.org/doi/abs/10.1596/978-0-8213-9734-3

[44] E. A. DeMeo, W. Grant, M. R. Milligan, and M. J. Schuerger, "Wind Plant Integration [Wind Power Plants]," *IEEE Power Energy Mag.*, vol. 3, no. 6, pp. 38–46, Nov 2005.

[45] R. Tanabe, K. Yasuda, R. Yokoyama, and H. Sasaki, "Flexible Generation Mix under Multi-objectives and Uncertainties," *IEEE Trans. Power Syst.*, vol. 8, no. 2, pp. 581–587, May 1993.

[46] E. Mazhari, J. Zhao, and N. Celik, "Hybrid Simulation and Optimization-Based Capacity Planner for Integrated Photovoltaic Generation with Storage Units," in *Proc. 2009 Winter Simulation Conference*, Dec. 2009.

[47] W. Yi-bo, L. Hua, W. Chun-sheng, and X. Hong-hua, "Large-scale Grid-connected Photovoltaic Power Station's Capacity Limit Analysis under Chance-constraints," in *Proc. International Conference on Sustainable Power Generation and Supply, SUPERGEN '09.*, Apr. 2009, pp. 1–6.

[48] B. H. Chowdhury, "Analysis of Wind Power Integration with Power System Planning," in *Proc. 25th Intersociety Energy Conversion Engineering Conference, IECEC-90.*, vol. 5, aug 1990, pp. 207 –212.

[49] S. Kamalinia and M. Shahidehpour, "Generation Expansion Planning in Wind-thermal Power Systems," *Proc. IET Gener. Transm. Dis.*, vol. 4, no. 8, pp. 940 –951, august 2010.

[50] F. Careri, C. Genesi, P. Marannino, M. Montagna, S. Rossi, and I. Siviero, "Generation Expansion Planning in the Age of Green Economy," *IEEE Trans. Power Syst.*, vol. 26, no. 4, pp. 2214–2223, 2011.

[51] J. Ma, V. Silva, R. Belhomme, D. Kirschen, and L. Ochoa, "Evaluating and Planning Flexibility in Sustainable Power Systems," *IEEE Trans. Sustain. Energy*, vol. 4, no. 1, pp. 200–209, 2013.

[52] Y. Zhou, L. Wang, and J. D. McCalley, "Designing Effective and Efficient Incentive Policies for Renewable Energy in Generation Expansion Planning," *Applied Energy*, vol. 88, no. 6, pp. 2201 – 2209, 2011.

[53] R. Hemmati, R. Hooshmand, and A. Khodabakhshian, "Comprehensive Review of Generation and Transmission Expansion Planning," *Proc. IET Gener. Transm. Dis.*, vol. 7, no. 9, pp. 955–964, 2013.

[54] R. D. Tabors, S. R. Connors, C. G. Bespolka, D. C. White, and C. J. Andrews, "A Framework for Integrated Resource Planning: The Role of Natural Gas Fired Generation in New England," *IEEE Trans. Power Syst.*, vol. 4, no. 3, pp. 1010–1016, Aug 1989.

[55] E. Hirst and C. Goldman, "Key Issues in Integrated Resource Planning for Electric Utilities," *IEEE Trans. Power Syst.*, vol. 5, no. 4, pp. 1105–1111, Nov 1990.

[56] D. Chattopadhyay, R. Banerjee, and J. Parikh, "Integrating Demand Side Options in Electric Utility Planning: A Multiobjective Approach," *IEEE Trans. Power Syst.*, vol. 10, no. 2, pp. 657–663, May 1995.

[57] P. S. Neelakanta and M. H. Arsali, "Integrated Resource Planning using Segmentation Method based Dynamic Programming," *IEEE Trans. Power Syst.*, vol. 14, no. 1, pp. 375–385, Feb 1999.

[58] H. Stoll, *Least-cost electric utility planning*. Wiley, 1989.

[59] R. N. Allan and R. Billinton, *Reliability Evaluation of Power Systems*. Springer, 1996.

[60] J. A. White, K. S. Grasman, K. E. Case, K. L. Needy, and D. B. Pratt, *Fundamentals of Engineering Economic Analysis: First Edition*. Wiley, 2013.

[61] A. J. Conejo, E. Castillo, R. Minguez, and R. Garcia-Bertrand, *Decomposition Techniques in Mathematical Programming: Engineering and Science Applications*. Berlin: Springer-Verlag, 2006.

[62] E. Castillo, A. Conejo, C. Castillo, R. Minguez, and D. Ortigosa, "Perturbation Approach to Sensitivity Analysis in Mathematical Programming," *Journal of Optimization Theory and Applications*, vol. 128, pp. 49–74, 2006.

[63] A. Saltelli, *Global Sensitivity Analysis: The Primer*. Wiley, 2008.

[64] J. Sobieszczanski-Sobieski, J. F. Barthelemyy, and K. M. Riley, "Sensitivity of Optimal Solutions of Problem Parameters," *AIAA Journal*, vol. 20, pp. 1291–1299, 1982.

[65] F. Milano, A. Conejo, and R. Zarate-Minano, "General Sensitivity Formulas for Maximum Loading Conditions in Power Systems," *Proc. IET Gener. Transm. Dis.*, vol. 1, no. 3, pp. 516–526, May 2007.

[66] J. Wittwer, "Monte Carlo Simulation Basics." [Online]. Available: http://www.vertex42.com/ExcelArticles/mc/MonteCarloSimulation.html

[67] S. S. Rao, *Engineering Optimization: Theory and Practice*. New Age International, 1996.

[68] J. Bisschop, *AIMMS Optimization Modeling*. Lulu Enterprises Incorporated, 2006. [Online]. Available: http://www.aimms.com

[69] R. E. Rosenthal, *GAMS - A User's Guide*. [Online]. Available: www.gams.com/dd/docs/bigdocs/GAMSUsersGuide.pdf

[70] *CPLEX 12*, Solver Manual. [Online]. Available: www.gams.com/dd/docs/solvers/cplex.pdf

[71] W. Muneer, "Large-Scale Solar PV Investment Planning Studies," M.A.Sc thesis, University of Waterloo, Waterloo, Ontario, Canada, 2011.

[72] *MATLAB Documentation*, The Mathworks Inc., 2011. [Online]. Available: www.mathworks.com/help/techdoc/

[73] E. Suhir, *Applied Probability for Engineers and Scientists*. McGraw-Hill, 1997.

[74] M. Shahidehpour, H. Yamin, and Z. Li, *Market Operations in Electric Power Systems: Forecasting, Scheduling, and Risk Management*. IEEE, Wiley-Interscience, 2002.

[75] "Ontario Transmission System," Independent Electricity System Operator (IESO), Aug. 2009. [Online]. Available: www.ieso.ca/imoweb/pubs/marketReports/OntTxSystem_2009aug.pdf

[76] A. Hajimiragha, "Sustainable Convergence of Electricity and Transport Sectors in the Context of Integrated Energy Systems," Ph.D. Thesis, University of Waterloo, Waterloo, Ontario, Canada, 2010.

[77] Photovoltaic and Solar Resource Map. Natural Resources Canada (NRCAN). [Online]. Available: www.pv.nrcan.gc.ca

[78] "Market Data," Independent Electricity System Operator (IESO), Ontario. [Online]. Available: www.ieso.ca/imoweb/marketdata/marketDATA.asp

[79] "Assumptions to the Annual Energy Outlook," U.S. Energy Information Administration, Tech. Rep., 2009.

[80] J. Parikh and D. Chattopadhyay, "A Multi-area Linear Programming Approach for Analysis of Economic Operation of the Indian Power System," *IEEE Trans. Power Syst.*, vol. 11, no. 1, pp. 52–58, Feb 1996.

[81] "Assumptions to the Annual Energy Outlook," U.S. Energy Information Administration, Tech. Rep., 2012.

[82] N. Rodriguez, R. Tidball, J. Bluestein, and S. Knoke, "Cost and Performance Assumptions for Modeling Electricity Generation Technologies," National Renewable Energy Laboratory, Tech. Rep., 2010.

[83] A. Evans, V. Strezov, and T. Evans, "Comparing the Sustainability Parameters of Renewable, Nuclear and Fossil Fuel Electricity Generation Technologies," in *World Energy Congress, Montreal 2010*, 2010.

[84] Population and dwelling count, 2011 Census. Statistics Canada. [Online]. Available: http://www12.statcan.gc.ca/census-recensement/index-eng.cfm

[85] "OPG Reports - Financial Results," Ontario Power Generation (OPG), Tech. Rep., 2011. [Online]. Available: http://www.opg.com/investor/pdf/2011_Q4_FullRpt.pdf

[86] "Quarterly Report to Shareholders," Transcanada Corporation, Tech. Rep., 2012. [Online]. Available: http://www.transcanada.com/docs/Investor_Centre/TCC-2012-Q1-Quarterly-Report.pdf

[87] D. B. Layzell, J. Stephen, and S. M. Wood, "Exploring the Potential for Biomass Power in Ontario," BIOCAP Canada Foundation, Tech. Rep., 2006. [Online]. Available: www.biocap.ca/files/Ont_bioenergy_OPA_Feb23_Final.pdf

[88] "The Economics of Nuclear Power," World Nuclear Association, Tech. Rep., 2012, accessed: Apr. 2012. [Online]. Available: www.world-nuclear.org/info/Economic-Aspects/Economics-of-Nuclear-Power

[89] I. Das, K. Bhattacharya, C. Cañizares, and W. Muneer, "Sensitivity-Indices-Based Risk Assessment of Large-Scale Solar PV Investment Projects," *IEEE Trans. Sustain. Energy*, vol. 4, no. 2, pp. 370–378, April 2013.

[90] I. Das, K. Bhattacharya, and C. Cañizares, "Optimal Incentive Design for Targeted Penetration of Renewable Energy Sources," *IEEE Trans. Sustain. Energy*, 2014, accepted for publication.